NASA CONTRACTOR REPORT

NASA CR-1350
C.1

NASA CR-1350

INCREMENTAL ANALYSIS OF LARGE DEFORMATIONS IN MECHANICS OF SOLIDS WITH APPLICATIONS TO AXISYMMETRIC SHELLS OF REVOLUTION

by Saeed Yaghmai

Prepared by
UNIVERSITY OF CALIFORNIA
Berkeley, Calif.
for

NATIONAL AERONAUTICS AND SPACE ADMINISTRATION • WASHINGTON, D. C. • JUNE 1969

NASA CR-1350

INCREMENTAL ANALYSIS OF LARGE DEFORMATIONS IN MECHANICS OF SOLIDS WITH APPLICATIONS TO AXISYMMETRIC SHELLS OF REVOLUTION

By Saeed Yaghmai

Prepared under Grant No. NGR-05-003-014 by
UNIVERSITY OF CALIFORNIA
Berkeley, Calif.

for

NATIONAL AERONAUTICS AND SPACE ADMINISTRATION

For sale by the Clearinghouse for Federal Scientific and Technical Information
Springfield, Virginia 22151 – CFSTI price $3.00

ABSTRACT

A general incremental variational method for the analysis of geometrically and physically non-linear problems in continuum mechanics is developed. This variational method is applicable to any type of material properties. In particular, non-linear constitutive laws for elastic, and elastic-plastic materials are considered. Starting from the basic principles in continuum mechanics, such as the invariance requirements and the thermodynamic laws, general incremental constitutive equations have been derived for non-linear elastic materials. For the elastic-plastic materials an incremental constitutive law is considered where deformations are infinitesimal but rotations are finite.

The method has been specialized and applied to the analysis of large deflections of elastic-plastic axisymmetrically deformed shells of revolution. The displacement formulation of the finite element method has been exploited for this problem and a digital computer program is written for the numerical analysis. Several examples of circular plate, shallow shell, and thin axisymmetric shells of arbitrary meridional form are presented to illustrate the convergence and accuracy of the method.

ACKNOWLEDGMENTS

I wish to express my deepest gratitude to my research advisor, Professor E. P. Popov, for his supervision and continuous encouragement and interest during the course of this work. I am also grateful to the other members of my thesis committee, Professor M. M. Carroll for some interesting discussions and his review and comments of the work, and Professor E. L. Wilson for reading the manuscript. In addition, I acknowledge the advice and help of some graduate students at the University of California, in particular Messrs. P. Sharifi, P. Larsen, and D. Kavlie, for checking of the computer program and the preparation of examples.

This research was supported in part by the National Aeronautics and Space Administration under Research Grant NGR-05-003-014 and by the National Science Foundation by Grant GK-750. The computer time and facilities were provided by the Computer Center of the University of California at Berkeley. I express my appreciation for all this support.

Thanks are due to the people of Iran who made my graduate study possible by a government scholarship through the National Iranian Oil Company.

Finally, I would like to thank Mrs. A. Martin and Mrs. C. Bryant for typing this manuscript and Mr. W. Kot for drawing all the Figures.

TABLE OF CONTENTS

NOMENCLATURE

A list of all important symbols in the text is compiled here. The symbols which are introduced in some sections of the text but which are not referred to later are not included. Some of the symbols may have two meanings in different sections; these are clearly defined and should not confuse the reader. For the symbols which have either lengthy definitions or no particular name the reader is referred to the place in the text where they were first introduced.

A tensor component with an asterisk (*) superscript denotes a physical component. Repeated indices indicate summation over the range of the indices unless otherwise stated. Latin indices range from 1 - 3, and Greek indices from 1 - 2.

$\bar{a}, a, A$	surface area in the initial, first and second configurations, respectively
A	increment of free energy function
${}^{1}A, {}^{2}A$	free energy function of configurations 1 and 2, respectively
$\underset{\sim}{a}_{\alpha}, \underset{\sim}{A}_{\alpha}$	in plane base vectors of the middle surface of the shell in configurations 1 and 2, respectively
$\underset{\sim}{a}_{3}, \underset{\sim}{A}_{3}$	unit vector normal to the middle surface of the shell in configurations 1 and 2, respectively
$a_{\alpha\beta}, a^{\alpha\beta}$	covariant and contravariant components of the middle surface metric tensor in configuration 1
$A_{ijk\ell}$	as defined in (II.51)
$b_{\alpha\beta}$	the second invariant form of the middle surface of the shell in configuration 1
b^{α}_{β}	curvature tensor of the middle surface of the shell in configuration 1

c	edge of the shell
C_{ij}	Green's deformation tensor between configurations 1 and 2
${}^1C_{ij}, {}^2C_{ij}$	Green's deformation tensors at configurations 1 and 2, respectively
$C_{ijk\ell}$	elastic-plastic moduli tensor
$C'_{ijk\ell}$	physical components of elastic-plastic moduli tensor, defined in (II.77)
$\bar{C}_{\alpha\beta\gamma\delta}$	elastic-plastic moduli tensor for generalized plane stress, see (III.28)
E	Young's modulus
E_t	tangent modulus
e_s	linear part of the meridional strain of the middle surface of the shell
e_θ	linear part of the circumferential strain of the middle surface of the shell
e_{ij}	linear part of Lagrange strain tensor from configuration 1 to 2
${}^1e_{ij}, {}^2e_{ij}$	linear part of the Lagrange strain tensor in configurations 1 and 2, respectively
F	hardening function defined in (II.42)
f	yield function
f_i	increment of body force per unit mass
g	plastic potential
$\underset{\sim}{\bar{g}}_i, \underset{\sim}{g}_i, \underset{\sim}{G}_A$	base vectors in the initial, first, and second configurations, respectively
$\bar{g}_{ij}, g_{ij}, G_{AB}$	metric tensors in the initial, first, and second configurations, respectively
h	thickness of the shell
H	hardening function defined in (II.43)
$\underset{\sim}{i}_j$	unit base vectors
J_1, J_2, J_3	invariants of the deviatoric stress tensor
ℓ	cord length of an element

M_s, M_θ	increment of the meridional and circumferential bending moments measured per unit length of the middle surface of the shell in configuration 1
${}^1M_s, {}^1M_\theta$	meridional and circumferential bending moments per unit length of the middle surface of the shell in configuration 1
N_s, N_θ	increment of the meridional and circumferential in plane forces per unit length of the middle surface of the shell in configuration 1
${}^1N_s, {}^1N_\theta$	meridional and circumferential in plane forces per unit length of the middle surface of the shell in configuration 1
$\bar{n}_i, n_i, N_A$	direction cosines of the outward normal to the boundary surfaces in the initial, first and second configurations
p_s, p_n	meridional and normal force increments measured per unit area of the middle surface of the shell in configuration 1
Q_s	increment of shear force per unit area of the middle surface of the shell in configuration 1
r	radial coordinate as shown in Figure III.1
${}^1r, {}^2r$	rate of heat production per unit mass in configurations 1 and 2, respectively
R_s, R_θ	meridional and circumferential principal radii of curvature of the shell in configuration 1
s	arc length
${}^1S, {}^2S$	entropy per unit mass in configurations 1 and 2
$s_{ij}, \bar{s}_{ij}$	increments of Piola symmetric stress tensor measured per unit of area a and $\bar{a}$, respectively
${}^2s_{ij}, {}^2\bar{s}_{ij}$	Piola symmetric stress tensor in configuration 2 measured per unit of area a and $\bar{a}$, respectively
$t_i, \bar{t}_i$	increments of surface traction measured per unit of area a and $\bar{a}$, respectively
${}^1t_i, {}^1\bar{t}_i$	surface tractions in configuration 1 measured per unit of area a and $\bar{a}$, respectively
${}^2t_i, {}^2\bar{t}_i$	surface tractions in configuration 2 measured per unit of area a and $\bar{a}$, respectively
u	meridional displacement increment of the middle surface of the shell, see Figure III.2

$\underset{\sim}{u}'$	increment of the displacement vector of a generic point in the shell space
u_1, u_2	increments of displacements of the middle surface of the shell, see Figure IV.1
$\bar{u}_i, u_i$	increments of the displacements in terms of the coordinates of the initial and first configurations, respectively
${}^1u_i, {}^1\bar{u}_i$	displacements between the initial state and the first configuration in terms of the coordinates of configuration 1 and initial state, respectively
${}^2u_i, {}^2\bar{u}_i$	displacements between the initial state and the second configuration in terms of the coordinates of configuration 2 and initial state, respectively.
$\bar{v}, v, V$	volumes of the initial, first, and second configurations, respectively
w	normal displacement increment of the middle surface of the shell, see Figure III.2
W_p	plastic work
W_v	virtual work
$\bar{x}^{ij}, x^{ij}, X^{AB}$	curvilinear coordinates of the initial state, and configurations 1 and 2, respectively
$\bar{z}_i, z_i, Z_A$	Cartesian coordinates of the initial state, and configurations 1 and 2, respectively
α_i	generalized coordinates
β	angle shown in Figure IV.1
Γ^k_{ij}	Christoffel symbols
δ	virtual variation
δ_{ij}	Kronecker delta
ε_{ij}	Lagrange strain tensor between configurations 1 and 2
${}^1\varepsilon_{ij}, {}^2\varepsilon_{ij}$	Lagrange strain tensors at configurations 1 and 2
$\varepsilon^e_{ij}, \varepsilon^p_{ij}$	elastic and plastic parts of Lagrange strain tensor between configurations 1 and 2
${}^1\varepsilon^e_{ij}, {}^1\varepsilon^p_{ij}$	elastic and plastic parts of Lagrange strain tensor in configuration 1

$\varepsilon_{ss}, \varepsilon_{\theta\theta}$	physical components of the meridional and circumferential Lagrangian strain of the shell between configurations 1 and 2
$\varepsilon_s, \varepsilon_\theta$	physical components of the meridional and circumferential Lagrangian strain of the middle surface of the shell between configurations 1 and 2
$\bar{\varepsilon}^p$	equivalent plastic strain, see (II.41)
ζ	ratio of tangent modulus to elastic modulus, also coordinate along the thickness of the shell
η	local coordinate for an element as in Chapter IV, see Figure IV.1
η_{ij}	non-linear part of Lagrange strain tensor between configurations 1 and 2
θ	circumferential coordinate of the shell, see Figure III.1; also temperature as in Chapter I
κ	hardening parameter
κ_s, κ_θ	change of the meridional and circumferential curvatures of the middle surface of the shell between configurations 1 and 2
$\kappa_s^{\circ}, \kappa_\theta^{\circ}$	linear parts of κ_s, and κ_θ, respectively
$\kappa_s^{1}, \kappa_\theta^{1}$	non-linear parts of κ_s, and κ_θ, respectively
λ	Lamé constant, see (II.1); also the geometric parameter of shallow shells, see Chapter III - section III.1.2
$\overset{\circ}{\bar{\lambda}}, d\bar{\lambda}$	as defined in (II.26) and (II.44)
μ	Lamé constant, see (II.1); also the dterminant of space shifter tensor, see (E.5)
μ_β^α	space shifter tensor, see (E.3)
ν	Poisson's ratio
ξ	local coordinate for an element, see Figure IV.1
ξ_{ij}	the difference between strains ${}^2\varepsilon_{ij}$ and ${}^1\varepsilon_{ij}$
$\bar{\rho}_o, \rho_o, \rho$	mass density in the initial state, and configurations 1 and 2, respectively
$\bar{\sigma}$	equivalent stress
τ_{ij}	Cauchy stress components in configuration 1

τ'_{ij}	deviatoric compponents of Cauchy stress tensor in configuration 1
ϕ	meridional angle of the shell
χ	as defined in (III.5)
ω_n, ω_s	normal and meridional physical components of the rotation vector of the middle surface of the shell between configurations 1 and 2
$\omega_{ij}, {}^1\omega_{ij}, {}^2\omega_{ij}$	rotation terms in the strain tensors ε_{ij}, ${}^1\varepsilon_{ij}$ and ${}^2\varepsilon_{ij}$, respectively
Ω	as defined in (III.31)
{ }	column vector
< >	row vector
[ ]	matrix
[A]	displacement transformation matrix, see (IV.57)
[B]	as defined in (IV.29)
[C]	matrix of elastic-plastic moduli
[D]	rigidity matrix, see (III.60)
{e}	vector of linear components of strain, see (IV.24)
[F]	as defined in (IV.36)
[G]	as defined in (IV.48)
$[k_\alpha^{(o)}]$	incremental stiffness matrix of an element in coordinates α due to the linear parts of increments of strain, see (IV.30)
$[k_\alpha^{(1)}]$	initial stress stiffness matrix for an element in coordinates $\{\alpha\}$, see (IV.50)
$[k_\alpha]$	incremental stiffness matrix for an element in coordinates $\{\alpha\}$, see (IV.56)
[k]	incremental stiffness matrix of an element in global coordinate system, see (IV.65)
[K]	incremental stiffness matrix of the shell, see (IV.66)
$\{{}^1N\}, [{}^1N]$	vector and diagonal matrix of stress resultants in configuration 1 of the shell, see (III.56) and (IV.41)

$\{\tilde{p}\}$	as defined in (III.52)
$\{Q\}$	increment of equivalent nodal point force
$\{Q_\alpha\}$	increment of equivalent nodal point force in generalized coordinates $\{\alpha\}$
$\{R\}$	increment of external nodal loads of the shell
$\{r\}$	increment of nodal displacements of the shell
$[T]$	transformation matrix, see (IV.60)
$\{\alpha\}$	generalized coordinates
$\{\varepsilon\}$	Lagrange strain between configurations 1, and 2, see (III.59)
$\{\eta\}$	non-linear part of Lagrange strain $\{\varepsilon\}$, see (III.55)
$\{\overline{\eta}\}$	as defined in (IV.36)
$[\phi]$	as defined in (IV.52)
$\{\chi\}$	as defined in (IV.45)
$[\chi]$	as defined in (IV.46)

INTRODUCTION

The consideration of geometrical and/or material nonlinearities in the analysis of many structures is quite important for various reasons, e.g., for the precision demanded in the prediction of the actual behavior of such structures under severe environmental and loading conditions and also for economical considerations. As an example, consider thin shells of revolution. The buckling behavior of these structures is essentially of nonlinear character and the prediction of their post buckling characteristics without such consideration is not possible. Even under prebuckling conditions the analysis of the behavior of some shells of revolution like a membrane torus or a thin shallow cap inevitably requires nonlinear analysis. Also, the necessity for utilizing engineering materials more efficiently and economically in such areas as aerospace industry requires the incorporation of physical and geometrical nonlinearities in the analysis of shell type structures.

There are no general methods of solution of nonlinear boundary value problems in engineering. Only a few very simple nonlinear problems can be solved by exact analytical methods [1,2]. Even the classical approximate solutions such as asymptotic expansions and weighted residual methods can be applied to relatively simple problems [1,2,3] and resort must be made to numerical procedures of analysis. In the past two decades the advent of high-speed digital computers has renewed the efforts at reconsidering and extending some classical approximate methods such as weighted residual and Ritz method, numerical finite difference techniques, and the development of new concepts like invariant imbedding and other numerical procedures.

The finite difference method has been studied rather well mathematically [145]. The difficulty with the application of this numerical technique in the problems of continuum mechanics is that it is not suitable to express some boundary conditions easily and cannot accommodate quite irregular changes of geometrical and material properties.

Invariant imbedding is the transformation of the boundary value problem into an initial value problem by introducing new variables and parameters [4,146]. This approach, together with the quasilinearization technique, which is an extension of Newton-Raphsor method for functional analysis, can be formulated into a predictor corrector formula which may prove useful in the solution of some nonlinear boundary value problems in mechanics of solids. The disadvantage of this method is that instead of one original problem a family of problems must be solved, resulting in more computational effort. In certain problems the additional calculations provide some extra informations which are desirable to know.

Another discrete approximation to the boundary value problems is the finite element method [5,6], which is ar extension of the classical Ritz method for the solution of variational problems. In the finite element method the domain of the problem is discretized into a number of disjoint subdomains called elements, a set of points of which (usually on the boundary) are called nodes. Then the integrand of the functional integral is approximated by a set of assumed functions which are expressed in terms of the values of the integrand functions at the nodes by suitable interpolation formulas satisfying the continuity conditions at the nodes.

In the problems of continuum mechanics the finite element method is easily adaptable to matrix formulation which can be readily used for the analysis by computers. The method is capable of approximating quite

irregular boundary shapes and complicated boundary conditions, and can handle arbitrary variations of the physical and geometrical parameters in the domain of the problem.

The above three methods can be used with an iterative and/or incremental integration scheme. The choice of either one of these depends, among other factors, on the physical characteristics of the problem. For example, for a non-conservative system like a continuum with the incremental constitutive law of plasticity an incremental procedure should be adopted. The combination of the finite element method with an incremental forward integration procedure on some variable of the problem is quite suitable for the analysis of many problems on digital computers.

The purpose of the present work is to develop an incremental variational method of analysis for the problems in continuum mechanics considering both the geometrical and physical nonlinearities, and to apply the method for the large displacement analysis of elastic-plastic shells of revolution using the displacement formulation of the finite element method.

Several forms of the incremental variational expressions of the equilibrium of the continuum are considered in Chapter I and Appendix C. From among these one expression which is based on a moving reference configuration is chosen and used in subsequent developments. The fact that such a variational expression leads to correct incremental equations of equilibrium and boundary conditions is shown in Appendix A. Also, in this chapter, after a preliminary review of the laws of thermodynamics and invariance principle for energy, the incremental nonlinear constitutive equations of elasticity are derived. For simplicity of understanding of the basic ideas, all of the presentations in Chapters I and II are in Cartesian coordinates.

In Chapter II the incremental constitutive equations for elastic materials are simplified for the isotropic case and for infinitesimal deformations but finite rotations. Based on these kinematic restrictions and for initially isotropic materials an incremental theory of plasticity for metals is deduced from the general theory of plasticity by Green and Naghdi [50]. It is shown that for initially isotropic materials the form of the elastic-plastic constitutive equations remains invariant in Cartesian and initially orthogonal convected curvilinear coordinates if the Cartesian tensors are replaced by the physical components of their corresponding curvilinear tensors. This invariance is very useful in applying the formulations in Cartesian coordinates to shells of revolution.

Chapters III, IV, and V are on the application of the incremental method to the large displacement analysis of axisymmetrically deformed shells of revolution. The kinematic relations for axisymmetric shells of revolution are derived in Chapter III. Also in this chapter the elastic-plastic constitutive equations of Chapter II, and the incremental expression of virtual work of Chapter I are specialized for axisymmetric shells of revolution. Finite element formulation of the variational expression in Chapter I is given in Chapter IV and the various stiffness matrices resulting from it are demonstrated. For the finite element analysis of axisymmetric shells of revolution a curved element developed in [140] is employed and the displacement formulation of the finite element method for linear incremental analysis is set up. A convenient procedure for the formation of the initial stress stiffness matrix is demonstrated. Some numerical examples are given in Chapter V and the convergence of the solutions are studied.

CHAPTER I: THEORY OF THE INCREMENTAL METHOD OF ANALYSIS IN CONTINUUM MECHANICS

I.1 Review of Literature on Incremental Methods of Analysis in Continuum Mechanics

The incremental method of analysis in continuum mechanics is closely related to the developments in the theory of the continuum which is under initial stress. Two approaches have been followed in the formulation of the theory of deformable bodies under initial stress. In the first approach exact constitutive equations have been sought for the superposition of small displacements or displacement gradients upon arbitrarily large deformations. Tensorial definitions have been used for strains and corresponding stresses have been defined. The second approach is more intuitive and relies on approximations within the kinematics of deformation and the constitutive equations.

According to Truesdell [7] the investigations in the exact theory date back to Cauchy who arrived at the correct form of the constitutive equations of an elastic body under initial stress [8]. A brief historical account of the developments in the theory of elasticity of deformable bodies under initial stress is given in [7]. Cauchy's constitutive relations were derived by Murnaghan [3] by means of Green's theory of elastic energy. Both Cauchy and Murnaghan's equations are limited to the superposition of infinitesimal displacement gradients on large initial deformations. A more restrictive theory in which the superposed displacements themselves are infinitesimal was developed by Green, Rivlin, and Shield [10].

All of these results indicate that the isotropy of an initially isotropic material is lost even if the displacement gradients of the superposed displacements are infinitesimal.

Another group of investigators have adopted the nontensorial strain quantity based on the definition of extension (the so-called engineering definition of strain) as a measure of deformation. They separate pure deformations and rotations and use constitutive equations which involve only pure deformations--thus separating the physics of the problem from the geometry. This approach has been followed by Southwell [11], Biezeno and Hencky [12], and has been extensively discussed and used by Biot since 1934 [13]. The difficulty with such a strain measure is that it is not a tensorial entity and cannot be used easily in curvilinear coordinates unless some approximations are made. Also, in general, it is an irrational function of displacement gradients unless approximations of the third order are committed*. The resulting non-linear expression of strain has a restricted form in which the linear strains are infinitesimal. Even rotations are limited to the first order to make the transformations among the various stress measures practically useful.**

It can be said that the theories developed by this approach are limited in scope and generality and usually leave many approximations to be made by the user, a feature which may prove both helpful and misleading. A parallel and more restricted development in the theory of elastic stability was reported by Prager [14] who superposes infinitesimal displacements on large ones and performs the superposition of stresses by the Piola unsymmetric stress tensor. He assumes that the incremental constitutive equations are linear and isotropic.

---

*Biot, M.A. [13], pp. 19

**Biot, M.A. [13], pp. 10, 21.

In an attempt to extend Biot's ideas to the analysis of large deformations, Felippa [15] wrote an expression for virtual work in which he uses the Lagrangian strain increment together with the Biezerio-Hencky type of stress. It can be shown that these stresses and strains are not conjugate in the sense that their product does not represent work unless the deformations are infinitesimal in which case Biot's relations are obtained. Therefore, his theory is applicable to problems in which deformations are infinitesimal but rotations are of first order.

The increasing interest in the non-linear analysis of structures has accelerated the application of the incremental method of analysis to such problems. The use of incremental procedure together with the finite element technique (with or without iterative procedures) is gaining momentum in the analysis of nonlinear problems in structural mechanics. However, so far no rigorous attempt has been made to give a general theory for the incremental analysis and in most cases the lack of understanding of the theory of the continuum under initial stress is evident. This is partly due to the simplicity of the problems analyzed for which relatively good results can be obtained even if crude approximations are made. The common feature of most of these incremental procedures is the presence of the so called geometric or the initial stress stiffness matrix which accounts for the effect of change of the geometry on equilibrium equations. Since the investigations in this area are applications to various structural problems and do not present a unified theory a detailed survey of them will not be presented but rather the trend of developments will be outlined. More detailed study

of the papers on circular plates and shells of revolution will be given in Chapter 3.

The use of the geometric stiffness matrix in the linearized incremental method of analysis was first reported by Turner, et al. [16] for stringers and triangular membrane elements. Gallagher and Padlog [17] derived the geometric stiffness matrix for beam columns from the expression of potential energy. Argyris and his co-workers have advocated the separation of rigid body motions and deformations of the elements in the finite element method of analysis and have derived corresponding geometric stiffness matrices for one, two and three dimensional bodies [18], [19], [20], [21]. An account of the developments in the incremental approach for nonlinear analysis of structures up to 1965 is given by Martin [22]. In both [22] and [23] Martin tries to present a more consistent method of deriving the initial stress stiffness matrix. Similar attempt was made by Oden [24] who uses the potential energy of the structural system. The application of the geometric stiffness matrix for the analysis of linear eigenvalue stability problems for beam columns is reported by Gallagher and Padlog [17]. The stability analysis for plane stress problems is considered by Turner, et al. [25], for plate problems by Hartz [26] and Kapur and Hartz [27], and for shells by Gallagher, et al. [28], [29] and Navaratna [30]. The problems of post buckling of plates is studied by Murray [31] who uses an iterative incremental procedure, and of plates and cylindrical shells by Schmit, Bogner, and Fox [32]. The importance of retaining higher order terms in the formulation of the incremental method for the analysis of certain structures was pointed out by Purdy and Przemieniecki [33]. Mallet and Marcal [34] discuss the methods of formulation of direct and incremental

procedures and arrive at various degrees of non-linearities.

In this chapter a general incremental method of analysis is presented in which the size of an increment is arbitrary. The incremental equations of equilibrium are given in the form of the expression of virtual work which renders itself to direct methods of solution of the variational problems. In order to make the presentation self-contained, a summary of the laws of thermodynamics and field equations are given in section I.2. The treatment follows the work of Truesdell and Noll [36], Green and Adkins [37], and Green and Rivlin [38]. The incremental form of the nonlinear constitutive equations for elastic materials is derived from the laws of thermodynamics. A more restrictive form of the constitutive equations for the elastic-plastic continuum is given in chapter 2. The theory is presented in Cartesian coordinates so that the understanding of the main ideas becomes easy. However, for the sake of completeness of presentation the derivations are also carried out in curvilinear coordinates in Appendix A. In section I.5 it is demonstrated that the constitutive equations for isotropic elastic-plastic materials in orthogonal curvilinear coordinates will be the same as those in Cartesian coordinates if the Cartesian tensors are replaced by the physical components of the curvilinear tensors. This invariance will be very helpful in the application of the incremental method for the solution of problems which are formulated in orthogonal curvilinear coordinates.

Choice of proper notations becomes a problem in a treatise of this form which deals with several types of stresses, strains, and coordinates. Each new variable is defined when it first appears. A collection of all the notations is appended. Both vectorial and

indicial notations are used. The summation convention holds. Latin indices range from 1 to 3, and Greek indices indicate 1 and 2.

I.2 The Field Equations and Thermodynamic Laws

Consider two configurations of a deformable body on its path of deformation from an initial state characterized by at most an isotropic state of stress to a final configuration (see Figure I.1). These are called configurations 1 and 2. The volume, boundary surface and the coordinates of the material points of the body in the initial, first and second configurations are denoted by $\overline{v},\overline{a},\overline{z}_i$, v,a,z_i, and V,A,Z_A respectively. The balance of energy in configuration 1 can be written as

$$\frac{D}{Dt}\int_{\overline{v}} \overline{\rho}_o\left(\frac{1}{2}\, v_m v_m + {}^1U\right)d\overline{v} = \int_{\overline{v}} \overline{\rho}_o\left({}^1\overline{f}_m v_m + {}^1r\right)d\overline{v} + \int_{\overline{a}} \left({}^1t_m \overline{v}_m - \overline{h}\right)d\overline{a} \qquad (I.1)$$

where $\frac{D}{Dt}$ represents the material derivative holding $\overline{z}_i$ fixed, $\overline{\rho}_o$ is the mass density in the initial state, $\underset{\sim}{v}$ is the velocity, ${}^1U$, ${}^1\underset{\sim}{\overline{f}}$, ${}^1r$ are the internal energy, body force, and rate of heat production, respectively, per unit mass, ${}^1\underset{\sim}{\overline{t}}$ is the traction in configuration 1 measured per unit of area $\overline{a}$, (see Figure I.2), and $\overline{h}$ is the rate of heat flux per unit of area $\overline{a}$.

The invariance requirement of the energy equality (I.1) under superposed uniform translational and angular velocities leads to the following equations [38]: the equations of equilibrium

$$\left({}^1s_{ij}\,\frac{\partial z_k}{\partial \overline{z}_j}\right)_{,i} + \overline{\rho}_o\ {}^1\overline{f}_k = \overline{\rho}_o\ \dot{v}_k \qquad (I.2)$$

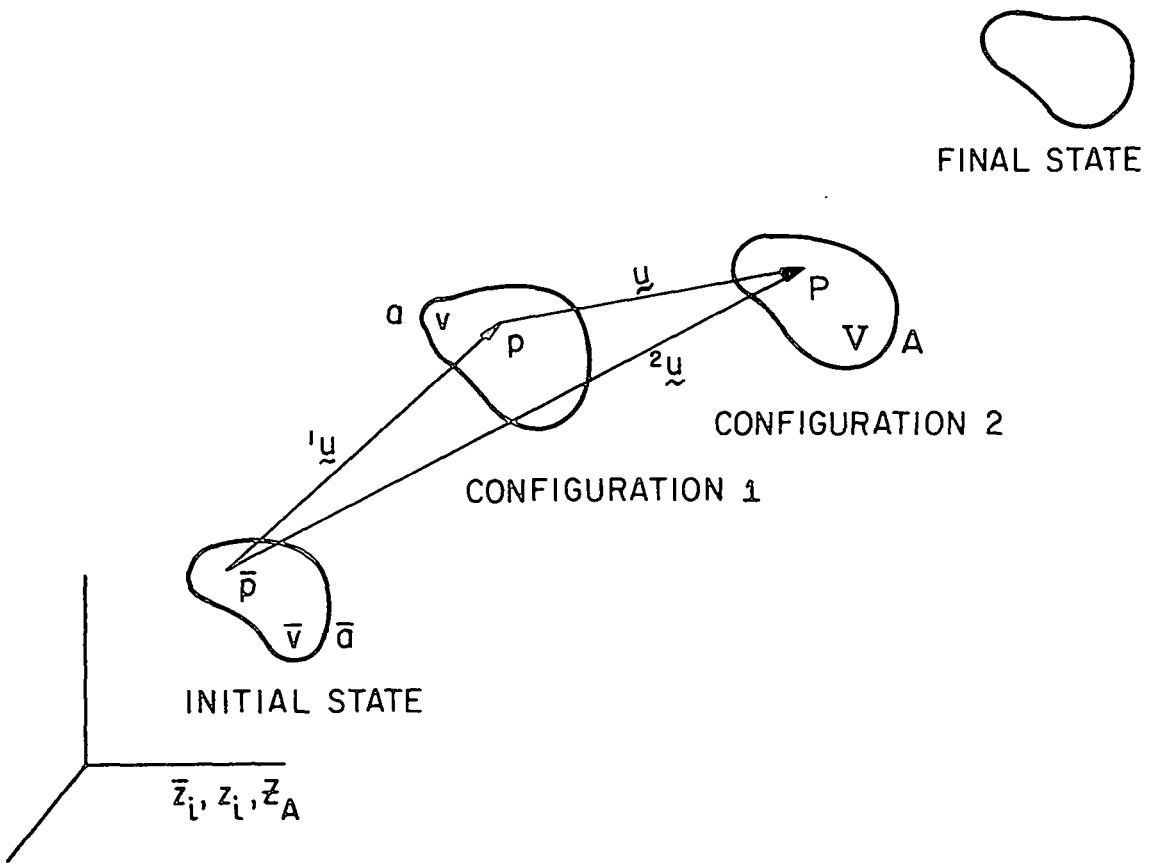
FINAL STATE
a
v
p
u
P
V
A
^2u
CONFIGURATION 2
^1u
CONFIGURATION 1
$\bar{p}$
$\bar{v}$
$\bar{a}$
INITIAL STATE
$\bar{z}_i, z_i, \bar{z}_A$

FIG. I-1

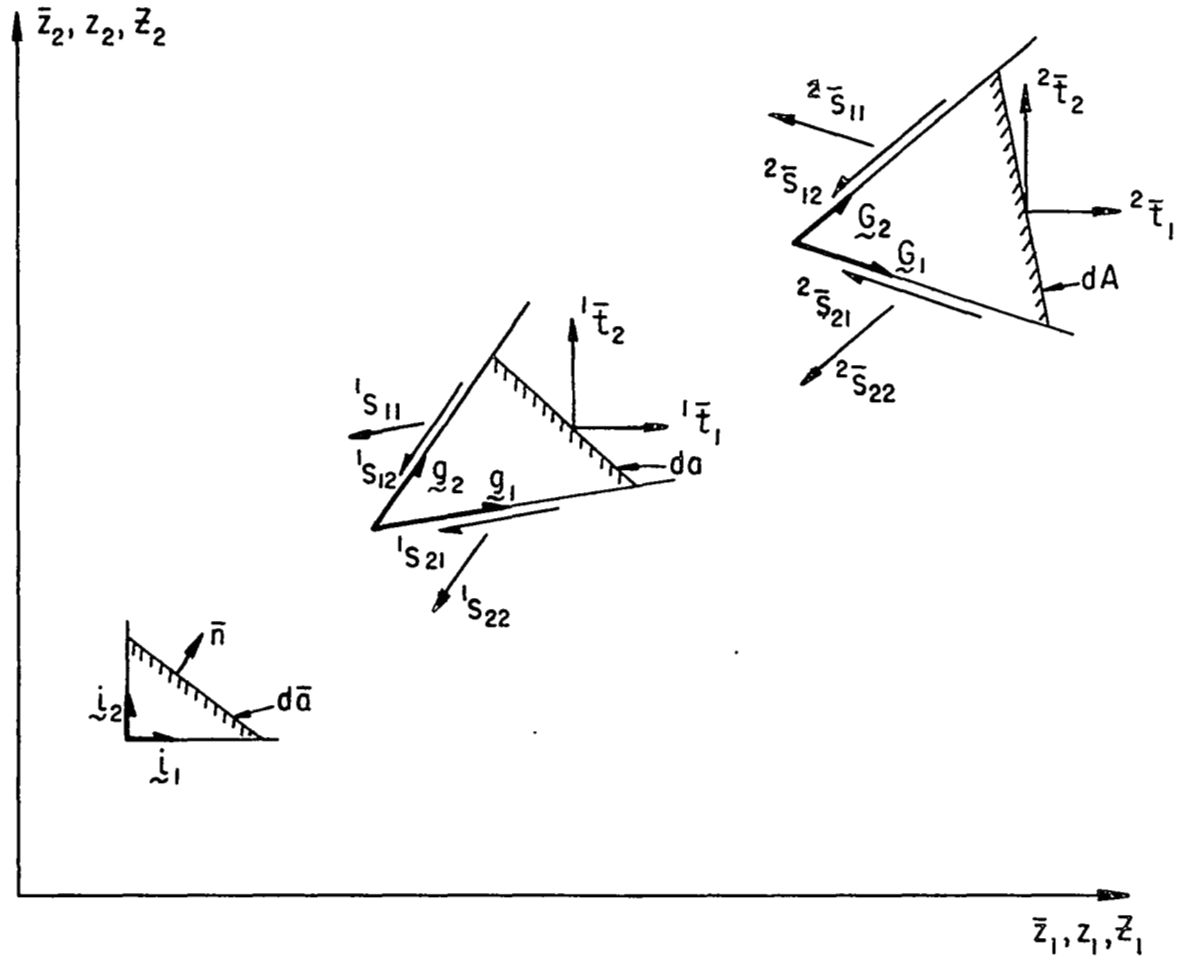
$\bar{z}_2, z_2, \bar{z}_2$
$^2\bar{s}_{11}$
$^2\bar{t}_2$
$^2\bar{s}_{12}$
$^2\bar{t}_1$
$\underset{\sim}{G}_2$
$\underset{\sim}{G}_1$
dA
$^2\bar{s}_{21}$
$^2\bar{s}_{22}$
$^1\bar{t}_2$
$^1s_{11}$
$^1\bar{t}_1$
$^1s_{12}$
$\underset{\sim}{g}_2$
$\underset{\sim}{g}_1$
da
$^1s_{21}$
$^1s_{22}$
$\bar{n}$
$\underset{\sim}{i}_2$
$d\bar{a}$
$\underset{\sim}{i}_1$
$\bar{z}_1, z_1, \bar{z}_1$

FIG. I-2

and

$$ {}^{1}s_{ij} = {}^{1}s_{ji} \quad , \tag{I.3} $$

Cauchy's equation

$$ {}^{1}\bar{t}_{k} = {}^{1}s_{ij} \frac{\partial z_k}{\partial \bar{z}_j} \bar{n}_i \tag{I.4} $$

and heat flux equation

$$ \bar{h} = \bar{q}_k \bar{n}_k \tag{I.5} $$

where ${}^{1}s_{ij}$ are the components of the Piola symmetric stress tensor, the dot over v_k denotes material derivative of v_k, $\bar{n}$ is the unit normal vector to surface $\bar{a}$ (see Figure I.2), and ${}^{1}\bar{q}_k$ is the rate of heat flux in configuration 1 across a converted coordinate surface which in the initial state is perpendicular to base vector $\underset{\sim}{i}_k$. The Piola symmetric stress tensor ${}^{1}s_{ij}$ is associated with the deformed base vectors $\underset{\sim}{g}$ (see Figure I.2). For example, ${}^{1}s_{mn}$ denotes a force acting on configuration 1 parallel to base vector $\underset{\sim}{g}_n$ and on a surface which had unit area in the initial state and which was perpendicular to base vector $\underset{\sim}{i}_m$. Therefore, this stress acts in configuration 1 but is measured per unit of area in the initial configuration. Another field equation denotes the conservation of mass which has already been assumed in (I.1). Substitution of (I.2), (I.3), (I.4) and (I.5) in (I.1) leads to the following local energy equality.

$$ \bar{\rho}_o {}^{1}r + \bar{\rho}_o {}^{1}\dot{U} + {}^{1}s_{k\ell} {}^{1}\dot{\varepsilon}_{k\ell} - {}^{1}\bar{q}_{k,k} = 0 \tag{I.6} $$

where ${}^{1}\varepsilon_{\ell k}$ is the Lagrange strain tensor in configuration 1.

The second law of thermodynamics states that

$$\frac{D}{Dt} \int_{\bar{V}} \bar{\rho}_o \, {}^1S \, d\bar{v} - \int_{\bar{V}} \bar{\rho}_o \frac{{}^1r}{\theta} \, d\bar{v} + \int_{\bar{a}} \frac{\bar{h}}{\theta} \, d\bar{a} \geq 0 \tag{I.7}$$

where ${}^1S$ is the entropy per unit mass, and θ is the temperature. Substitution of (I.5) into (I.7) results in the following local expression for the second law of thermodynamics

$$\bar{\rho}_o \, {}^1\dot{S} - \bar{\rho}_o \frac{{}^1r}{\theta} + {}^1\bar{q}_{k,k} - \frac{{}^1\bar{q}_k \theta_{,k}}{\theta} \geq 0 \tag{I.8}$$

Helmholtz free energy function ${}^1A$ is defined by

$${}^1A = {}^1U - {}^1S\theta \tag{I.9}$$

Substitution of (I.9) into (I.6) and (I.8) gives

$$\bar{\rho}_o \, {}^1r - \bar{\rho}_o({}^1\dot{A} + {}^1S\dot{\theta} + {}^1\dot{S}\theta) - {}^1\bar{q}_{k,k} + {}^1s_{k\ell} \, {}^1\dot{\varepsilon}_{k\ell} = 0 \tag{I.10}$$

and

$$-\bar{\rho}_o \, ({}^1\dot{A} + {}^1S\dot{\theta}) + {}^1s_{k\ell} \, {}^1\dot{\varepsilon}_{k\ell} - \frac{{}^1\bar{q}_k \theta_{,k}}{\theta} \geq 0 \tag{I.11}$$

I.3 The Principle of Virtual Work

A generic point $\bar{p}$ in the initial state will occupy positions p and P in configurations 1 and 2, respectively. The displacement vectors between these positions are shown in Figure I.1. The equations of equilibrium at configurations 1 and 2 can be written in the form of the expressions of virtual work in different manners depending on the choice of the reference configuration for the variables involved, and also on the vectors in terms of which the virtual displacements are expressed. For example, the variables in configuration 1 can be written with reference to the coordinates of any configuration desired; also the virtual displacements for point p can be written as $\delta(\overset{1}{\underset{\sim}{u}})$ or $\delta\underset{\sim}{u}$ and for point P can be written as $\delta\underset{\sim}{u}$ or $\delta(\overset{2}{\underset{\sim}{u}})$. Three incremental expressions of virtual work are considered. The first one in which configuration 1 is taken as the reference and $\delta\underset{\sim}{u}$ as the virtual displacement is derived in this chapter and used in the subsequent developments. The second expression of virtual work uses the initial configuration as the reference and $\delta\overset{1}{\underset{\sim}{u}}$, $\delta\overset{2}{\underset{\sim}{u}}$ as the virtual displacements. For hyperelastic materials this formulation can be recast in the form of the variation of the incremental internal energy. The third expression of virtual work uses the initial configuration and $\delta\underset{\sim}{u}$. These last two expressions are derived in Appendix C.

The expression of virtual work W_v at configuration 2 is

$$W_v = \int_A \underset{\sim}{T} \cdot \delta \underset{\sim}{u} \, dA + \int_V \rho \, F \cdot \delta u \, dV \qquad (I.12)$$

where $\underset{\sim}{T}$ is the surface traction per unit of area A, ρ is the mass density in configuration 2, and $\underset{\sim}{F}$ is the body force per unit of mass.

Equation (I.12) can be written in terms of the coordinates of configuration 1 by choosing proper definitions for traction and body force. One such traction is defined by

$$^2\underset{\sim}{t} = \underset{\sim}{T} \frac{dA}{da} \qquad (I.13)$$

where $^2\underset{\sim}{t}$ is the traction in configuration 2 and measured per unit of area in configuration 1, and da is the element of surface area in configuration 1.

The stresses associated with traction $^2\underset{\sim}{t}$ can be defined in various ways, one of which is the symmetric Piola stress tensor. Consider the neighborhood of a generic point p of the deformable body in configuration 1 and the same neighborhood in configuration 2. For simplicity of presentation a two dimensional picture of such neighborhood is shown in Figure I.3, although the theoretical development is carried out for a three dimensional body. The Cauchy stresses in this neighborhood in configuration 1 are τ_{ij} which are associated with the unit base vectors $\underset{\sim}{i}_k$. The Piola symmetric stresses of our interest which act in the same neighborhood in configuration 2 are called $^2s_{ij}$. These stresses are associated with the deformed base vectors $\underset{\sim}{G}_i$. For example

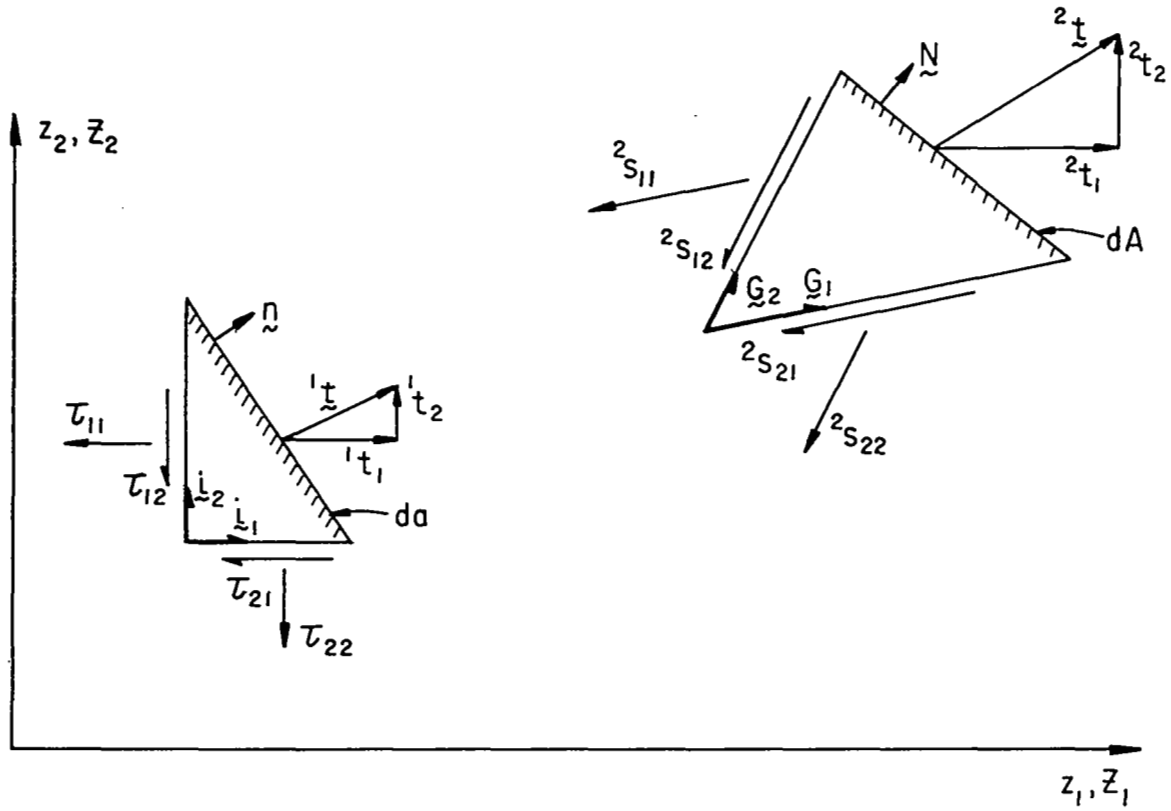
$z_2, \bar{z}_2$
$\underset{\sim}{n}$
$^1\underset{\sim}{t}$
$^1t_2$
$^1t_1$
τ_{11}
τ_{12}
$\underset{\sim}{i}_2$
$\underset{\sim}{i}_1$
da
τ_{21}
τ_{22}
$\underset{\sim}{N}$
$^2\underset{\sim}{t}$
$^2t_2$
$^2t_1$
$^2s_{11}$
$^2s_{12}$
dA
$\underset{\sim}{G}_2$
$\underset{\sim}{G}_1$
$^2s_{21}$
$^2s_{22}$
$z_1, \bar{z}_1$

FIG. I·3

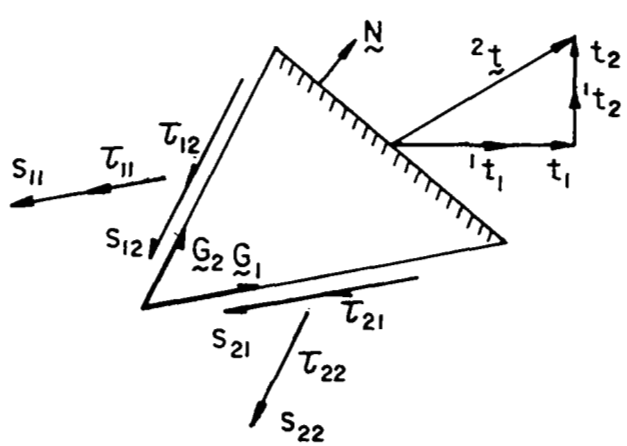
$\underset{\sim}{N}$
$^2\underset{\sim}{t}$
t_2
$^1t_2$
$^1t_1$
t_1
τ_{12}
s_{11}
τ_{11}
s_{12}
$\underset{\sim}{G}_2$ $\underset{\sim}{G}_1$
τ_{21}
s_{21}
τ_{22}
s_{22}

FIG. I·4

${}^2s_{mn}$ denotes a force acting in configuration 2 on a surface which had a unit area in configuration 1 and was perpendicular to base vector i_m, and which is parallel to the base vector $\underset{\sim}{G}_n$. Therefore, these stresses are in configuration 2 but are measured per unit area in configuration 1. The relationship between ${}^2\underset{\sim}{t}$ and the stresses ${}^2s_{ij}$ is of the same form as equation (I.4).

$$ {}^2t_k = {}^2s_{ij} \frac{\partial Z_k}{\partial z_j} n_i \qquad \text{(I.14)} $$

where $\underset{\sim}{n}$ is the unit normal vector to surface $\underset{\sim}{a}$.

The magnitude of the components of stress tensor ${}^2s_{ij}$ can be arbitrarily divided into two parts (see Figure I.4).

$$ {}^2s_{ij} = \tau_{ij} + s_{ij} \qquad \text{(I.15)} $$

in which τ_{ij} have the same magnitude as the corresponding Cauchy stresses in configuration 1 but are associated with the base vectors $\underset{\sim}{G}$, and s_{ij} are symmetric stress components which have magnitudes equal to the difference between the stresses ${}^2s_{ij}$ and τ_{ij}. Substitution of equations (I.15), (I.14), and (I.13) into the first integral on the right hand side of equation (I.12) results in

$$ \int_A \underset{\sim}{T} \cdot \delta\underset{\sim}{u} \, dA = \int_a (\tau_{ij} + s_{ij}) \frac{\delta Z_k}{\delta z_j} n_i \, \delta u_k \, da \qquad \text{(I.16)} $$

This surface integral can be replaced by an equivalent volume integral by means of Gauss transformation. In view of the symmetry of

s_{ij} and τ_{ij}, the final result is

$$\int_A \underset{\sim}{T} \cdot \delta u \, dA = \int_v ({}^2s_{ij} \, Z_{k,j}),_i \delta u_k dv + \int_v (\tau_{ij} + s_{ij}) \delta \varepsilon_{ji} dv \tag{I.17}$$

in which ε_{ij} is the Lagrangian strain from configuration 1 to 2.

$$\varepsilon_{ij} = \frac{1}{2} (u_{i,j} + u_{j,i} + u_{k,i} \, u_{k,j}) \tag{I.18}$$

Considering the law of conservation of mass, the second integral on the right hand side of equation (I.12) can be written as

$$\int_v \rho F \cdot \delta u \, dv = \int_v \rho_o \cdot {}^2f_k \, \delta u_k \, dv \tag{I.19}$$

where ${}^2f_k$ denotes the body force per unit mass acting in configuration 2, but measured in terms of the coordinates in configuration 1.

Substitution of (I.17) and (I.19) into (I.12) yields

$$W_v = \int_v (\tau_{ij} + s_{ij}) \delta \varepsilon_{ij} \, dv + \int_v [({}^2s_{ij} \, Z_{k,j}),_i + \rho_o \, {}^2f_k] \delta u_k \, dv \tag{I.20}$$

The integrandin the second integral on the right hand side is the expression for the equilibrium of the body and is equal to zero. Therefore

$$W_v = \int_v (\tau_{ij} + s_{ij}) \delta \varepsilon_{ij} \, dv$$

or

$$\int_a {}^2t_i \, \delta u_i \, da + \int_v \rho_o \, {}^2f_i \, \delta u_i \, dv = \int_v (\tau_{ij} + s_{ij}) \, \delta\varepsilon_{ij} \, dv \tag{I.21}$$

The expression for virtual work at configuration 1 can be written as

$$\int_a {}^1t_i \, \delta u_i \, da + \int_v \rho_o \, {}^1f_i \, \delta u_i \, dv = \int_v \tau_{ij} \, \delta e_{ij} \, dv \tag{I.22}$$

in which ${}^1t_i$ is the traction acting per unit of area of a, ${}^1f_1$ is the body force acting per unit of mass in configuration 1, and e_{ij} is the linear part of Lagrangian strain between configurations 1 and 2.

$$e_{ij} = \frac{1}{2}(u_{i,j} + u_{j,i}) \tag{I.23}$$

Subtraction of (I.22) from (I.21) gives

$$\int_a ({}^2t_i - {}^1t_i)\delta u_i da + \int_v \rho_o ({}^2f_i - {}^1f_i)\delta u_i dv = \int_v (\tau_{ij}\delta\eta_{ij} + s_{ij}\delta\varepsilon_{ij})dv \tag{I.24}$$

where

$$\eta_{ij} = \varepsilon_{ij} - e_{ij} = \frac{1}{2} u_{k,i} \, u_{k,j} \tag{I.25}$$

is the nonlinear part of the increment of Lagrangian strain between configurations 1 and 2.

Let

and

$$\begin{aligned} t_i &= {}^2t_i - {}^1t_i \, , \\ f_i &= {}^2f_i - {}^1f_i \end{aligned} \tag{I.26}$$

which denote the increments of traction and body force between configurations 1 and 2 both measured in terms of the coordinates of configuration 1. Substitution of these in the relation (I.24) yields

$$\int_a t_i \, \delta u_i \, da + \int_v \rho_o \, f_i \, \delta u_i \, d_v = \int_v (\tau_{ij} \, \delta \eta_{ij} + s_{ij} \delta \varepsilon_{ij}) dv \qquad (I.27)$$

This is the incremental expression of virtual work which in effect is a statement of the equilibrium equations of the body at configuration 2 in terms of the variables which are expressed in the coordinates of configuration 1. The proof that (I.27) leads to the incremental equilibrium equations and the corresponding boundary conditions is given in Appendix A where the principle of virtual work is derived in curvilinear coordinates.

Equation (I.27) is an expression for equilibrium of the deformable body. It is not restricted to any particular constitutive law which the material of the continuum may obey.

I.4 Incremental Constitutive Equations of Elasticity

The constitutive equations of the continuum are written based on mathematical approximations of physical observations subject to the laws of thermodynamics, and some invariance requirements like the principle of material frame indifference [37], [40]. For an elastic continuum it can be shown that

$$ {}^{1}s_{ij} = \bar{\rho}_o \frac{\partial {}^{1}A}{\partial {}^{1}\varepsilon_{ij}} \quad , \tag{I.28} $$

$$ {}^{1}S = - \frac{\partial {}^{1}A}{\partial \theta} \tag{I.29} $$

and

$$ \bar{q}_k \theta_{,k} \geq 0 \tag{I.30} $$

where

$$ \begin{aligned} {}^{1}A &= {}^{1}A({}^{1}\varepsilon_{ij}, \theta) \\ {}^{1}S &= {}^{1}S({}^{1}\varepsilon_{ij}, \theta) \\ {}^{1}s_{ij} &= {}^{1}s_{ij}({}^{1}\varepsilon_{k\ell}, \theta) \\ \bar{q}_i &= \bar{q}_i({}^{1}\varepsilon_{ij}, \theta, \theta_{,k}) \end{aligned} \tag{I.31} $$

For the deformable body in Figure I.1, the laws of thermodynamics for a variable configuration 2 can be written as

$$\bar{\rho}_o {}^2r - \bar{\rho}_o({}^2\dot{A} + {}^2\dot{S}\theta) - {}^2\bar{q}_{k,k} + {}^2\bar{s}_{k\ell}\, {}^2\dot{\varepsilon}_{k\ell} = 0 \quad , \tag{I.32}$$

and

$$- \bar{\rho}_o({}^2\dot{A} + {}^2S\dot{\theta}) + {}^2\bar{s}_{k\ell}\, {}^2\dot{\varepsilon}_{k\ell} - \frac{{}^2\bar{q}_k \theta,_k}{\theta} \geq 0 \tag{I.33}$$

in which

$$\begin{aligned}
{}^2A &= {}^2A({}^1\varepsilon_{ij}, \xi_{ij}, \theta) \ , \\
{}^2S &= {}^2S({}^1\varepsilon_{ij}, \xi_{ij}, \theta) \ , \\
{}^2\bar{s}_{ij} &= {}^2\bar{s}_{ij}({}^1\varepsilon_{ij}, \xi_{ij}, \theta) \ , \\
{}^2\bar{q}_i &= {}^2\bar{q}_i({}^1\varepsilon_{k\ell}, \xi_{k\ell}, \theta, \theta,_k) \ , \\
{}^2r &= {}^2r({}^1\varepsilon_{k\ell}, \xi_{k\ell}, \theta, \theta,_k) \ ,
\end{aligned}$$

${}^2\bar{s}_{ij}$ is the Piola symmetric stress tensor in configuration 2 measured per unit of area $\bar{a}$ (see Figure I.2), and ξ_{ij} is defined in Appendix B as

$$\xi_{ij} = \frac{\partial z_k}{\partial \bar{z}_i} \frac{\partial z_\ell}{\partial \bar{z}_j} \varepsilon_{k\ell} \tag{I.35}$$

It is possible to divide the functions in (I.34) into two parts

$$\begin{aligned}
{}^2A &= {}^1A({}^1\varepsilon_{ij}, \theta) + A({}^1\varepsilon_{ij}, \xi_{ij}, \theta) \\
{}^2S &= {}^1S({}^1\varepsilon_{ij}, \theta) + S({}^1\varepsilon_{ij}, \xi_{ij}, \theta) \\
{}^2\bar{s}_{ij} &= {}^1s_{ij}({}^1\varepsilon_{ij}, \theta) + \bar{s}_{ij}({}^1\varepsilon_{ij}, \xi_{ij}, \theta) \\
{}^2\bar{q}_i &= {}^1\bar{q}_i({}^1\varepsilon_{k\ell}, \theta, \theta,_k) + \bar{q}({}^1\varepsilon_{k\ell}, \xi_{k\ell}, \theta, \theta,_k) \\
{}^2r &= {}^1r({}^1\varepsilon_{k\ell}, \theta, \theta,_k) + r({}^1\varepsilon_{k\ell}, \xi_{k\ell}, \theta, \theta,_k)
\end{aligned} \tag{I.36}$$

Substitution of (I.36) into (I.33) results in

$$({}^{1}s_{k\ell} - \bar{\rho}_o \frac{\partial {}^{1}A}{\partial {}^{1}\varepsilon_{k\ell}}){}^{1}\dot{\varepsilon}_{k\ell} - \bar{\rho}_o({}^{1}S + \frac{\partial {}^{1}A}{\partial \theta})\dot{\theta} - \frac{{}^{2}\bar{q}_k \theta_{,k}}{\theta} + ({}^{2}\bar{s}_{k\ell} - \bar{\rho}_o \frac{\partial A}{\partial \xi_{k\ell}})\dot{\xi}_{k\ell} +$$

$$(s_{k\ell} - \bar{\rho}_o \frac{\partial A}{\partial {}^{1}\varepsilon_{k\ell}}){}^{1}\dot{\varepsilon}_{k\ell} - \bar{\rho}_o(S + \frac{\partial A}{\partial \theta})\dot{\theta} \geq 0 , \qquad \text{(I.37)}$$

which in view of (I.28) and (I.29) becomes

$$({}^{2}\bar{s}_{k\ell} - \bar{\rho}_o \frac{\partial A}{\partial \xi_{k\ell}})\dot{\xi}_{k\ell} + (s_{k\ell} - \bar{\rho}_o \frac{\partial A}{\partial {}^{1}\varepsilon_{k\ell}}){}^{1}\dot{\varepsilon}_{k\ell} - \bar{\rho}_o(S + \frac{\partial A}{\partial \theta})\dot{\theta} - \frac{{}^{2}\bar{q}_k \theta_{,k}}{\theta} \geq 0 \qquad \text{(I.38)}$$

In the same manner the energy equality (I.32) reduces to

$$\bar{\rho}_o r + \rho_o(\dot{A} + \dot{\theta}S + \theta\dot{S}) - \bar{q}_{k,k} - {}^{2}\bar{s}_{k\ell}\,\dot{\xi}_{k\ell} - s_{k\ell}\,{}^{1}\dot{\varepsilon}_{k\ell} = 0 \qquad \text{(I.39)}$$

Since ${}^{1}\dot{\varepsilon}_{k\ell}$, $\dot{\xi}_{k\ell}$, and $\dot{\theta}$ can be chosen arbitrarily, following a similar argument presented by Coleman and Noll [40] it can be concluded that

$$\bar{s}_{k\ell} = \bar{\rho}_o \frac{\partial A}{\partial {}^{1}\varepsilon_{k\ell}} , \qquad \text{(I.40)}$$

$${}^{2}\bar{s}_{k\ell} = \bar{\rho}_o \frac{\partial A}{\partial \xi_{k\ell}} , \qquad \text{(I.41)}$$

$$S = - \frac{\partial A}{\partial \theta} , \qquad \text{(I.42)}$$

and

$${}^{2}\bar{q}_k\, \theta_{,k} \geq 0 . \qquad \text{(I.43)}$$

These are the incremental constitutive equations for an elastic continuum.

All the discussion in this section has dealt with stresses ${}^{1}\underline{s}_{ij}$, ${}^{2}\underline{s}_{ij}$, and $\bar{s}_{ij}$ which are measured per unit of area $\bar{a}$ in the initial state. In order to be able to use the constitutive equations (I.40), and (I.41) in the expression of virtual work (I.27), they must be expressed in terms of stresses ${}^{2}s_{ij}$, and s_{ij} which are measured per unit of area a in configuration 1. The following transformations hold between the Cauchy stress tensor in configuration 2 and the Piola stresses ${}^{2}s_{ij}$ and ${}^{2}s_{ij}$ [29], [31].

$$ {}^{2}s_{ij} = \frac{\rho_o}{\rho} \frac{\partial z_i}{\partial Z_M} \frac{\partial z_j}{\partial Z_N} \tau_{MN} , \tag{I.44} $$

$$ \tau_{MN} = \frac{\rho}{\rho_o} \frac{\partial Z_M}{\partial \bar{z}_m} \frac{\partial Z_N}{\partial \bar{z}_n} {}^{2}\bar{s}_{mn} . \tag{I.45} $$

Substitution of (I.45) into (I.44) gives

$$ {}^{2}s_{ij} = \frac{\rho_o}{\rho_o} z_{i,m} z_{j,n} {}^{2}\bar{s}_{mn} , \tag{I.46} $$

and also substitution of (I.15), and $(I.36)_3$ into (I.46) results in

$$ s_{ij} = \frac{\rho_o}{\rho_o} z_{i,m} z_{j,n} \bar{s}_{mn} \tag{I.47} $$

The incremental constitutive equations in terms of ${}^{2}s_{ij}$ and s_{ij} can be obtained by substituting (I.46), and (I.47) into (I.40) and (I.41).

$$ {}^{2}s_{ij} = \rho_o z_{i,m} z_{j,n} \frac{\partial A}{\partial \xi_{mn}} \tag{I.48} $$

$$ s_{ij} = \rho_o z_{i,m} z_{j,n} \frac{\partial A}{\partial {}^{1}\varepsilon_{mn}} \tag{I.49} $$

I.5 Constitutive Equations in Curvilinear Coordinates

In some problems it is necessary to use curvilinear coordinates. Compared with the constitutive equations in Cartesian coordinates, the constitutive equations in curvilinear coordinates are difficult to write, to interpret physically, and to use in the solution of practical problems. It has been shown by Carroll [41],[42] that for isotropic and transversely isotropic simple solids the constitutive equations in terms of Cauchy stress in Cartesian coordinates remain invariant in orthogonal curvilinear coordinates if the Cartesian tensors are replaced by the physical components of the curvilinear tensors. This invariance is demonstrated in this section for elastic materials when the constitutive equations are expressed in terms of Piola symmetric stress tensor. The form invariance of Piola symmetric stress tensor simplifies the proof. In Chapter II it is proved that the invariance of constitutive equations also holds for a special theory of plasticity.

If the curvilinear coordinate system in the initial state $\bar{x}^i$ is orthogonal then the transformation between the local Cartesian coordinates (associated with unit base vector) on $\bar{x}^i$ and the global Cartesian coordinate system $\bar{z}_i$ can be performed by the orthogonal transformation matrix R_{ij} having the property

$$R_{im} R_{mj} = \delta_{ij} \tag{I.50}$$

where δ_{ij} is the Kronecker delta.

The physical components of the Piola symmetric stress tensor in orthogonal curvilinear coordinates are defined in Appendix D. They are given by

$${}_1s^*_{ij} = (\bar{g}_{ii}\, \bar{g}_{jj})^{\frac{1}{2}}\, {}_1s^{ij} \qquad \text{(no sum)} . \tag{I.51}$$

The physical components of the Lagrangian strain tensor are defined as

$$ {}^{1}\varepsilon^{*}_{ij} = (\bar{g}_{ii}\ \bar{g}_{jj})^{\frac{1}{2}}\ {}^{1}\varepsilon_{ij} \qquad \text{(no sum)} \ . \tag{I.52} $$

Since these physical components are associated with unit base vectors in the curvilinear coordinates in the initial configuration, they transform to their global Cartesian counterparts by

$$ {}^{1}s^{*}_{ij} = R_{im}R_{jn}\ {}^{1}s_{mn} \tag{I.53} $$

$$ {}^{1}\varepsilon^{*}_{ij} = R_{im}R_{jn}\ {}^{1}\varepsilon_{mn} \tag{I.54} $$

where ${}^{1}s_{mn}$ and ${}^{1}\varepsilon_{mn}$ are the stress and strain tensors in the global Cartesian coordinate system.

The Cartesian form of the constitutive equations is

$$ {}^{1}s_{ij} = {}^{1}s({}^{1}\varepsilon_{k\ell}) \tag{I.55} $$

If the material is isotropic then (I.55) must remain invariant under any orthogonal transformation. In particular for the orthogonal transformation R_{ij} then

$$ R_{im}\ R_{jn}\ {}^{1}s_{ij} = {}^{1}s(R_{ik}\ R_{j\ell}\ {}^{1}\varepsilon_{k\ell}) \ . \tag{I.56} $$

Substitution of (I.53) and (I.54) into (I.56) results in

$$ {}^{1}s^{*}_{mn} = {}^{1}s({}^{1}\varepsilon^{*}_{ij}) \tag{I.57} $$

Comparison of (I.57) and (I.55) indicates that the form of the constitutive equation has remained invariant. This result is very helpful in dealing with the shell problem.

CHAPTER II: LARGE DISPLACEMENTS, SMALL DEFORMATIONS

II.1 Isotropic Elastic Materials

The constitutive equations

$$\bar{s}_{k\ell} = \bar{\rho}_o \frac{\partial A({}^1\varepsilon_{k\ell}, \xi_{k\ell})}{\partial {}^1\varepsilon_{k\ell}} \tag{I.40}$$

and

$${}^2\bar{s}_{k\ell} = \bar{\rho}_o \frac{\partial A({}^1\varepsilon_{k\ell}, \xi_{k\ell})}{\partial \xi_{k\ell}} \tag{I.41}$$

are quite general. If the free energy function A is known in terms of ${}^1\varepsilon_{k\ell}$ and $\xi_{k\ell}$ then $\bar{s}_{k\ell}$ and ${}^2\bar{s}_{k\ell}$ can be determined. Assuming that A is an analytic function it can be expanded as a power series of ${}^1\varepsilon_{k\ell}$ and $\xi_{k\ell}$. In particular for isotropic materials A can be expressed as a function of the invariants of ${}^1\varepsilon_{k\ell}$ and $\xi_{k\ell}$. For certain problems a finite number of terms in the power series expansion is enough to approximate A and hence the constitutive equations accurately. In the special case where deformations are infinitesimal but displacements and rotations are not, the retention of the terms in the power series of A up to the second power of ${}^1\varepsilon_{k\ell}$ and $\xi_{k\ell}$ is enough. Then equations (I.40) and (I.41) will lead to linear relations between the stresses $\bar{s}_{k\ell}$, ${}^2\bar{s}_{k\ell}$ and the strains ${}^1\varepsilon_{k\ell}$ and $\xi_{k\ell}$.

For isotropic elastic materials ${}^2A$ can be written as

$$\rho_o {}^2A = \frac{\lambda}{2} ({}^2\varepsilon_{ii})^2 + \mu ({}^2\varepsilon_{ij})({}^2\varepsilon_{ij}) \tag{II.1}$$

where λ and μ are the Lame's constants. In (II.1) the strain ${}^2\varepsilon_{ij}$ is limited to infinitesimal deformations

$$ {}^2\varepsilon_{ij} = {}^2e_{ij} + \frac{1}{2}({}^2e_{ik}\,{}^2\omega_{kj} + {}^2e_{jk}\,{}^2\omega_{ki} + {}^2\omega_{ik}\omega_{kj}) \qquad \text{(II.2)} $$

where

$$ {}^2e_{ij} = \frac{1}{2}\,({}^2\bar{u}_{i,j} + {}^2\bar{u}_{j,i}) $$

$$ {}^2\omega_{ij} = \frac{1}{2}\,({}^2\bar{u}_{i,j} - {}^2\bar{u}_{j,i}) $$

The displacements ${}^2\bar{u}_i$ being in the direction of coordinate systems of the initial configuration (see Figure I.1). It is shown in appendix B that

$$ {}^2\varepsilon_{ij} = {}^1\varepsilon_{ij} + \xi_{ij} \ , \qquad \text{(II.3)} $$

where

$$ \xi_{ij} = z_{m,i}z_{n,j}\,\varepsilon_{mn} \ . \qquad \text{(I.35)} $$

Substitution of (II.3) and (I.35) into (II.1) results in

$$ {}^2A({}^2\varepsilon_{ij}) = {}^1A({}^1\varepsilon_{ij}) + A({}^1\varepsilon_{ij},\xi_{ij}) \qquad \text{(II.4)} $$

where

$$ \rho_o{}^1A = \frac{\lambda}{2}\,({}^1\varepsilon_{ii})^2 + \mu\,({}^1\varepsilon_{ij})({}^1\varepsilon_{ij}) \ , \qquad \text{(II.5)} $$

and

$$ \rho_o A = \frac{\lambda}{2}\,\xi_{ii}^2 + \mu\,\xi_{ij}\xi_{ij} + 2(\frac{\lambda}{2}\,{}^1\varepsilon_{ii}\xi_{jj} + \mu\,{}^1\varepsilon_{ij}\xi_{ij}) \ . \qquad \text{(II.6)} $$

Equations (1.40) and (1.41) become

$$ \bar{s}_{k\ell} = \lambda\delta_{k\ell}\ \xi_{ii} + 2\mu\,\xi_{k\ell} \ , \qquad \text{(II.7)} $$

$$^{2}\bar{s}_{k\ell} = \lambda\delta_{k\ell}\,(^{2}\varepsilon_{ii}) + 2\mu\,(^{2}\varepsilon_{k\ell}) \tag{II.8}$$

and the constitutive equations (I.48) and (I.49) become

$$^{2}s_{ij} = \frac{\rho_o}{\bar{\rho}_o}\, z_{i,k}\, z_{j,\ell}\,[\lambda\delta_{k\ell}\,(^{2}\varepsilon_{ii}) + 2\mu\,(^{2}\varepsilon_{k\ell})] \tag{II.9}$$

and

$$s_{ij} = \frac{\rho_o}{\bar{\rho}_o}\, z_{i,k}\, z_{j,\ell}\,[\lambda\delta_{k\ell}\,\xi_{ii} + 2\mu\,\xi_{k\ell}] \tag{II.10}$$

II.2 Remarks on Some Recent Developments in the Theory of Plasticity

The study of plastic deformations of materials has been under consideration for almost a century. However, most of the investigations have been limited to infinitesimal deformations and even then the diversity of opinions and observations has led to various special theories of plasticity. Detailed account of these is given in Hill's book [59] and the review papers by Naghdi [43] and Koiter [44]. Only very recently the construction of a large deformation theory of plasticity, based on the principles of thermodynamics and the invariance requirements in continuum mechanics was undertaken by some investigators. A brief review of some of the recent developments in the theory of inviscid plasticity is given in this section and some remarks are made to show the relationship among them.

Since many assumptions existed in the theory of plasticity, it was desirable to introduce concepts from which several of the assumptions could be derived consistently. One such hypothesis, now called Drucker's postulate, was presented by Drucker [45]. It states that the work done by an external agency on an elasto-plastic material going through a closed cycle of stress is non negative. That is,

$$W_D \geq 0 \ . \tag{II.11}$$

The Mises-Prager plastic potential stress-strain relations and the convexity of loading surface are derived from this postulate. Later, Il'iushin, who was motivated by the observation that in general Drucker's postulate does not assert the irreversibility of plastic deformations, introduced another postulate [46] which states that the

work done by an external agency on an elasto-plastic material going through a closed cycle of strain is positive. In particular

$$W_I > W_D \geq 0 \ . \qquad \text{(II.12)}$$

This hypothesis leads to normality rule, however, it implies the sufficiency rather than the necessity of convexity of the yield surface.

The use of the laws of thermodynamics in the construction of the theory of plasticity is a more logical approach than the other methods which use the conclusions based on a limited class of physical observations. The investigations in this area prior to 1960 are very few and are mainly on infinitesimal theory of plasticity [43]. Sedov recognized three configurations in the process of elasto-plastic deformations of the continuum [47] (see Figure II.1): an initially free of stress state, a current configuration with complete elasto-plastic deformations, and an intermediate configuration which is obtained when the stresses in the body at current configuration are released. Thus the total deformation is composed of an elastic part which is between configurations (c) and (b) and a plastic part between (a) and (b). In general the intermediate state is not Euclidean. Sedov develops a theory of plasticity based on this kinematical model and some thermodynamical considerations. Drucker's postulate is used in a thermodynamical context and the associated flow rule is derived. Backman also introduced the concept of the three configurations [48]. However, he defines the elastic and plastic components of strains directly in terms of the displacement gradients. Due to the non-Euclidean character of the

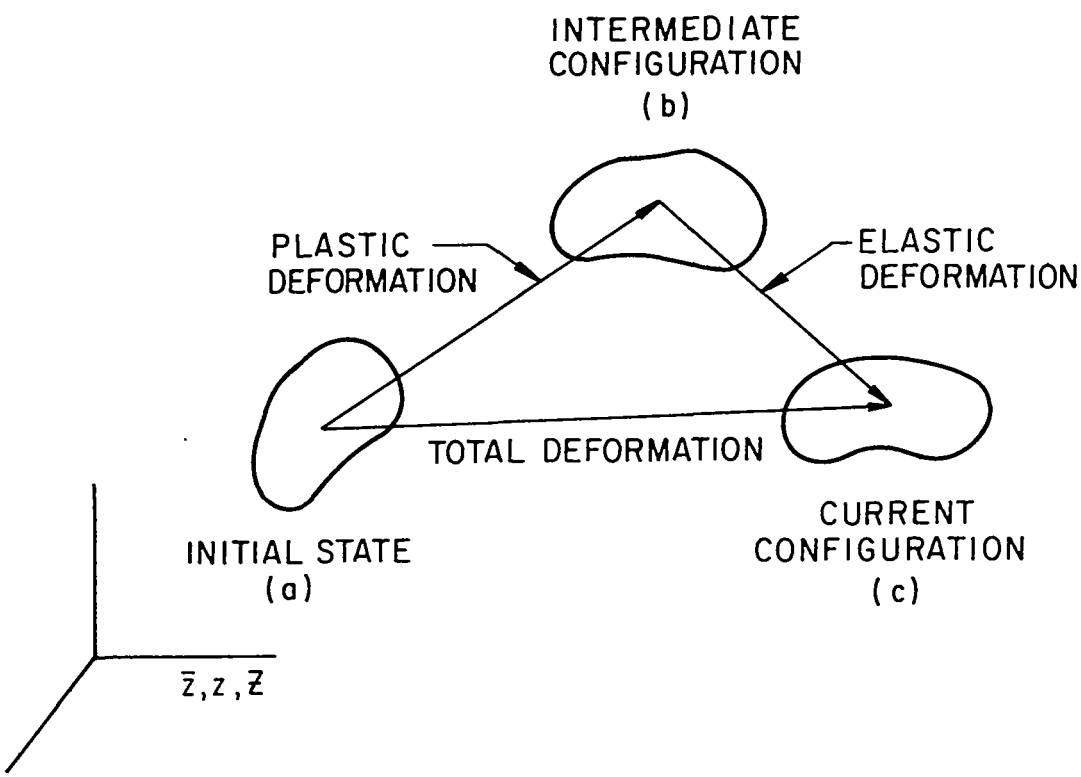
INTERMEDIATE
CONFIGURATION
(b)
PLASTIC
DEFORMATION
ELASTIC
DEFORMATION
TOTAL DEFORMATION
INITIAL STATE
(a)
CURRENT
CONFIGURATION
(c)
$\bar{z}, z, \bar{\bar{z}}$

FIG. II - 1

intermediate configuration the definition of elastic and plastic components of strain in terms of the kinematics of deformation is not in general correct. Lee, and Liu [49] recognize the non-Euclidean character of the intermediate configuration and define the kinematics of deformation by

$$[F] = [F^e][F^P] \tag{II.13}$$

where

$$[F] = \frac{\partial Z_A}{\partial \bar{z}_j} ; \tag{II.14}$$

and $[F^e]$, and $[F^P]$ are linear transformations between configurations (b) and (c) and (a) and (b) respectively (see Figure II.1). These transformations are not in general the displacement gradients between the corresponding configurations. Lee and Liu develop a particular theory of plasticity for the application to a one-dimensional wave propagation problem.

Recently Green and Naghdi [50], [51] developed a general nonlinear theory of plasticity which utilizes the thermodynamical laws and the invariance requirements in the theory of continuum mechanics. For the kinematics of deformation it is assumed that Lagrangian strain tensor can be divided into two parts as

$$\varepsilon_{ij} = \varepsilon^e_{ij} + \varepsilon^P_{ij} \tag{II.15}$$

where ε^e_{ij} , and ε^P_{ij} are called the elastic and plastic components of strain respectively and they have the same invariance properties as ε_{ij} . No kinematical interpretation is given for ε^e_{ij} and ε^P_{ij} , and

they are found from the constitutive equations only. It can be shown that the kinematic idea in [47], [49], and [50] are equivalent. The Lagrangian strain between configurations (a) and (c) can be written as follows in matrix notation

$$2[\varepsilon] = [F]^T[F] - [I] \tag{II.16}$$

where $[I]$ is the identity matrix. Substitution of (II.13) into (II.16) gives

$$2[\varepsilon] = [F^P]^T[F^e]^T[F^e][F^P] - [I] \ . \tag{II.17}$$

Subtraction and addition of the product $[F^P]^T[F^P]$ from (II.17) and rearrangement of the terms on the right hand side results in

$$2[\varepsilon] = ([F^P]^T[F^P] - [I]) + [F^P]^T([F^e]^T[F^e] - [I])[F^P] \ . \tag{II.18}$$

The first and second terms on the right hand side of (II.18) can be defined as plastic and elastic parts of strain. Thus

$$[\varepsilon] = [\varepsilon^P] + [\varepsilon^e] \tag{II.19}$$

which is the same as (II.15).

It is shown by Green and Naghdi [50] that the second law of thermodynamics puts a restriction on the plastic deformation. This restriction is more general than Drucker's postulate. In particular it is shown that for the infinitesimal uniaxial tension test the plastic volume change is not zero unless Drucker's postulate is adopted [52]. Thus they conclude that Drucker's postulate is not general enough but is a good assumption for some materials like metals. In the

same paper [52] they specialize the general non-linear theory and obtain a bilinear stress-strain representation for a uniaxial tension test.* The theory of plasticity in [50] has been extended for the elastic-plastic multipolar continua [53], and also to Cosserat surface [54].

Following Coleman and Noll's approach [40], Dillon [55] has arrived from the second law of thermodynamics at the result that the loading and unloading stress-strain relations are different for materials in which the dependent thermodynamical variables are functions of deviators of stress and strain. Thus, he rationally arrives at a feature essential in plasticity. Another approach in the study of the theory of plasticity was followed by Pipkin and Rivlin [56] who use a functional theory for the rate independent materials and essentially dynamical concepts. They use Il'iushin's plasticity postulate.

---

* It seems that the assumed form of the hardening parameter in [50] leads at most to a bilinear stress-strain characteristic in uniaxial tension. The hardening parameter must be given a more general form in order to obtain a curvilinear one-dimensional stress-strain representation.

II.3 A Special Form of the Theory of Plasticity

The general theory of plasticity developed by Green and Naghdi [50] can be specialized for application to specific problems. For any material it is possible to introduce further constitutive restrictions and hence reduce the general theory to a more tractable form. For example, in the case of metals Drucker's postulate and von Mises yield condition are good constitutive assumptions which simplify the general theory appreciably.

In this section after a short review of the general equations, the elastic-plastic constitutive equations for homogeneous and initially isotropic materials are studied. Drucker's postulate and von Mises yield condition are assumed and specific forms of the hardening law are considered. The treatment will be limited to isothermal processes.

Consider a deformable body on its path of deformation from an initial state to a final configuration (see Figure I.1). At time t the material points of the continuum have coordinates z_i and all together form configuration 1. In this configuration the isothermal yield function which is a regular surface containing the origin in the stress space may be expressed by

$$f({}^1s_{ij}, {}^1\varepsilon^P_{ij}) = \kappa \qquad \text{(II.20)}$$

where κ is the hardening parameter depending on the whole history of motion of the body and ${}^1\varepsilon^P_{ij}$ is called the plastic strain tensor and is given by

$$ {}^{1}\varepsilon_{ij} = {}^{1}\varepsilon^{P}_{ij} + {}^{1}\varepsilon^{e}_{ij} \qquad \text{(II.21)} $$

in which ${}^{1}\varepsilon^{e}_{ij}$ is the elastic strain tensor. Both ${}^{1}\varepsilon^{P}_{ij}$ and ${}^{1}\varepsilon^{e}_{ij}$ have the same invariant properties as ${}^{1}\varepsilon_{ij}$ but they are determined only from the constitutive relations and not the kinematics of deformation.

Green and Naghdi [50] have shown that if there exists a linear relationship between ${}^{1}\dot{\varepsilon}^{P}_{ij}$ and ${}^{1}\dot{s}_{ij}$ then

$$ {}^{1}\dot{\varepsilon}^{P}_{ij} = \lambda \, \beta_{ij} \frac{\partial f}{\partial {}^{1}s_{mn}} {}^{1}\dot{s}_{mn} , \qquad \lambda > 0 \qquad \text{(II.22)} $$

during loading where

$$ f = \kappa , \; \dot{\kappa} \neq 0 \qquad \frac{\partial f}{\partial {}^{1}s_{mn}} {}^{1}\dot{s}_{mn} > 0 \qquad \text{(II.23)} $$

In (II.22) λ is a scalar function of ${}^{1}s_{mn}$ and ${}^{1}\varepsilon^{P}_{mn}$, and β_{ij} is a symmetric tensor which can be written as the derivative of some potential function $g({}^{1}s_{ij} , {}^{1}\varepsilon^{P}_{ij})$

$$ \beta_{ij} = \frac{\partial g}{\partial {}^{1}s_{ij}} \qquad \text{(II.24)} $$

Therefore,

$$ {}^{1}\dot{\varepsilon}^{P}_{ij} = \dot{\lambda} \frac{\partial g}{\partial {}^{1}s_{ij}} \qquad \text{(II.25)} $$

where

$$ \dot{\lambda} = \lambda \frac{\partial f}{\partial {}^{1}s_{mn}} {}^{1}\dot{s}_{mn} \quad . \qquad \text{(II.26)} $$

As in the infinitesimal theory of plasticity three types of behavior are postulated for the material. These are:

Loading, during which $^{1}\dot{\varepsilon}^{P}_{ij} \neq 0$ and is given by (II.22) and

$$f = \kappa \ , \ \dot{\kappa} \neq 0 \ , \ \frac{\partial f}{\partial {}^{1}s_{mn}} \, {}^{1}\dot{s}_{mn} > 0 \ ; \tag{II.23}$$

Neutral loading for which $^{1}\varepsilon^{P}_{ij} = 0$, and

$$f = \kappa \ , \ \dot{\kappa} = 0 \ , \ \frac{\partial f}{\partial {}^{1}s_{mn}} \, {}^{1}\dot{s}_{mn} = 0 \tag{II.27}$$

Unloading from a plastic state during which $^{1}\dot{\varepsilon}^{P}_{ij} = 0$, and

$$f = 0 \ , \ \dot{\kappa} = 0 \ , \ \frac{\partial f}{\partial {}^{1}s_{mn}} \, {}^{1}\dot{s}_{mn} < 0$$

or (II.28)

$$f < 0 \ , \ \dot{\kappa} = 0 \ .$$

In general the measure of hardening κ is a functional of the entire history of deformation and temperature. A representation of κ for isothermal deformations is

$$\kappa = F\left(\int_{-\infty}^{t} \dot{h} \right) \tag{II.29}$$

$$\dot{h} = \dot{h}({}^{1}s_{ij}, \ {}^{1}\varepsilon^{P}_{ij}, \ {}^{1}\dot{s}_{ij}, \ {}^{1}\dot{\varepsilon}^{P}_{ij}) \tag{II.30}$$

For an inviscid continuum $\dot{h}$ is independent of the time scale and homogeneous of degree one in $^{1}\dot{s}_{ij}$, and $^{1}\dot{\varepsilon}^{P}_{ij}$. Then in view of (II.22) κ can be written as

$$\kappa = F\left(\int^{{}^{1}\varepsilon^{P}_{ij}} dh \right) \tag{II.31}$$

$$dh = dh\ ({}^{1}s_{ij},\ {}^{1}\varepsilon^{P}_{ij},\ d{}^{1}\varepsilon^{P}_{ij}) \tag{II.32}$$

The initial yield surface is only a function of stresses, and for initially isotropic materials it is a function of invariants of stress tensor. In particular it has been found that for metals hydrostatic stress of the order of the yield stress does not affect the yielding and plastic deformation [57]. Therefore, the initial yield surface can be written as

$$f(J_2, J_3) = k \tag{II.33}$$

where k is a constant and J_2 and J_3 are the second and third invariants of the deviatoric Cauchy stress tensor τ_{ij}.

$$J_2 = \frac{1}{2}\ \tau'_{ij}\ \tau'_{ij} \tag{II.34}$$

$$J_3 = \tau'_{ik}\ \tau'_{k\ell}\ \tau'_{\ell i} \tag{II.35}$$

$$\tau'_{ij} = \tau_{ij} - \frac{1}{3}\,\delta_{ij}\ \tau_{kk} \tag{II.36}$$

Experimental evidence indicates that for metals the yield function can be approximated by von Mises yield criterion [43, 58] which is

$$f = J_2 = k \tag{II.37}$$

Equation (II.20) shows the set of all loading surfaces. The shape of these surfaces depends on the scalar functional κ. In the infinitesimal theory of plasticity different mathematical models, called hardening rules, have been proposed to approximate the form

of the subsequent yield surfaces after the initial yielding [43]. These hardening rules can be used in the large deformation theory also. One of these is the isotropic hardening law which asserts that the shape of the yield surfaces at higher stresses is a uniform expansion of the initial yield surface. Mathematically this can be written as

$$f({}^1s_{ij}) = \kappa \tag{II.38}$$

For von Mises yield condition the isotropic hardening law is of the form (see Figure II.2)

$$\bar{\sigma} = \kappa$$

where (II.39)

$$\sqrt{3J_2} = \bar{\sigma}$$

Two simple measures of hardening have been proposed in the infinitesimal theory of plasticity [57]. The first one states that κ is a function of plastic work, and the second states that it is a function of the so-called equivalent plastic strain. It is assumed in this work that these two measures can be used also in the large deformation theory. If the increments of plastic work and equivalent plastic strain are defined by

$$dW_P = {}^1s_{ij}\, d\, {}^1\varepsilon^P_{ij}\ , \tag{II.40}$$

and

$$d\bar{\varepsilon}^P = [\frac{2}{3}\, d\, ({}^1\varepsilon^P_{ij})\, d\, ({}^1\varepsilon^P_{ij})]^{\frac{1}{2}} \tag{II.41}$$

respectively then the functional κ in (II.31) can be written as

$$\kappa = F(\int^{{}^1\varepsilon^P_{ij}} dW_P) \tag{II.42}$$

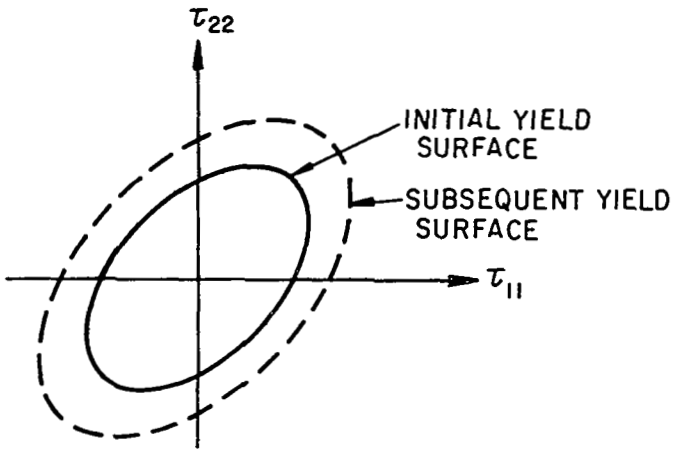

FIG. II-2 ISOTROPIC HARDENING

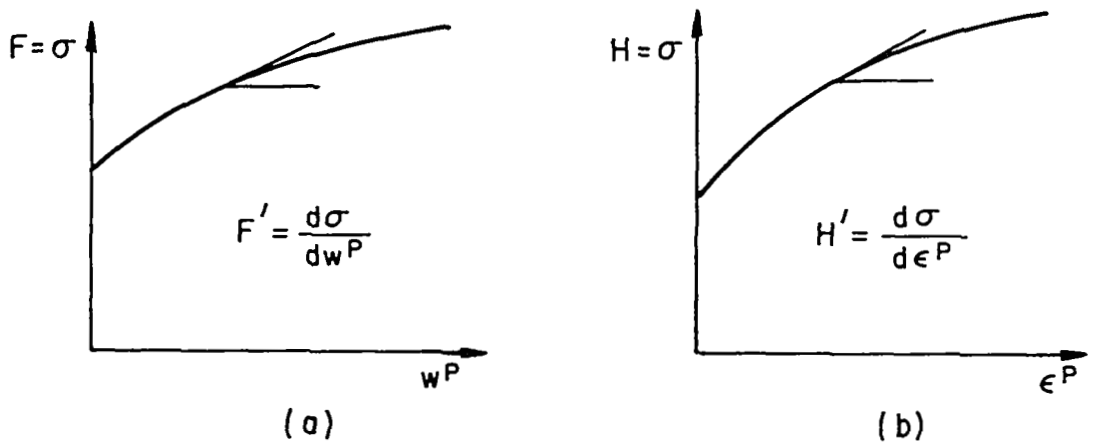

FIG. II-3 HARDENING CURVES FOR SIMPLE TENSION

and

$$\kappa = H\left(\int^{{}^{1}\varepsilon^{P}_{ij}} d\bar{\varepsilon}^{P}\right) \tag{II.43}$$

In the solution of problems the form of the function κ as determined from some experiment, e.g., simple tension test is used (see Figure II.3).

Another constitutive assumption which simplifies the general theory appreciably is Drucker's normality rule which asserts that the increment of plastic strain vector is normal to the yield surface. This requirement indicates that the plastic potential g in (II.24) is the same as f, and equation (II.25) becomes

$$d^{1}\varepsilon^{P}_{ij} = d\bar{\lambda}\,\frac{\partial f}{\partial {}^{1}s_{ij}} \quad . \tag{II.44}$$

where for the von Mises yield criterion

$$\frac{\partial f}{\partial {}^{1}s_{ij}} = \frac{\partial f}{\partial\, \tau_{mn}}\,\frac{\partial\, \tau_{mn}}{\partial {}^{1}s_{ij}} \tag{II.45}$$

$$= \frac{3}{2}\,\frac{\tau'_{mn}}{\bar{\sigma}}\left(\frac{\rho_o}{\bar{\rho}_o}\, z_{n,i}\, z_{n,j}\right) .$$

Since

$$\tau'_{mn} = \frac{\rho_o}{\bar{\rho}_o}\left(Z_{m,i}\, Z_{n,j} - \frac{1}{3}\,\delta_{mn}\, {}^{1}C_{ij}\right) {}^{1}s_{ij} \quad , \tag{II.46}$$

Therefore,

$$\frac{\partial f}{\partial {}^{1}s_{ij}} = \frac{3}{2\bar{\sigma}}\, B_{ijmn}\, {}^{1}s_{mn} \tag{II.47}$$

where

$$B_{ijmn} = \left(\frac{\rho_o}{\bar{\rho}_o}\right)^2 \left({}^1C_{mi}\,{}^1C_{nj} - \frac{1}{3}\,{}^1C_{ij}\,{}^1C_{mn}\right) \qquad \text{(II.48)}$$

and

$${}^1C_{mn} = 2\,{}^1\varepsilon_{mn} - \delta_{mn} \qquad \text{(II.49)}$$

II.4 Stress-Strain Relations

The relationship between the stress and elastic part of strain can be written as

$$d({}^1s_{ij}) = A_{ijk\ell}\, d({}^1\varepsilon^e_{k\ell}) \tag{II.50}$$

where

$$A_{ijk\ell} = \lambda\, \delta_{ij}\, \delta_{k\ell} + \mu(\delta_{ik}\, \delta_{j\ell} + \delta_{jk}\, \delta_{i\ell}). \tag{II.51}$$

During loading

$$\frac{\partial f}{\partial {}^1s_{ij}}\, d({}^1s_{ij}) = \frac{\partial \kappa}{\partial {}^1\varepsilon^P_{ij}}\, d({}^1\varepsilon^P_{ij})\ . \tag{II.52}$$

Substitution of (II.50), (II.21), and (II.25) into (II.52), results in

$$d\overline{\lambda} = \frac{\dfrac{2f}{\partial {}^1s_{rt}}\, A_{rtuv}\, d({}^1\varepsilon_{uv})}{\dfrac{\partial f}{\partial {}^1s_{k\ell}} \left(\dfrac{\partial \kappa}{\partial {}^1\varepsilon^P_{k\ell}} + \dfrac{\partial f}{\partial {}^1s_{ij}}\, A_{ijk\ell}\right)} \tag{II.53}$$

Hence the plastic strain increment (II.44) becomes

$$d({}^1\varepsilon^P_{ij}) = \frac{\dfrac{\partial f}{\partial {}^1s_{ij}}\, \dfrac{\partial f}{\partial {}^1s_{rt}}\, A_{rtk\ell}}{b}\, d({}^1\varepsilon_{k\ell}) \tag{II.54}$$

where

$$b = \frac{\partial f}{\partial {}^1s_{pq}} \left(\frac{\partial \kappa}{\partial {}^1\varepsilon^P_{pq}} + \frac{\partial f}{\partial {}^1s_{uv}}\, A_{uvpq}\right) \tag{II.55}$$

Substitution of (II.54), and (II.21), into (II.50) gives

$$d({}^{1}s_{ij}) = C_{ijpq}\, d({}^{1}\varepsilon_{pq}) \tag{II.56}$$

where

$$C_{ijpq} = A_{ijpq} - b^{-1} A_{ijk\ell} A_{uvpq} \frac{\partial f}{\partial {}^{1}s_{uv}} \frac{\partial f}{\partial {}^{1}s_{k\ell}} \tag{II.57}$$

The derivative $\frac{\partial \kappa}{\partial {}^{1}\varepsilon^{P}_{pq}}$ in (II.55) depends on the form of hardening parameter κ. For work hardening (II.42) this derivative can be written as

$$\frac{\partial \kappa}{\partial {}^{1}\varepsilon^{P}_{mn}} = {}^{1}s_{mn} \frac{\partial \kappa}{\partial W^{P}} . \tag{II.58}$$

$\frac{\partial \kappa}{\partial W^{P}}$ can be determined from a simple tension test where it will be the slope of the hardening curve F' (see Figure II.3(a)). Therefore

$$\frac{\partial \kappa}{\partial {}^{1}\varepsilon^{P}_{mn}} = F' \, {}^{1}s_{mn} \tag{II.59}$$

For strain hardening (II.43) the derivative $\frac{\partial \kappa}{\partial {}^{1}\varepsilon^{P}_{ij}}$ can be written as

$$\frac{\partial \kappa}{\partial {}^{1}\varepsilon^{P}_{mn}} = H' \, {}^{1}s_{mn} \frac{\partial \bar{\varepsilon}^{P}}{\partial W^{P}} \tag{II.60}$$

where H' is the slope of the stress-plastic strain curve in simple tension (see Figure II.3(b)). The relationship between dW^{P} and $d\bar{\varepsilon}^{P}$ can be determined as follows. Substitution of (II.44) into (II.41) results in

$$d\bar{\varepsilon}^P = [\frac{2}{3}(d\bar{\lambda})^2 \frac{\partial f}{\partial {}^1s_{ij}} \frac{\partial f}{\partial {}^1s_{ij}}]^{\frac{1}{2}} \tag{II.61}$$

from which $d\bar{\lambda}$ can be found

$$d\bar{\lambda} = \frac{d\bar{\varepsilon}^P}{(\frac{2}{3} \frac{\partial f}{\partial {}^1s_{ij}} \frac{\partial f}{\partial {}^1s_{ij}})^{\frac{1}{2}}} \tag{II.62}$$

Substitution of (II.62), (II.44), (II.47) and (II.40) into (II.60) gives

$$\frac{\partial \kappa}{\partial {}^1\varepsilon^P_{mn}} = \frac{\alpha^2 H'}{\bar{\sigma}} {}^1s_{mn} \ , \tag{II.63}$$

where

$$\alpha^2 = \frac{B_{ijk\ell} B_{ijrt} {}^1s_{k\ell} {}^1s_{rt}}{B_{pquv} {}^1s_{pq} {}^1s_{uv}} \tag{II.64}$$

II.5 Constitutive Equations in Curvilinear Coordinates

The form invariance of the constitutive equations in Cartesian and orthogonal curvilinear coordinates discussed in section I.5 also holds for inviscid plastic materials with constitutive relation (II.22). Substitution of (II.21) into (II.50) gives

$$d({}^1s_{ij}) = A_{ijpq}\ d({}^1\varepsilon_{pq}) - A_{ijk\ell}\ d({}^1\varepsilon^P_{k\ell})\ . \qquad \text{(II.65)}$$

Since this is an isotropic relationship the corresponding equation in curvilinear coordinates in terms of Cartesian components would be

$$d({}^1s_{ij})^* = (A_{ijpq})^*\ d({}^1\varepsilon_{pq})^* - (A_{ijk\ell})^*\ d({}^1\varepsilon^P_{k\ell})^* \qquad \text{(II.66)}$$

where the asterisks over the tensors indicates Cartesian components. Due to the linear relationship between $d^1\varepsilon^P_{ij}$ and $\frac{\partial f}{\partial {}^1s_{ij}}$ in (II.44) then

$$d({}^1\varepsilon^P_{ij})^* = d\overline{\lambda}\ (\frac{\partial f}{\partial {}^1s_{ij}})^*\ . \qquad \text{(II.67)}$$

$d\overline{\lambda}$ is a scalar and can be written in terms of the physical components of the tensors in (II.53). Therefore, substitution of (II.67) in (II.65) gives

$$d({}^1s_{ij})^* = (C_{ijpq})^*\ d({}^1\varepsilon_{pq})^* \qquad \text{(II.68)}$$

II.6 Approximate Constitutive Equations

The time rate of change of stress and strain ${}^{1}s_{ij}$ and ${}^{1}\varepsilon_{ij}$ can be written as

$$ {}^{1}\dot{s}_{uv} = \lim_{\Delta t \to 0} \left(\frac{{}^{2}\bar{s}_{uv} - {}^{1}s_{uv}}{\Delta t} \right) = \lim_{\Delta t \to 0} \left(\frac{\bar{s}_{uv}}{\Delta t} \right) \tag{II.69} $$

$$ {}^{1}\dot{\varepsilon}_{uv} = \lim_{\Delta t \to 0} \left(\frac{{}^{2}\varepsilon_{uv} - {}^{1}\varepsilon_{uv}}{\Delta t} \right) = \lim_{\Delta t \to 0} \left(\frac{\xi_{uv}}{\Delta t} \right) \tag{II.70} $$

The stress-strain relationship (II.56) can be approximated by substituting $\bar{s}_{uv}$ for $d({}^{1}s_{uv})$ and ξ_{uv} for $d({}^{1}\varepsilon_{uv})$. Then

$$ \bar{s}_{ij} = C_{ijpq}\, \xi_{pq} \tag{II.71} $$

Substitution of (I.35), and (I.47) into (II.71) results in

$$ s_{k\ell} = \frac{\rho_o}{\bar{\rho}_o} \left(z_{k,m}\, z_{\ell,n}\, C_{mnrs}\, z_{u,r}\, z_{v,s} \right) \varepsilon_{uv} \tag{II.72} $$

The corresponding relation in curvilinear coordinates is

$$ (s^{k\ell})^{*} = \frac{\rho_o}{\bar{\rho}_o} (x^{k}_{,m})^{*} (x^{\ell}_{,n})^{*} (x^{u}_{,r})^{*} (x^{v}_{,s})^{*} (C^{mnrs})^{*} (\varepsilon_{uv})^{*} \tag{II.73} $$

where the asterisk over the tensors signifies the physical components. The physical components of the displacement gradients can be written as

$$ (x^{k}_{,m})^{*} = \left(\frac{\partial x^{k}}{\partial \bar{x}^{m}} \right)^{*} = \sqrt{g_{kk} \bar{g}^{mm}}\; x^{k}_{,m} \qquad \text{(no sum)}. \tag{II.74} $$

If an initially orthogonal convected curvilinear coordinate system is used, then

$$x^{k}_{,m} = \delta^{k}_{m} \ . \tag{II.75}$$

Substitution of (II.74) and (II.75) into (II.73) gives

$$(s^{k\ell})^* =$$

$$\frac{\rho_o}{\overline{\rho}_o} \sqrt{(g_{kk}\bar{g}^{kk})(g_{\ell\ell}\bar{g}^{\ell\ell})(g_{rr}\bar{g}^{rr})(g_{ss}\bar{g}^{ss})}\,(C^{k\ell rs})^*(\varepsilon_{rs})^* \tag{II.76}$$

For simplicity define

$$\begin{aligned} s_{k\ell} &= (s^{k\ell})^* \ , \\ \varepsilon_{rs} &= (\varepsilon_{rs})^* \ , \\ C_{k\ell rs} &= (C^{k\ell rs})^* \ , \end{aligned} \tag{II.77}$$

and

$$C'_{k\ell rs} = \frac{\rho_o}{\overline{\rho}_o} \sqrt{(g_{kk}\bar{g}^{kk})(g_{\ell\ell}\bar{g}^{\ell\ell})(g_{rr}\bar{g}^{rr})(g_{ss}\bar{g}^{ss})}\,(C^{k\ell rs})^* \ ,$$

then equation (II.73) becomes

$$s_{k\ell} = C'_{k\ell rs}\ \varepsilon_{rs} \ . \tag{II.78}$$

CHAPTER III: LARGE DEFLECTION ANALYSIS OF ELASTIC-PLASTIC AXISYMMETRIC SHELLS OF REVOLUTION

Many investigators have tried to construct general non-linear bending theories for shells. The problem is not yet resolved completely and certain fundamental questions like the reduction of the general three-dimensional constitutive equations for thin shells, or the development of a general two-dimensional theory present difficulties. Indeed there is not yet a unique definition for a shell type continuum. A complete review of the developments in the nonlinear theory of shells is out of the scope of this work, however, some major contributions will be mentioned.

Two different approaches have been followed in the construction of linear and nonlinear bending theories of shells. The first method consists of reducing the general three-dimensional equations for shells in which one geometric dimension is much smaller than the other two. Synge and Chien [61] developed an intrinsic theory for elastic shells; they treated linear constitutive equations. Green and Zerna [62], and Naghdi [61] have expressed the non-linear kinematics in terms of displacements and treated linear elastic constitutive relations. A theory of elastic shells with small deformations and non-linear elastic response was constructed by Wainwright [63]. Naghdi and Nordgren [64] developed a particular theory subject to Kirchhoff's hypothesis; they consider large displacements and non-linear elastic constitutive equations. Recently Green, Laws, and Naghdi [65] have constructed non-linear thermodynamical theories for rods and shells using the

three-dimensional theory of classical continuum mechanics.

In the second approach the shell is considered as a Cosserat surface, i.e., a two-dimensional continuum to each point of which a director is assigned. The kinematics of a shell considered as a Cosserat surface was given by Ericksen and Truesdell [66]. Special theories in which the director is identified with the inextensional normal to the surface and which remains normal after deformation, corresponding to the usual Kirchhoff's hypothesis, were developed by Sanders [67], Leonard [68] and Koiter [69]. A general theory of a Cosserate surface was constructed by Green, Naghdi, and Wainwright [70] who discuss both the kinematics and the constitutive equations for the surface. Green, Naghdi, and Osborn have developed the elastic-plastic constitutive equations for a Cosserat surface [54].

The equations for the non-linear analysis of shells of revolution can be derived from any of the above theories. A set of equations, which have been widely used by investigators in solving practical problems, have been derived by E. Reissner [71] for linearly elastic shells of revolution. He assumes Kirchhoff's hypothesis and his development is restricted to infinitesimal deformations but large displacements.

The importance of nonlinear analysis of shells of revolution was discussed before. In practical problems closed form solutions for such cases do not exist and resort must be made to numerical techniques. In this chapter after a review of the numerical methods of solution of shells of revolution, shallow caps, and circular plates, the incremental approach developed in Chapters 1 and 2 is specialized for the large deflection elastic-plastic analysis of axisymmetrically deformed thin shells of revolution. The formulation is suitable for the direct

numerical methods of analysis of variational problems, and in Chapter 4 the problem will be solved by the finite element technique.

III.1. Review of Numerical Methods

In this section the numerical methods of analysis of shells of revolution are considered. Three forms of this structure, namely, circular plates, shallow spherical caps and axisymmetric shells of revolution are discussed separately. The division in presentation is not intended to show the diversity of the general methods used in analyzing the nonlinear behavior of these structures, but rather it is dictated because of the existence of rather vast amount of literature for each case.

III.1.1. Axisymmetric shells of revolution

Several numerical methods such as finite difference, invariant imbedding, and finite element techniques have been used for the large deflection bending and membrane analysis of shells of revolution. Finite difference method with iterative schemes has been used by some investigators for linearly elastic shells of revolution [72-76]. Witmer, et al., [77] used finite difference together with a lumped parameter technique for elastic-plastic materials. They used von Mises yield condition and the associated flow rule of plasticity. Inconsistencies arise in their method in the plastic range unless the number of lumped layers in the thickness of the shell is large. A combination of finite difference method and Newton-Raphson iterative scheme was used by Stricklin, Hsu, and Pian [78]. They utilized a special theory of plasticity with the Tresca yield condition. In general, the finite difference method is difficult to use for certain boundary conditions and since the variation of shell geometry and material properties must be expressed analytically the method loses its value when these variables cannot be easily represented analytically or by curve fitting.

The invariant imbedding technique which reformulates the boundary value problem into an initial value problem was applied by Kalnins and Lestingi [79] for elastic shells of revolution. The instabilities in this numerical technique have been pointed out by Fox [80]. The disadvantage of the method is that instead of one problem a family of problems should be solved [79,81].

The finite element method is capable of hacling various boundary conditions and sharp variations or jumps in the geometrical and material properties. The displacement formulation of the finite element method has been used for the post buckling analysis of elastic cylindrical shells by Schmidt, Bogner and Fox [32]. They used an iterative scheme and compatible elements in the form of cylindrical strips. Stricklin, et al. [82,83] have treated the symmetric and asymmetric large deflections of elastic axisymmetric shells of revolution. Their incremental scheme is not consistent because strains and stresses are expressed in two different configurations of the shell. Navaratna, et al., [84] solve the linear bifurcation buckling of elastic shells of revolution by superposing asymmetric buckling modes on the axisymmetric prebuckling deformations.

The nonlinear membrane analysis of elastic shells of revolution has been considered by many investigators. The case of small deformations and large rotations has been treated by asymptotic expansions [85,89], asymptotic expansion with the Ritz method [88], numerical integration with an iterative scheme [86], and asymptotic integration [87]. The problem of large deformations and rotations has been solved by matched asymptotic expansion [90,91]. It is found in [90] that the circumferential membrane force in a toroidal shell is remarkably different when both large

deformations and rotations are considered. A general non-linear membrane theory of shells which includes the effect of finite strains has been derived by Rajan [92]. Salmon [94] has treated the membrane solution of large plastic deformations of a cylindrical shell. He utilized both the incremental and the deformation laws of plasticity and observed that as the length of the cylinder increases the results of the two theories agree rather well. His results also confirm the validity of the approximate method used by Weil [93] in the case of long cylinders.

III.1.2. Shallow caps

The analysis of spherical caps has been the subject of a great number of investigations. The nonlinear behavior of this structure is sensitive to several factors such as the geometrical parameter $\lambda^2 \doteq \sqrt{12(1-\nu^2)}\,\frac{h}{t}$ where ν is the Poisson's ratio, h is the rise and t is the thickness of the shell; the type of applied load; the initial imperfections; and the material property. The influence of these factors on the pattern of displacements and buckling is so significant that up to now there is no complete agreement between the theoretical and experimental results. The nonlinear differential equations of shallow shells were derived by Marguerre [95]. Also, E. Reissner gives a set of equations for shallow caps [96]. In both cases the deformations are considered to be infinitesimal but deflections are finite.

The problem of finite displacements and buckling of shallow spherical caps under uniform normal load was investigated both experimentally and theoretically by Kaplan and Fung in 1954 [97]. In the theoretical method axisymmetric deformations were assumed and a perturbation technique was used with the central deflection as the perturbation parameter.

Great discrepancy was noted between the experimental and theoretical buckling loads for values of $\lambda > 4$. Since that time a great deal of effort has been made by many investigators to close the gap between the experimental and the theoretical results. In the early researches the mode of deflection was assumed to be symmetric and buckling was thought to occur by a symmetric snap through process. The results of such investigations [98-101] do not agree both with the experimental results [97] and also among themselves for $\lambda > 4$, although they all use the same set of differential equations [95]. Among the various numerical procedures for the analysis of axisymmetric large deflection of uniformly loaded spherical caps the integral method of Budiansky [101], power series method of Weinitschke [102], the residual method of Thurston [103], and the direct iterative technique of Archer [104] give the same upper bound solution for the buckling load. Lower bound solutions for the buckling load were given by Reiss, Greenberg, and Keller [98] using power series expansion and by Thurston [103]. Budiansky [101] and Thurston [103] studied the effect of initial imperfections on the axisymmetric buckling of uniformly loaded shallow spherical shells. Budiansky, who used smooth imperfections, concluded that for $\lambda > 5$ the inclusion of imperfections cannot close the gap between the experimental and theoretical results. Thurston, using rough imperfections, points out that the inclusion of imperfections in the analysis of caps is important. The experimental results by Krenzke and Kiernan [105], on highly accurate aluminum specimens, which show higher buckling loads than Kaplan and Fung's experiment support Thurston's point of view.

Since the theoretical results on the symmetrical buckling of uniformly loaded shallow spherical shells do not agree with experimental

evidence for $\lambda > 5$ it was concluded by some investigators that the process of buckling may be unsymmetric although the initial and final configurations are symmetric. Weinitschke [106] superimposed small asymmetric deflections on finite axisymmetric displacements and obtained buckling loads which are close to experimental values of [97]. Huang [107] solved the variational formulation of the unsymmetric snap through buckling numerically and obtained buckling loads higher than the experimental results in [97] but lower than the axisymmetric theoretical calculations. His results are close to the experimental buckling loads of Krenzke and Kiernan [105].

Contrary to uniform or partially uniform loading, the theoretical and experimental results of shallow spherical caps under concentrated load agree rather well [108-112]. It is found that, unlike the uniformly loaded cap, the snap through occurs at very high loads. The experimental results in [111] indicate that symmetric snap through occurs for $\lambda < 6.5$ and asymmetric buckling occurs for $\lambda > 10.2$. The theoretical study of spherical caps under concentrated load has also revealed the fact that buckling of the bifurcation type may occur even before snap through happens [110-114].

Experimental results of uniformly loaded spherical sandwich shallow shells by Lin [115] emphasize the importance of including the nonlinear behavior of material in the buckling analysis.

III.1.3. Circular plates

The governing differential equations for the bending analysis of infinitesimal deformation but finite deflections of thin elastic plates were derived by von Karman [116]. For the case of axisymmetrically loaded and supported circular plates the von Karman equations reduce to two coupled

second order non-linear ordinary differential equations. Corresponding equations for circular plates can be obtained by simplifying E. Reissner's equations for axisymmetric shells of revolution [71].

Two approaches have been followed for the solution of the differential equations of large displacement bending analysis of elastic circular plates. In the first approach the von Karman equations are further simplified and then solved exactly. This method was used by Berger [117], who neglected the strain energy due to the second invariant of middle surface strains, and by Goldberg [118], who neglected the Gaussian curvature in the compatibility equation for membrane strains. Both Berger and Goldberg arrived at a set of uncoupled equilibrium equations. Berger's simplification was later used for the vibration analysis of circular plates [119] and for the problem of circular plates on elastic foundations [120].

In the other approach approximate solutions have been sought for von Karman's or E. Reissner's equations by different mathematical methods. Power series expansion method, where the variables are expressed in powers of the radius from the center of the plate, was used by Way [121]. Bromberg [122] used a perturbation method by expanding the variables in terms of the perturbation parameter $k = \frac{R}{12(1-\nu^2)} \left(\frac{pR}{Eh}\right)^{1/3}$ where R, and h, are the radius and thickness of the plate, respectively, p is the intensity of the applied uniform load, and E and ν are the Young's modulus and Poisonn's ratio, respectively. As pointed out in [122], the perturbation method gives correct results for $k \leq 1$, and the power series method for $1 \leq k \leq 15$. For larger values of k, however, boundary layer effects become important near the edge of the plate and the above two methods fail to give accurate results. In such a case a boundary layer

solution, employing asymptotic expansion, has been used. This method was proposed and used for the solution of the problem of circular plates by Friedrichs and Stoker [123] and was later modified by Bromberg [122]. Hart and Evans [124] have applied the method of asymptotic expansion for the annular plates. Keller and Reiss [125] applied an iterative scheme to the boundary layer solution in [123]. Their method together with finite difference equations have been used by Hamada and Seguchi [126] for the analysis of annular plates.

The large deflection analysis of elastic-plastic circular plates has been considered by several investigators. The order of geometric nonlinearity is the same as in von Karman's theory. For the material nonlinearity different constitutive laws have been employed. Rigid plastic materials were analyzed by Sawczuk [127] for static loads and by Jones for dynamic and impulsive loads [128,129]. Deformation theory of plasticity was used by Ohashi and Murakami [130,131] for elastic perfectly plastic materials. The results of their calculations fall within the range of Budiansky's criterion for the physical validity of the deformation theory of plasticity [132] and the comparison of their theoretical and experimental results is satisfactory. Using the deformation law of plasticity Naghdi [133] and Ohashi and Kamiya [134] analyze the large deflections of circular plates with hardening materials. A lumped parameter method was employed by Crose and Ang [135], who divide the plate thickness into three layers. The top and bottom layers are thin and are in a state of plane stress, and the middle layer has infinite shear stiffness and no resistance to bending. They use flow theory of plasticity.

The observation common in all of the above investigations on the large deflection of elastic-plastic circular plates is that the effect of

membrane forces in the plastic range is significant even for relatively small displacements, and that the load carrying capacity of the plates is more than that given by bending collapse load.

III.2 The Strain-Displacement Relations

The coordinate system on the middle surface of a shell of revolution in configuration 1 is chosen to be orthogonal and coincide with the principal lines of curvature (see Figure III.1). It is assumed that the deformation of the shell follows Kirchhoff's hypothesis which asserts that the unit normal vector to the middle surface in configuration 1 remains normal to the middle surface of the shell in configuration 2 and that its length does not change. Then the convected form of the coordinate system x^i remains orthogonal and coincides with the principal curvature lines in configuration 2 for axisymmetrically loaded and supported shells of revolution.

It is shown in Appendix E that the strain-displacement relations for axisymmetrically deformed shells of revolution when Kirchhoff's hypothesis prevails are

$$\begin{aligned}\varepsilon_{ss} = {} & e_s + \frac{1}{2} e_s^2 + \frac{\chi^2}{2} + \zeta[(\omega_{s,s} + \frac{\omega_n}{R_s}) + \\ & \frac{e_s}{R_s} + e_s(\omega_{s,s} + \frac{\omega_n}{R_s}) - \chi(\omega_{n,s} - \frac{\omega_s}{R_s})] + \\ & \zeta^2[\frac{1}{R_s}(\omega_{s,s} + \frac{\omega_n}{R_s}) + \frac{1}{2}(\omega_{s,s} + \frac{\omega_n}{R_s})^2 + \\ & \frac{1}{2}(\omega_{n,s} - \frac{\omega_s}{R_s})^2] \quad ,\end{aligned} \tag{III.1}$$

and

$$\begin{aligned}\varepsilon_{\theta\theta} = {} & e_\theta + \frac{1}{2} e_\theta^2 + \zeta[\omega_r(1 + e_\theta) + \frac{e_\theta}{R_\theta}] + \\ & \zeta^2[\frac{\omega_r}{R} + \frac{1}{2}\omega_r^2] \quad ,\end{aligned} \tag{III.2}$$

where

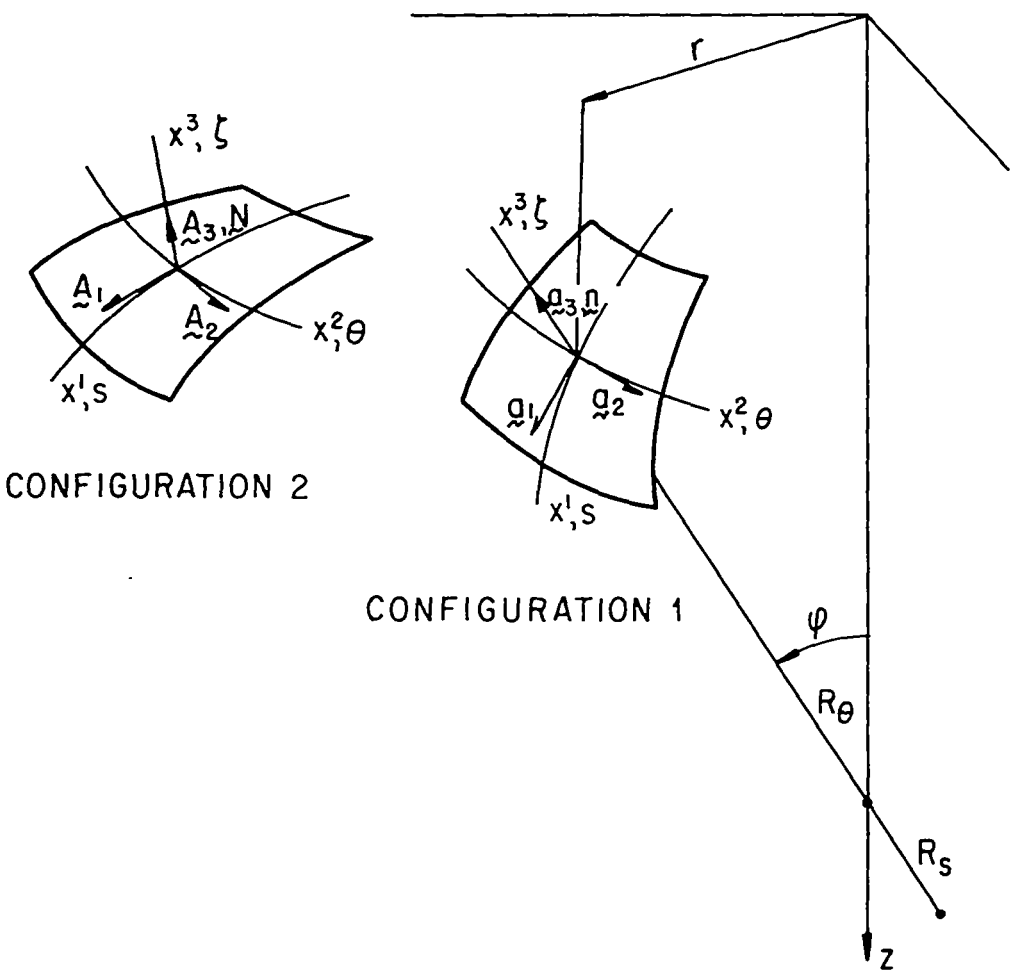
x^3, ζ
$\underset{\sim}{A}_3, \underset{\sim}{N}$
$\underset{\sim}{A}_1$
$\underset{\sim}{A}_2$
x^2, θ
x^1, s
CONFIGURATION 2
r
x^3, ζ
$\underset{\sim}{a}_3, \underset{\sim}{n}$
$\underset{\sim}{a}_1$
$\underset{\sim}{a}_2$
x^2, θ
x^1, s
CONFIGURATION 1
φ
R_θ
R_s
z

FIG. III·1

$$e_\theta = \frac{1}{r}(u\cos\phi + w\sin\phi) \ , \tag{III.3}$$

$$e_s = u,_s + \frac{w}{R_s} \ , \tag{III.4}$$

$$\chi = \frac{u}{R_s} - w,_s \ , \tag{III.5}$$

$$\omega_n = \cos\omega - 1 = \frac{1 + e_s}{(1 + 2e_s + e_s^2 + \chi)^{1/2}} - 1 \ , \tag{III.6}$$

$$\omega_s = \sin\omega - \frac{\chi}{(1 + 2e_s + e_s^2 + \chi)^{1/2}} \ , \tag{III.7}$$

and

$$\omega_r = \frac{\omega_s\cos\phi + \omega_n\sin\phi}{r} : \tag{III.8}$$

ε_{ss} and $\varepsilon_{\theta\theta}$ are the physical components of meridional and circumferential strain tensor. u and w are the physical components of meridional and normal displacements of the middle surface of the shell (see Figure III.2).

If the shell is thin, expressions (III.1) and (III.2) can be simplified further by assuming that $\zeta^2 \approx 0$. Then

$$\varepsilon_{ss} = e_s + \frac{1}{2}e_s^2 + \frac{\chi^2}{2} + \zeta[(\omega_{s,s} + \frac{\omega_n}{R_s}) + \frac{e_s}{R_s} + e_s(\omega_{s,s} + \frac{\omega_n}{R_s}) - \chi(\omega_{n,s} - \frac{\omega_s}{R_s})] \ , \tag{III.9}$$

and

$$\varepsilon_{\theta\theta} = e_\theta + \frac{1}{2}e_\theta^2 + \zeta[\omega_r(1 + e_\theta) + \frac{e_\theta}{R_\theta}] \ . \tag{III.10}$$

Also for thin shells whose deformations are infinitesimal such that $e_\theta^2 \ll e_\theta$, and $e_s^2 \ll e_s$, but whose rotations are large with the restriction that $\chi^n \ll \chi$, $n > 2$, the strain displacement relations

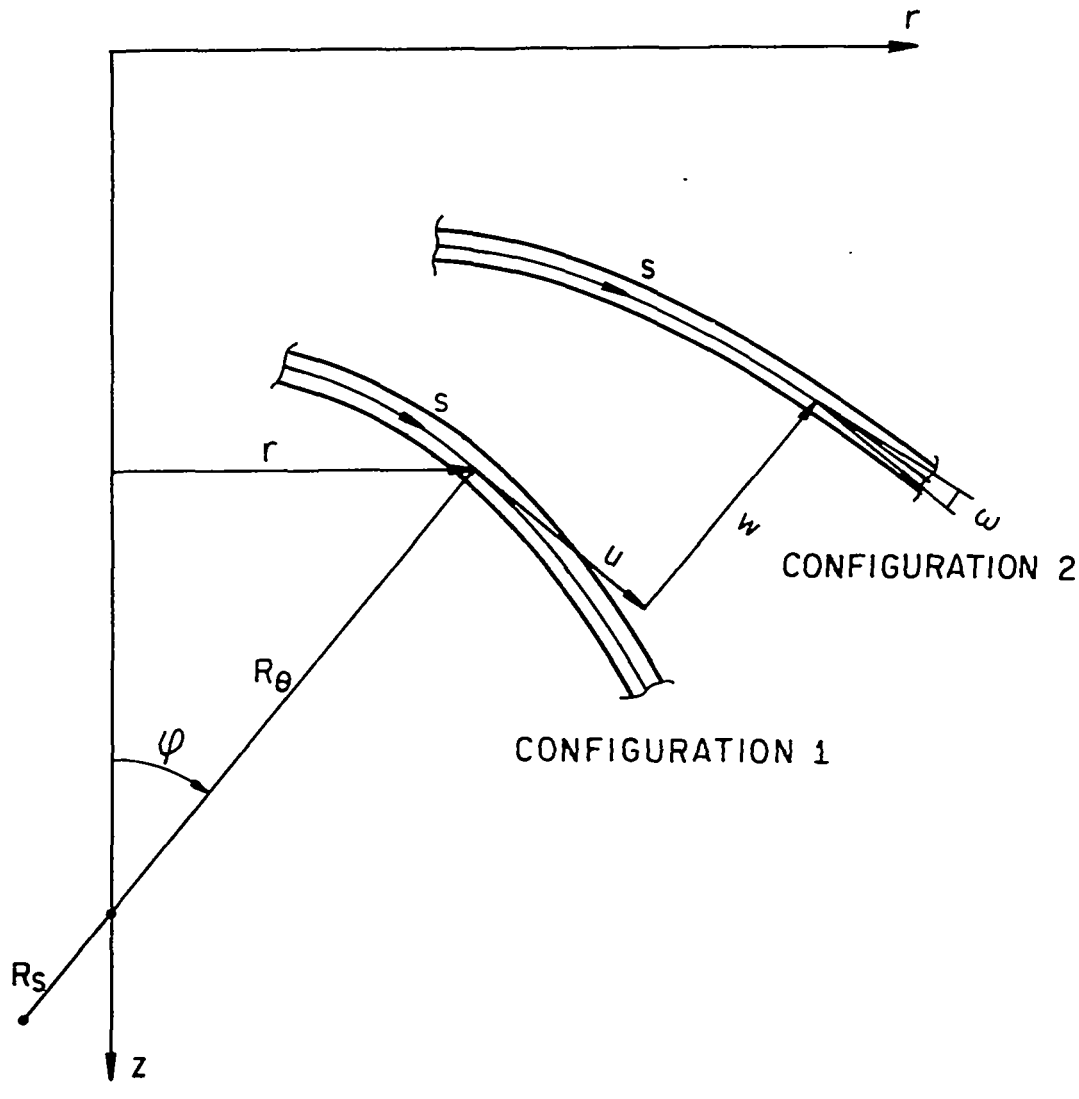

FIG. III-2

(III.9) and (III.10) can be simplified still further. Then

$$(1 + 2e_s + e_s^2 + \chi)^{-\frac{1}{2}} \approx 1 - \frac{1}{2}(2e_s + e_s^2 + \chi^2) , \tag{III.11}$$

$$\omega_s = \chi - \chi e_s , \tag{III.12}$$

$$\omega_n = -\frac{\chi^2}{2} , \tag{III.13}$$

and the strain-displacement equations become

$$\varepsilon_{ss} = \varepsilon_s + \zeta \kappa_s , \tag{III.14}$$

and

$$\varepsilon_{\theta\theta} = \varepsilon_\theta + \zeta \kappa_\theta , \tag{III.15}$$

where

$$\varepsilon_s = e_s + \frac{\chi^2}{2} \tag{III.16}$$

$$\varepsilon_\theta = e_\theta \tag{III.17}$$

$$\kappa_s = (\chi_{,s} + \frac{e_s}{R_s}) + (\frac{\chi^2}{2R_s} - \chi e_{s,s}) \tag{III.18}$$

$$\kappa_\theta = (\frac{\cos\phi}{r}\chi + \frac{e_\theta}{R_\theta}) + \frac{1}{r}[-\frac{\sin\phi}{2}\chi^2 + \cos\phi(e_\theta - e_s)\chi] \tag{III.19}$$

κ_s and κ_θ are the meridional and tangential change of curvatures. The strains ε_{ss} and $\varepsilon_{\theta\theta}$ can be written as the sum of a linear and a non-linear part

$$\begin{Bmatrix} \varepsilon_{ss} \\ \varepsilon_{\theta\theta} \end{Bmatrix} = \begin{Bmatrix} e_{ss} \\ e_{\theta\theta} \end{Bmatrix} + \begin{Bmatrix} \eta_{ss} \\ \eta_{\theta\theta} \end{Bmatrix} \tag{III.20}$$

where the linear part is

$$\begin{Bmatrix} e_{ss} \\ e_{\theta\theta} \end{Bmatrix} = \begin{Bmatrix} e_s \\ e_\theta \end{Bmatrix} + \zeta \begin{Bmatrix} \kappa_s^\circ \\ \kappa_\theta^\circ \end{Bmatrix} \tag{III.21}$$

and the non-linear part is

$$\begin{Bmatrix} \eta_{ss} \\ \eta_{\theta\theta} \end{Bmatrix} = \begin{Bmatrix} \frac{\chi^2}{2} \\ 0 \end{Bmatrix} + \zeta \begin{Bmatrix} \kappa_s^1 \\ \kappa_\theta^1 \end{Bmatrix} \tag{III.22}$$

The linear and non-linear components of the curvature vector are

$$\begin{Bmatrix} \kappa_s^\circ \\ \kappa_\theta^\circ \end{Bmatrix} = \begin{Bmatrix} \chi_{,s} + \frac{e_s}{R_s} \\ \frac{\cos\phi}{r}\chi + \frac{e_\theta}{R_\theta} \end{Bmatrix}. \tag{III.23}$$

and

$$\begin{Bmatrix} \kappa_s^1 \\ \kappa_\theta^1 \end{Bmatrix} = \begin{Bmatrix} \frac{\chi^2}{2R_s} - \chi\, e_{s,s} \\ \frac{1}{r}\left[-\frac{\sin\phi}{2}\chi^2 + \cos\phi(e_\theta - e_s)\chi\right] \end{Bmatrix} \tag{III.24}$$

III.3. The Constitutive Equations

The symmetry of deformations and Kirchhoff's hypothesis require that ${}^1s^{\alpha 3} = 0$, $s^{\alpha 3} = 0$, ${}^1\varepsilon_{i3} = 0$, and $\varepsilon_{i3} = 0$. If the strains ${}^1\varepsilon_{33}$ and ε_{33} are not assumed to be zero but are such that $\varepsilon_{33} << 1$, ${}^1\varepsilon_{33} << 1$ and ${}^1\varepsilon_{33} << {}^1\varepsilon_{\alpha\beta}$, $\varepsilon_{33} << \varepsilon_{\alpha\beta}$ then the strain-displacement relationships of Section III.2. are still a good representation of the kinematics of deformation of the shell. If the shell is thin, then it can be assumed that ${}^1s^{33} = 0$, and $s^{33} = 0$. With these restrictions on stresses and strains the constitutive equations (II.78) can be written as

$$s_{\alpha\beta} = C'_{\alpha\beta\gamma\delta}\,\varepsilon_{\gamma\delta} + C_{\alpha\beta 33}\,\varepsilon_{33} \quad . \tag{III.25}$$

and

$$s_{33} = C'_{33\gamma\delta}\,\varepsilon_{\gamma\delta} + C'_{3333}\,\varepsilon_{33} \quad . \tag{III.26}$$

Solve (III.26) for ε_{33} and substitute in (III.25) to get

$$s_{\alpha\beta} = \overline{C}_{\alpha\beta\gamma\delta}\,\varepsilon_{\gamma\delta} \quad , \tag{III.27}$$

where

$$\overline{C}_{\alpha\beta\gamma\delta} = \frac{C'_{\alpha\beta\gamma\delta}\;C'_{3333} - C'_{\alpha\beta 33}\;C'_{33\gamma\delta}}{C'_{3333}} \tag{III.28}$$

III.3.1. Strain hardening materials

For materials which obey the strain hardening law (II.43) the stress strain relations (II.74) are reduced to

$$\begin{Bmatrix} s_{11} \\ s_{22} \end{Bmatrix} = \begin{bmatrix} \overline{C}_{1111} & \overline{C}_{1122} \\ \overline{C}_{2211} & \overline{C}_{2222} \end{bmatrix} \begin{Bmatrix} \varepsilon_{11} \\ \varepsilon_{22} \end{Bmatrix} \tag{III.29}$$

along the principal directions of the shell. The transformation coefficients

in (III.29) are calculated from (III.28). These are

$$\bar{C}_{1111} = \frac{A^3}{B}\frac{E}{\Omega}[\zeta + (1-\zeta)S_2^2] \quad ,$$

$$\bar{C}_{2222} = \frac{B^3}{A}\frac{E}{\Omega}[\zeta + (1-\zeta)S_1^2] \quad , \tag{III.30}$$

$$\bar{C}_{1122} = \bar{C}_{2211} = AB\frac{E}{\Omega}[\nu\zeta - (1-\zeta)S_1S_2] \quad ,$$

where

$$\Omega = (1-\nu^2)\zeta + (1-\zeta)(S_1^2 + 2\nu S_1S_2 + S_2^2) \tag{III.31}$$

$$A = \sqrt{g_{11}\,\bar{g}^{11}} \quad , \quad B = \sqrt{g_{22}\,\bar{g}^{22}} \tag{III.32}$$

where $\bar{g}^{ij}$ and g_{ij} are the metric tensors associated with the convected orthogonal curvilinear coordinates of the shell in the initial state and configuration 1, respectively. On the middle surface of the shell they coincide with $\bar{a}^{ij}$ and a_{ij}, respectively. Also

$$S_1 = \sqrt{3/2}\,\frac{a}{\alpha e} \quad , \quad S_2 = \sqrt{3/2}\,\frac{b}{\alpha e} \quad , \quad \alpha^2 = \frac{e^2}{a^2+b^2} \quad , \tag{III.33}$$

$$\begin{aligned} a &= B_{1111}\,{}^1s_{11} + B_{1122}\,{}^1s_{22} \quad , \\ b &= B_{2211}\,{}^1s_{11} + B_{2222}\,{}^1s_{22} \quad , \\ e^2 &= a\,{}^1s_{11} + b\,{}^1s_{22} \quad , \end{aligned} \tag{III.34}$$

and

$$\begin{aligned} B_{1111} &= \frac{2}{3}\,{}^1C_{11}^2\left(\frac{\rho_o}{\bar{\rho}_o}\right)^2 \\ B_{1122} &= B_{2211} = -\frac{1}{3}\,{}^1C_{11}\,{}^1C_{22}\left(\frac{\rho_o}{\bar{\rho}_o}\right)^2 \\ B_{2222} &= \frac{2}{3}\,{}^1C_{22}^2\left(\frac{\rho_o}{\bar{\rho}_o}\right)^2 \end{aligned} \tag{III.35}$$

Since the curvilinear coordinate axes are convected, then ${}^1C_{\alpha\beta}$ can be

directly expressed in terms of metric tensors. In particular

$$
\begin{aligned}
{}^{1}C_{11} &= \sqrt{(g_{ii}\,\bar{g}^{11})(g_{ii}\,\bar{g}^{11})}\;\;\delta_1{}^{i}\,\delta_1{}^{i} \quad \text{(no sum)} \\
&= g_{11}\,\bar{g}^{11} \quad , \qquad \text{(III.36)}
\end{aligned}
$$

and similarly

$$
{}^{1}C_{22} = g_{22}\,\bar{g}^{22} \quad . \qquad \text{(III.37)}
$$

Substitution of (III.36), (III.37), and (II.49) into (III.35) results in

$$
B_{1111} = \frac{2}{3}\,\frac{1 + 2\,{}^{1}\varepsilon_{11}}{1 + 2\,{}^{1}\varepsilon_{22}} \quad ,
$$

$$
B_{1122} = B_{2211} = -\frac{1}{3} \quad , \qquad \text{(III.38)}
$$

and

$$
B_{2222} = \frac{2}{3}\,\frac{1 + 2\,{}^{1}\varepsilon_{22}}{1 + 2\,{}^{1}\varepsilon_{11}} \quad .
$$

The relationship between the tensors ${}^{1}s_{ij}$ and τ^{ij} in convected coordinates is [31]

$$
{}^{1}s^{mn} = \frac{\bar{\rho}_o}{\rho_o}\,\tau^{mn} \quad . \qquad \text{(III.39)}
$$

If these stresses are expressed in terms of their physical components (similar to equations (D.9) and (D.12) in Appendix D) then (III.39) with $m = n = 1$ becomes

$$
{}^{1}s_{11} = \sqrt{\frac{g_{22}\,\bar{g}^{22}}{g_{11}\,\bar{g}^{11}}}\;\;\tau_{11} \quad . \qquad \text{(III.40)}
$$

Substitution of (III.36), (III.37), and (II.49) into (III.40) gives

$$ {}^{1}s_{11} = \sqrt{\frac{1 + 2\,{}^{1}\varepsilon_{22}}{1 + 2\,{}^{1}\varepsilon_{11}}}\ \tau_{11} \quad . \tag{III.41} $$

Similarly

$$ {}^{1}s_{22} = \sqrt{\frac{1 + 2\,{}^{1}\varepsilon_{11}}{1 + 2\,{}^{1}\varepsilon_{22}}}\ \tau_{22} \quad . \tag{III.42} $$

In view of equations (III.36) to (III.42), then

$$ A = \sqrt{1 + 2\,{}^{1}\varepsilon_{11}} \quad , \qquad B = \sqrt{1 + 2\,{}^{1}\varepsilon_{22}} \tag{III.43} $$

$$ S_1 = \frac{A}{\alpha B}\ \frac{(\tau_{11} - \frac{1}{2}\tau_{22})}{\bar{\sigma}} \quad , \quad S_2 = \frac{B}{\alpha A}\ \frac{(\tau_{22} - \frac{1}{2}\tau_{11})}{\bar{\sigma}} \quad , \tag{III.44} $$

$$ \alpha = \left(\frac{1}{S_1^{\,2} + S_2^{\,2}}\right)^{1/4} \tag{III.45} $$

and

$$ \bar{\sigma} = \tau_{11}^{\,2} - \tau_{11}\tau_{22} + \tau_{22}^{\,2} \quad , \qquad \zeta = \frac{E_t}{E} \tag{III.46} $$

III.3.2. Work hardening materials

For materials which obey the work hardening law (II.42) the transformation coefficients in (III.29) are

$$ \begin{aligned} \bar{C}_{1111} &= \frac{A^3}{B}\ \frac{E}{\bar{\Omega}}\ (F' + \bar{S}_2^{\,2}) \\ \bar{C}_{2222} &= \frac{B^3}{A}\ \frac{E}{\bar{\Omega}}\ (F' + \bar{S}_1^{\,2}) \end{aligned} \tag{III.47} $$

$$ \bar{C}_{1122} = \bar{C}_{2211} = AB\ \frac{E}{\bar{\Omega}}\ (\nu F' - \bar{S}_1\bar{S}_2) $$

where

$$ \bar{S}_1 = \frac{A}{B}\ \sqrt{E/\bar{\sigma}}\ \frac{(\tau_{11} - \frac{1}{2}\tau_{22})}{\bar{\sigma}} \quad , \quad S_2 = \frac{B}{A}\ \sqrt{E/\bar{\sigma}}\ \frac{(\tau_{22} - \frac{1}{2}\tau_{11})}{\bar{\sigma}} \tag{III.48} $$

and

$$ \bar{\Omega} = (1-\nu^2)F' + (\bar{S}_1^{\,2} + 2\nu\bar{S}_1\bar{S}_2 + \bar{S}_2^{\,2}) \quad . \tag{III.49} $$

III.4. The Expression for Virtual Work

The incremental equations of equilibrium between configurations 1 and 2 for the shell can be written in the form of an expression of virtual work. The general form of the expression of virtual work in curvilinear coordinates is given in equation (A.13) in Appendix A. The incremental expression of virtual work for axisymmetrically deformed shells of revolution was derived from (A.13) in Appendix F. If the shell is thin so that $\frac{\zeta}{R_s} << 1$, and $\frac{\zeta}{R_\theta} << 1$ then the equations (A.13), (F.16), (F.18), and (F.21) reduce to the following form in terms of physical components:

$$\int_{a_\tau} \delta\{V\}^T\{\tilde{p}\}\, da \int_c \delta\{V\}^T\{\tilde{P}\}\, dc = \int_\nu (\tau_{ss}\delta\eta_{ss} + \tau_{\theta\theta}\delta\eta_{\theta\theta} + s_{ss}\delta\epsilon_{ss} + s_{\theta\theta}\delta\epsilon_{\theta\theta})\, d\nu \qquad \text{(III.50)}$$

where

$$\{V\}^T = < u \; x \; \chi > \quad , \qquad \text{(III.51)}$$

$$\{\tilde{p}\}^T = < \tilde{p}_s \; \tilde{p}_n \; \tilde{m} > \quad , \qquad \text{(III.52)}$$

and

$$\{\tilde{P}\}^T = < \tilde{N}_s \; \tilde{Q}_s \; \tilde{M}_s > \quad . \qquad \text{(III.53)}$$

the tildas over the variables in (III.52) and (III.53) indicate that these quantities are specified. Substitution of (III.29) into (III.50) and integration over the thickness of the shell leads to

$$\int_{a_\tau} \delta\{V\}^T\{\tilde{p}\}\, da + \int_c \delta\{V\}^T\{\tilde{P}\}\, dc = \int_a (\delta\{\eta\}^T\{{}^1N\} + \delta\{\epsilon\}^T[D]\{\epsilon\}\, da \qquad \text{(III.54)}$$

where the nonlinear part of strain vector is

$$\{\eta\}^T = < \eta_s \; \eta_\theta \; \kappa_s{}^1 \; \kappa_\theta{}^1 > \quad ; \qquad \text{(III.55)}$$

and

$$\{{}^{1}N\}^{T} = < {}^{1}N_{s} \; {}^{1}N_{\theta} \; {}^{1}M_{s} \; {}^{1}M_{\theta} > \quad , \tag{III.56}$$

$$\begin{Bmatrix} {}^{1}N_{s} \\ \\ {}^{1}N_{\theta} \end{Bmatrix} = \int_{-h/2}^{h/2} \begin{Bmatrix} \tau_{ss} \\ \\ \tau_{\theta\theta} \end{Bmatrix} d\zeta \quad , \tag{III.57}$$

$$\begin{Bmatrix} {}^{1}M_{s} \\ \\ {}^{1}M_{o} \end{Bmatrix} = \int_{-h/2}^{h/2} \begin{Bmatrix} \tau_{ss} \\ \\ \tau_{\theta\theta} \end{Bmatrix} \zeta \, d\zeta \quad , \tag{III.58}$$

$$\{\varepsilon\}^{T} = < e_{s} \; e_{\theta} \; \kappa_{s} \; \kappa_{\theta} > \quad , \tag{III.59}$$

and the rigidity matrix is

$$[D]_{4\times4} = \begin{bmatrix} D_{11} & D_{12} \\ \\ D_{21} & D_{22} \end{bmatrix} \quad . \tag{III.60}$$

The components of [D] are

$$[D_{11}]_{2\times2} = \int_{-h/2}^{h/2} [\bar{C}(s,\zeta)] \, d\zeta \quad , \tag{III.61}$$

$$[D_{12}]_{2\times2} = [D_{21}]_{2\times2} = \int_{-h/2}^{h/2} [\bar{C}(s,\zeta)]\zeta \, d\zeta \quad , \tag{III.62}$$

and

$$[D_{22}]_{2\times2} = \int_{-h/2}^{h/2} [\bar{C}(s,\zeta)]\zeta^{2} \, d\zeta \quad . \tag{III.63}$$

CHAPTER IV: APPLICATION OF THE FINITE ELEMENT METHOD FOR THE ANALYSIS OF AXISYMMETRIC SHELLS OF REVOLUTION

The application of finite element method to structural problems has been discussed in [6, 136-138]. The direct stiffness procedure of the displacement formulation of finite element method which has been widely used for both linear and nonlinear analysis of structures has been explained and the various requirements on the assumed displacement fields has been discussed in several references, e.g. [6,15,25,34,136,138,139]. The incremental expression of virtual work given by equation (I.27) can be solved for the displacements by the displacement formulation of the finite element method. In this Chapter, first a nonlinear incremental procedure of solving (I.27) using the displacement approach of the finite element method is discussed and the basic steps are explained. Then, using the direct stiffness technique, the linear part of the incremental procedure is applied for the nonlinear analysis of elastic-plastic shells of revolution.

IV.1. Displacement Formulation for a Non-Linear Incremental Procedure

The incremental expression of virtual work in configuration 2 is given by Equation (I.27) as

$$\int_a t_i \delta u_i \, da + \int_v \rho_o f_i \delta u_i \, dv = \int_v (\tau_{ij} \delta \eta_{ij} + s_{ij} \delta \varepsilon_{ij}) \, dv \quad . \tag{I.27}$$

Assume that the material space of the body in configuration 1 is composed of a set of simply connected subregions called finite elements. Then Equation (I.27) can be thought of as the sum of similar expressions for

the elements. Let the displacement increments, $u_i(z_m)$, of the points in the elements be expressed in terms of the displacement increments, $r_j(z_n)$, of certain points or sets of points of the elements called the nodes (which are usually at the interfaces of the elements) by some interpolation functions $M_{ij}(z_m)$ as

$$u_i(z_m) = M_{ij}(z_m) r_j(z_n) \quad . \tag{IV.1}$$

The displacements $u_i(z_m)$ are continuous in the element and vanish beyond the boundaries of the element. Thus the element is the support for the functions $u_i(z_m)$. The combination of all such displacements for all the elements comprise the total incremental displacement field of the whole body. The element displacement and geometry representation should be such that the rigid body motion of the elements and the compatibility requirements at the element boundaries be satisfied. In addition, for the uniform convergence of solutions, the displacements must be such that uniform straining modes of the elements exist.

In the same way the tractions and body forces are expressed in terms of the magnitude of tractions and body forces at the nodes by some interpolation functions such as

$$t_i(z_k) = {}^{t}M_{im}(z_k)\ T_m(z_n) \tag{IV.2}$$

$$f_i(z_m) = {}^{f}M_{ij}(z_m)\ F_j(z_n) \tag{IV.3}$$

For materials where the relationship between s_{ij} and ε_{ij} in the elements can be expressed by*

$$s_{ij} = C_{ijk\ell}\, \varepsilon_{k\ell} \quad , \tag{IV.4}$$

$$\varepsilon_{k\ell} = \frac{1}{2}\,(u_{k,\ell} + u_{\ell,k} + u_{m,k}\, u_{m,\ell}) \quad , \tag{IV.5}$$

the substitution of (IV.1) - (IV.5) into (I.27) results in the following incremental force-displacement relationship:

$$R_k = K^{(o)}_{kn} + K^{(1)}_{kn})\, r_n + \underline{K^{(2)}_{kns}\, r_n r_s + K^{(3)}_{knsu}\, r_n r_s r_u} \tag{IV.6}$$

where

$$R_k = \int_a {}^{t}M_{im}\, M_{ik}\, T_m\, da + \int_v \rho_o\, {}^{f}M_{im}\, M_{ik}\, F_m\, dv \quad , \tag{IV.7}$$

$$K^{(o)}_{kn} = \frac{1}{4} \int_v C_{ijrt}(M_{ik,j} + M_{jk,i})(M_{rn,t} + M_{tn,r})\, dv \quad , \tag{IV.8}$$

$$K^{(1)}_{kn} = \frac{1}{2} \int_v \tau_{ij}(M_{mk,i} + M_{mn,j} + M_{mn,i}\, M_{mk,j})\, dv \quad , \tag{IV.9}$$

$$K^{(2)}_{kns} = \frac{1}{4} \int_v C_{ijrt}[(M_{ik,j} + M_{jk,i})\, M_{ms,r}\, M_{mn,t}$$

$$+ (M_{rs,t} + M_{ts,r})(M_{mk,i}\, M_{mn,j} + M_{mk,j}\, M_{mn,i})]\, dv \quad , \tag{IV.10}$$

and

*More complicated constitutive relations can be assumed. The stated relationship is sufficiently general for our purpose here.

$$K^{(3)}_{knsu} = \frac{1}{4}\int_V C_{ijrt}\, M_{ms,r}\, M_{mu,t}\, (M_{mk,i}\, M_{mn,j} + M_{mk,j}\, M_{mn,i})\, dv \quad . \tag{IV.11}$$

The stiffness matrix $K^{(o)}_{kn}$ is due to the linear part of $s_{ij}\delta\varepsilon_{ij}$ in (I.27). The stiffness matrix $K^{(1)}_{kn}$, called the tangent or initial stress stiffness matrix, is due to the $\tau_{ij}\eta_{ij}$ term in (I.27), and the matrices $K^{(2)}_{kns}$ and $K^{(3)}_{knsu}$ are due to the nonlinear terms in $s_{ij}\delta\varepsilon_{ij}$. It can be seen that the incremental force-displacement relationship in (IV.6) consists of a linear part and an underlined nonlinear part. In general, this relationship must be solved by successive approximations, e.g., iteration. The linear part of (IV.7) can be used as a first approximation in a direct incremental procedure.

When the nodal displacement increments are found from (IV.6) they are added to the total nodal displacements at configuration 1 to give the total nodal displacements at configuration 2

$$^2r_j(z_n) = {}^1r_j(z_n) + r_j(z_n) \quad . \tag{IV.12}$$

Substitution of $r_j(z_n)$ in (IV.1) and the result in (IV.5) and (IV.4) gives the increments of stresses s_{ij}. Then by (I.15), (I.46), and (I.45) the Cauchy stress components in configuration 2 are found.

IV.2. Discretization of Shell Geometry

The shell is subdivided into a number of doubly curved ring elements and a cap element. Khojasteh Bakht [140] has found that doubly curved elements for which the positions, slopes, and curvatures of the shell meridian match at the nodes and which are described in local Cartesian coordinate systems give very good results for small deflection analysis of axisymmetric shells of revolution. Also, he studied a degenerate form of this element which has all of the above properties except that meridian curvatures do not match at the nodes. He designates these two types of elements as FDR(2) and FDR(1), respectively. He found that for a hemispherical shell under internal pressure the results with nine FDR(1) elements is the same as the exact solution. In the displacement method of finite element procedure the curvatures at the nodes of adjacent elements do not remain the same. In the present incremental method of large deflection analysis,the nodal curvatures are used in finding the varying geometry of the elements. Therefore, in order not to introduce additional constraint on the deformation of elements (by matching the curvatures) FDR(1) elements are used in this dissertation.

The meridional profile of the middle surface of the curved element FDR(1) for an arbitrary shell of revolution is shown in Figure IV.1. The local Cartesian coordinate system for this element is denoted by ξ and η.* ξ is a normalized coordinate with value 0 at i and 1 at j. The angles are positive as shown in the figure and the following relation applies

*η as a local Cartesian coordinate for an element is uded only in this Chapter. It should not be confused with η_{ij}, the nonlinear part of Lagrangian strain.

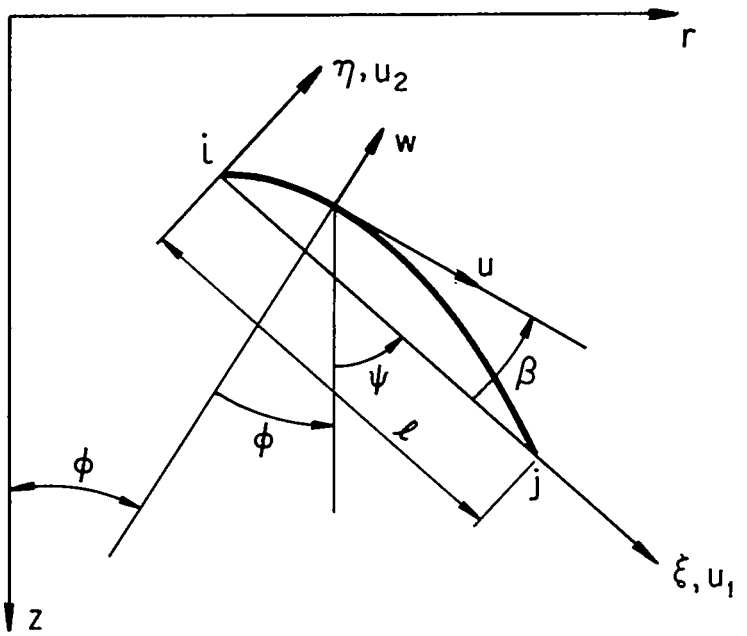

FIG. IV-1 DOUBLY CURVED ELEMENT

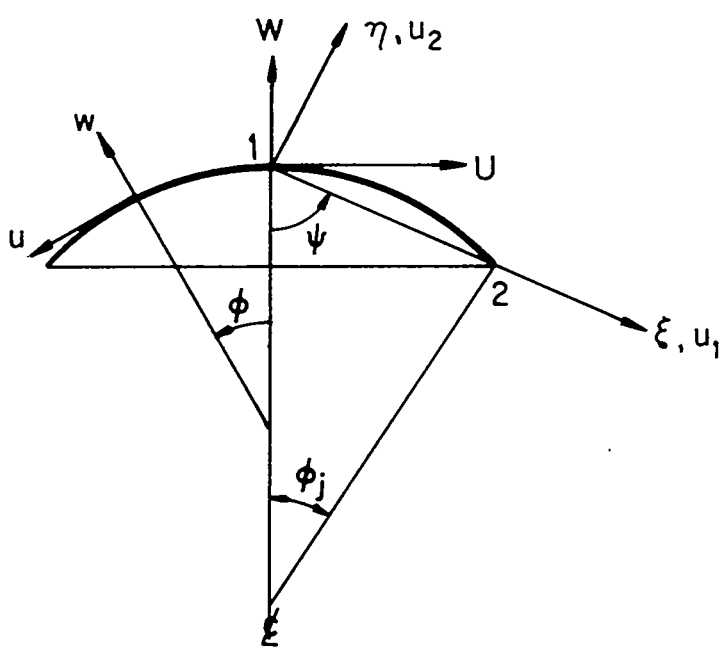

FIG. IV-2 CAP ELEMENT

$$\phi + \psi + \beta = \pi/2 \quad . \tag{IV.13}$$

In [140] the meridian of the FDR(1) element is represented by

$$\eta = \xi(1-\xi)(a_1+a_2\xi) \tag{IV.14}$$

where

$$a_1 = \tan \beta_i \tag{IV.15}$$

$$a_2 = -(\tan \beta_i + \tan \beta_j) \quad . \tag{IV.16}$$

The parameters in (IV.15) and (IV.16) are determined from

$$\Delta r = r_j - r_i$$

$$\Delta z = z_j - z_i$$

$$\Delta s = [\overline{\Delta r}^2 + \overline{\Delta z}^2]^{1/2} \tag{IV.17}$$

$$\sin \psi = \frac{\Delta r}{\Delta s} \quad , \quad \cos \psi = \frac{\Delta z}{\Delta s}$$

$$\sin \beta_n = \cos \phi_n \cos \psi - \sin \phi_n \sin \psi \qquad n = i,j$$

$$\cos \beta_n = \sin \phi_n \cos \psi + \cos \phi_n \sin \psi \quad .$$

The following relations which can be derived from the geometry of the substitute element will be used in some of the equations in the subsequent presentation.

$$\eta' = \frac{d\eta}{d\xi} = \tan \beta$$

$$\eta'' = \frac{d^2\eta}{d\xi^2} = -\frac{\ell}{R_s \cos^3\beta} \quad , \qquad \ell \text{ is the cord length}$$

$$r = r_i + \ell\xi(\sin \psi + \frac{\eta}{\xi} \cos \psi)$$

$$\frac{ds}{d\xi} = \frac{\ell}{\cos \beta} \qquad \text{(IV.18)}$$

$$\frac{1}{R_s} = -\frac{\eta''}{\ell} \cos^3\beta$$

$$\cos \phi = \cos \beta(\tan \beta \cos \psi + \sin \psi)$$

$$\sin \phi = \cos \beta(\cos \psi - \tan \beta \sin \psi)$$

IV.3. Displacement Pattern

Following the work in [140] the displacements of the middle surface of the elements will be chosen to be u_1 and u_2 (see Figure IV.1). These displacements are expanded in terms of the generalized displacement coefficients α_i. For a ring element these expansions are

$$u_1 = \alpha_1 + \alpha_2 \xi \quad ,$$

and (IV.19)

$$u_2 = \alpha_3 + \alpha_4 \xi + \alpha_5 \xi^2 + \alpha_6 \xi^3 \quad ,$$

where $0 \leq \xi \leq 1$. These displacement expansions satisfy the requirements of rigid body motion and compatibility for the elements of axisymmetrically loaded shells of revolution. It can be shown that they do not give all of the constant strains required for uniform convergence of the solution unless angle β is zero.* However, when the length of the meridian of the curved elements is chosen to be small and approximately equal to the cord lengths then the constant strain requirement will be satisfied sufficiently well.

The transformation between the displacements u_1, u_2 and u, w is as follows

$$\begin{Bmatrix} u \\ w \end{Bmatrix} = \begin{bmatrix} \cos\beta & \sin\beta \\ -\sin\beta & \cos\beta \end{bmatrix} \begin{Bmatrix} u_1 \\ u_2 \end{Bmatrix} \quad . \qquad \text{(IV.20)}$$

*This point was brought to the author's attention by Mr. P. Larsen, Graduate Student in the Division of Structural Engineering and Structural Mechanics, University of California, Berkeley, California.

At the top of a cap element for the axisymmetrically deformed shell of revolution the displacement u and the rotation ω vanish (see Figure IV.2). Hence from (IV.19), (IV.13), and (IV.20)

$$\alpha_1 = - \cos \psi \frac{\alpha_3}{\sin \psi} = - \cos \psi \, \alpha_3' \quad . \tag{IV.21}$$

Also, when $\omega = 0$ then $\sin \omega = 0$ and from (III.7) it can be seen that $\chi = 0$. Substitution of (IV.19) and (IV.20) into (III.5) gives

$$\alpha_2 = \tan \psi \, \alpha_4 = \alpha_4' \tag{IV.22}$$

Hence the displacement pattern for the cap element is

$$\begin{aligned} u_1 &= - \cos \psi \, \alpha_3' + \alpha_4' \, \xi \\ u_2 &= \sin \psi \, \alpha_3' + \tan \beta_1 \, \alpha_4' \, \xi + \alpha_5 \, \xi^2 + \alpha_6 \, \xi^3 \end{aligned} \tag{IV.23}$$

In the regions of the shell where the rate of change of meridional variables like meridional curvature and in plane force is high many elements must be used so that the linear expansion for u_1 can give reasonably accurate results.

IV.4. Strain-Displacement Relations

For the present numerical application the terms of the type $e_\theta \chi$, and $e_s \chi$ have been neglected in the curvature terms (III.24). Then the strain vector is

$$\{\varepsilon\} = \{e\} + \{\eta\} \tag{IV.24}$$

where

$$\{e\}^T = < e_s \; e_\theta \; \kappa_s{}^o \; \kappa_\theta{}^o > \tag{IV.25}$$

$$\{\eta\}^T = < \eta_s \; \eta_\theta \; \kappa_s{}^1 \; \kappa_\theta{}^1 > \tag{III.55}$$

$$\kappa_s{}^o = \chi_{,s} + \frac{e_s}{R_s} \quad , \quad \kappa_\theta{}^o = \frac{\cos \phi}{r} \chi + \frac{e_\theta}{R_\theta} \tag{IV.26}$$

$$\kappa_s{}^1 = \frac{\chi^2}{2R_s} \quad , \quad \kappa_\theta{}^1 = - \frac{\sin \phi}{2r} \chi^2 \quad . \tag{IV.27}$$

Substitution of (IV.20) in (III.3) - (III.5) gives

$$\begin{aligned} e_s &= \frac{\cos^2 \beta}{\ell} \left(\frac{du_1}{d\xi} + \tan \beta \frac{du_2}{d\xi} \right) \quad , \\ e_\theta &= \frac{1}{r} (\sin \psi \; u_1 + \cos \psi \; u_2) \quad , \\ \chi &= \frac{\cos^2 \beta}{\ell} \left(\tan \beta \frac{du_1}{d\xi} - \frac{du_2}{d\xi} \right) \quad . \end{aligned} \tag{IV.28}$$

IV.5. Element Stiffness Matrices

Four stiffness matrices were derived for the incremental force-displacement relation (IV.6). For a linear incremental procedure only $K^{(o)}$ and $K^{(1)}$ are required. These two matrices will be derived in this section for axisymmetric shells of revolution.

IV.5.1. Stiffness matrix $k^{(o)}$

It was demonstrated in Section IV.1. that in the general case the stiffness matrix $K^{(o)}$ is derived from the linear part of $s_{ij}\delta\varepsilon_{ij}$ in (I.27). For the axisymmetric shells of revolution $k^{(o)}$ is associated with the linear part of $\delta\{\varepsilon\}^T[D]\{\varepsilon\}$ in (III.54). The relationship between the linear part of strain, $\{e\}$, and the generalized coordinates $\{\alpha\}$ can be found by substitution of (IV.19), (IV.28), and (IV.26) into (IV.25). In matrix notation

$$\underset{4\times1}{\{e\}} = \underset{4\times4}{[B(\xi)]}\,\underset{4\times1}{\{\alpha\}} \qquad \text{(IV.29)}$$

where matrix $[B(\xi)]$ is given in Appendix G for both ring and cap elements. Therefore, when (III.54) is written for an element of the shell and in terms of coordinates ξ-η (see Figure IV.1), then

$$\underset{6\times6}{[K_\alpha^{(o)}]} = \int_o^1 \ell[B(\xi)]^T[D(\xi)][B(\xi)]r(\xi)(1+\eta'^2)^{1/2}\,d\xi \quad . \qquad \text{(IV.30)}$$

The components of the rigidity matrix $[D(\xi)]$ are obtained by the integrations in (III.61) - (III.63). These integrals are evaluated numerically. In order to follow the history of deformation of the shell in the elastic-plastic analysis sufficiently large number of points should be considered in the thickness of the shell and, therefore, simple methods of

numerical integration can be used. It has been found in [140,141] that rectangular rule of numerical integration is satisfactory. For this procedure the shell is divided into a number of layers along its thickness (see Figure IV.3). The material property matrices $[\bar{C}]$ are assumed to be constant in the thickness of each layer. Then

$$
\begin{aligned}
[D_{11}(\xi)]_{2\times2} &= [\bar{D}_1(\xi)]_{2\times2} \quad , \\
[D_{12}(\xi)]_{2\times2} &= [D_{21}(\xi)]_{2\times2} = [\bar{D}_2(\xi)]_{2\times2} - \frac{1}{2} h(\xi) [\bar{D}_1(\xi)]_{2\times2} \quad , \qquad \text{(IV.31)} \\
[D_{22}(\xi)]_{2\times2} &= [\bar{D}_3(\xi)]_{2\times2} - h(\xi) [\bar{D}_2(\xi)]_{2\times2} + \frac{1}{4} h^2(\xi) [\bar{D}_1(\xi)]_{2\times2} \quad ,
\end{aligned}
$$

where

$$
\begin{aligned}
[\bar{D}_1(\xi)]_{2\times2} &= \sum_{k=1}^{n} [\bar{C}(\xi,\bar{h}_k)]_{2\times2} (h_k - h_{k-1}) \quad , \\
[\bar{D}_2(\xi)]_{2\times2} &= \frac{1}{2} \sum_{k=1}^{n} [\bar{C}(\xi,\bar{h}_k)]_{2\times2} (h_k^2 - h_{k-1}^2) \quad , \qquad \text{(IV.32)} \\
[\bar{D}_3(\xi)]_{2\times2} &= \frac{1}{3} \sum_{k=1}^{n} [\bar{C}(\xi,\bar{h}_k)]_{2\times2} (h_k^3 - h_{k-1}^3) \quad , \\
\bar{h}_k &= \frac{1}{2} (h_k - h_{k-1} - h) \quad .
\end{aligned}
$$

If the layers have equal thickness, then

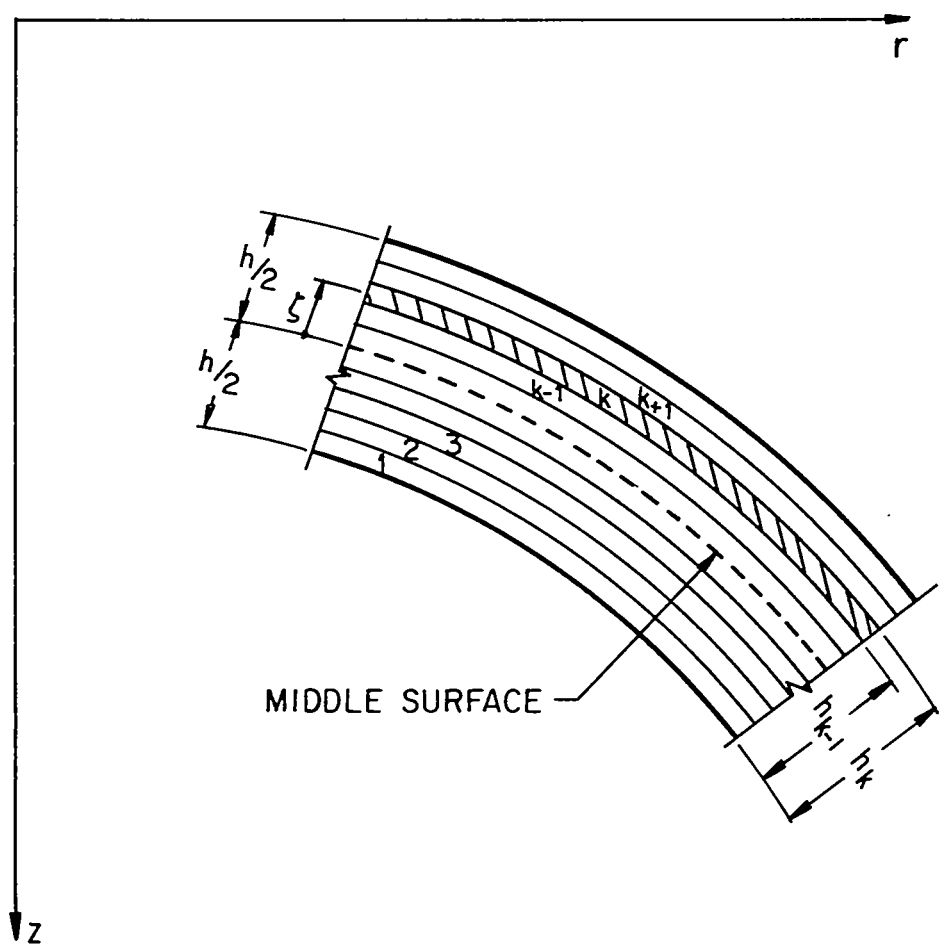

FIG. IV-3 SHELL THICKNESS

$$[\bar{D}_1(\xi)]_{2\times2} = \frac{h(\xi)}{n} \sum_{k=1}^{n} [\bar{C}(\xi,\bar{h}_k)]_{2\times2}$$

$$[\bar{D}_2(\xi)]_{2\times2} = \frac{h^2(\xi)}{n^2} \sum_{k=1}^{n} [\bar{C}(\xi,\bar{h}_k)]_{2\times2}(k - \tfrac{1}{2}) \qquad \text{(IV.33)}$$

$$[\bar{D}_3(\xi)]_{2\times2} = \frac{h^3(\xi)}{n^3} \sum_{k=1}^{n} [\bar{C}(\xi,h_k)]_{2\times2}(k^2 - k + \tfrac{1}{3}) \quad .$$

The value of the material property matrix $[\bar{C}(\xi,\zeta)]$ along the meridian of the element can be expressed in terms of its magnitude at the nodes by some suitable interpolation function. For sufficiently small elements linear interpolation can be used. Thus

$$[\bar{C}(\xi,\zeta)]_{2\times2} = (1-\xi)[\bar{C}(0,\zeta)]_{2\times2} + \xi[\bar{C}(1,\zeta)]_{2\times2} \quad . \qquad \text{(IV.34)}$$

In the same manner the variation of the shell thickness can be written as

$$h(\xi) = (1-\xi)\, h_i + \xi\, h_j \quad . \qquad \text{(IV.35)}$$

The integral in (IV.30) can be evaluated numerically. Gauss' integration formula is used for this purpose [142].

IV.5.2. Stiffness matrix $k^{(1)}$

The initial stress stiffness matrix $k^{(1)}$ is obtained from the term $\delta\{\eta\}^T\{N\}$ in (III.54). The components of the nonlinear strain vector $\{\eta(\xi)\}$ are given in (III.22) and (IV.27). Vector $\{\eta(\xi)\}$ can be written as

$$\{\eta(\xi)\}_{4\times1} = [F(\xi)]_{4\times4}\,\{\bar{\eta}(\xi)\}_{4\times1} \qquad \text{(IV.36)}$$

where

$$\underset{1\times4}{\{\eta(\xi)\}^T} = < \frac{\chi^2}{2} \quad 0 \quad \frac{\chi^2}{2} \quad \frac{\chi^2}{2} > \quad , \tag{IV.37}$$

and

$$\underset{4\times4}{[F(\xi)]} = \begin{bmatrix} 1 & 0 & 0 & 0 \\ 0 & 0 & 0 & 0 \\ 0 & 0 & \frac{1}{R_s} & 0 \\ 0 & 0 & 0 & \frac{-\sin\phi}{r} \end{bmatrix} \quad . \tag{IV.38}$$

Also let the stress resultants in configuration 1 be expressed by

$$\underset{4\times1}{\{{}^1N(\xi)\}} = \underset{4\times4}{[{}^1N(\xi)]} \; \underset{4\times1}{\{I\}} \tag{IV.39}$$

where

$$\underset{1\times4}{\{{}^1N(\xi)\}^T} = < {}^1N_s \quad {}^1N_\theta \quad {}^1M_s \quad {}^1M_\theta > \quad , \tag{IV.40}$$

$$\underset{4\times4}{[{}^1N(\xi)]} = \begin{bmatrix} {}^1N_s & 0 & 0 & 0 \\ 0 & {}^1N_\theta & 0 & 0 \\ 0 & 0 & {}^1M_s & 0 \\ 0 & 0 & 0 & {}^1M_\theta \end{bmatrix} \quad , \tag{IV.41}$$

and

$$\underset{1\times4}{\{I\}^T} = < 1 \quad 1 \quad 1 \quad 1 > \quad . \tag{IV.42}$$

The variation of $\delta\{\bar{\eta}(\xi)\}$ is

$$\underset{1\times4}{\delta\{\bar{\eta}(\xi)\}^T} = < \chi\delta\chi \quad 0 \quad \chi\delta\chi \quad \chi\delta\chi > \quad . \tag{IV.43}$$

This variation can be written as

$$\underset{4\times1}{\delta\{\overline{\eta}(\xi)\}} = \underset{4\times4}{[\chi(\xi)]} \; \underset{4\times4}{\{\delta\chi(\xi)\}} \tag{IV.44}$$

where

$$\underset{1\times4}{\delta\{\chi(\xi)\}^T} = \delta < \chi(\xi) \quad 0 \quad \chi(\xi) \quad \chi(\xi) > \quad , \tag{IV.45}$$

$$[\chi(\xi)] = \begin{bmatrix} \chi(\xi) & 0 & 0 & 0 \\ 0 & 0 & 0 & 0 \\ 0 & 0 & \chi(\xi) & 0 \\ 0 & 0 & 0 & \chi(\xi) \end{bmatrix} \quad , \tag{IV.46}$$

Substitution of (IV.36), (IV.39) and (IV.44) into $\delta\{\eta\}^T\{N\}$ gives

$$\underset{1\times4}{\delta\{\eta(\xi)\}^T} \; \underset{4\times1}{\{{}^1N(\xi)\}} = \underset{1\times4}{\delta\{\chi(\xi)\}^T} \; \underset{4\times4}{[F(\xi)]} \; \underset{4\times4}{[{}^1N(\xi)]} \; \underset{4\times1}{\{\chi(\xi)\}} \; . \tag{IV.47}$$

Also substitution of (IV.19) into $(IV.28)_3$ gives

$$\underset{4\times1}{\{\chi(\xi)\}} = \underset{4\times4}{[G(\xi)]} \; \underset{4\times1}{\{\alpha\}} \tag{IV.48}$$

where Matrix $[G(\xi)]$ is given in Appendix G for both ring and cap elements.

In view of (IV.48), expression (IV.47) becomes

$$\underset{1\times4}{\delta\{\eta(\xi)\}^T} \; \underset{4\times1}{\{{}^1N(\xi)\}} = \underset{1\times4}{\delta\{\alpha\}^T} \; \underset{4\times4}{[G(\xi)]^T} \; \underset{4\times4}{[F(\xi)]} \; \underset{4\times4}{[{}^1N(\xi)]} \; \underset{4\times4}{[G(\xi)]} \; \underset{4\times1}{\{\alpha\}} \; . \tag{IV.49}$$

Substitution of (IV.49) into (III.54) results in the following expression for the initial stress stiffness matrix of an element

$$\underset{6\times6}{[k_\alpha^{(1)}]} = \int_0^1 \ell[G(\xi)]^T[F(\xi)][{}^1N(\xi)][G(\xi)] \; r(\xi) \; (1+\eta'^2)^{1/2} \; d\xi \quad . \tag{IV.50}$$

IV.6. The Incremental Force-Displacement Relations

The displacement vector for an element is chosen to be

$$\underset{1\times3}{\{V(\xi)\}^T} = < u_1(\xi) \quad u_2(\xi) \quad \chi(\xi) > \quad . \tag{IV.51}$$

Substitution of (IV.19) and (IV.28) in (IV.51) results in

$$\underset{3\times1}{\{V(\xi)\}} = \underset{3\times6}{[\phi(\xi)]}\underset{6\times1}{\{\alpha\}} \tag{IV.52}$$

where $[\phi(\xi)]$ is given in Appendix G. Substitution of (IV.52) in (III.54) results in the following expression for the generalized force of the element.

$$\underset{6\times1}{\{Q_\alpha\}} = \int_0^1 \ell[\phi(\xi)]^T\{\tilde{p}(\xi)\}r(\xi)(1+\eta'^2)^{1/2}\, d\xi \tag{IV.53}$$

where, for a linear interpolation, the surface force vector $\{\tilde{p}(\xi)\}$ can be written as

$$\underset{3\times1}{\{\tilde{p}(\xi)\}} = (1-\xi)\underset{3\times1}{\{\tilde{p}_i\}} + \xi\underset{3\times1}{\{\tilde{p}_j\}} \quad . \tag{IV.54}$$

The linear incremental force-displacement relations for an element in coordinate system $\{\alpha\}$ is

$$\underset{6\times1}{\{Q_\alpha\}} = \underset{6\times6}{[k_\alpha]}\underset{6\times1}{\{\alpha\}} \tag{IV.55}$$

where

$$\underset{6\times6}{[k_\alpha]} = \underset{6\times6}{[k_\alpha^{(o)}]} + \underset{6\times6}{[k_\alpha^{(1)}]} \tag{IV.56}$$

At the nodes of the element, equation (IV.52) has the form

$$\underset{6\times1}{\{q\}} = \underset{6\times6}{[A]}\underset{6\times1}{\{\alpha\}} \tag{IV.57}$$

where $\{q\}$ is the vector of nodal displacements in ξ-η coordinate system

$$\underset{1\times6}{\{q\}} = \langle V_i : V_j \rangle \quad . \tag{IV.58}$$

The coefficients α are obtained in terms of $\{q\}$ by inversion of (IV.57)

$$\underset{6\times1}{\{\alpha\}} = \underset{6\times6}{[A^{-1}]}\ \underset{6\times1}{\{q\}} \tag{IV.59}$$

where matrix $[A^{-1}]$ is given in Appendix G. The relationship between the components of nodal point displacement vector in ξ-η coordinates, $\{q\}$, and the corresponding components in the surface coordinates, $\{r\}$ is given by

$$\underset{6\times1}{\{q\}} = \underset{6\times6}{[T]}\ \underset{6\times1}{\{r\}} \tag{IV.60}$$

where

$$\underset{1\times6}{\{r\}^T} = \langle r_i : r_j \rangle$$

$$\underset{1\times3}{\{r_i\}^T} = \langle u_i\ w_i\ \chi_i \rangle \tag{IV.61}$$

The matrix $[T]$ is given in Appendix G. Transformation of (IV.55) into surface coordinates results in the following incremental force-displacement relation

$$\underset{6\times1}{\{Q\}} = \underset{6\times6}{[k]}\ \underset{6\times1}{\{r\}} \tag{IV.62}$$

where

$$\underset{6\times1}{\{Q\}} = \underset{6\times6}{[T]^T}\ \underset{6\times6}{[A^{-1}]^T}\ \underset{6\times1}{\{Q_\alpha\}} \quad , \tag{IV.63}$$

$$\underset{6\times1}{\{r\}} = \underset{6\times6}{[T]^T}\ \underset{6\times6}{[A]}\ \underset{6\times1}{\{\alpha\}} \quad , \tag{IV.64}$$

and

$$\underset{6\times6}{[k]} = \underset{6\times6}{[T]^T}\ \underset{6\times6}{[A]^T}\ \underset{6\times6}{[k_\alpha]}\ \underset{6\times6}{[A^{-1}]}\ \underset{6\times6}{[T]} \tag{IV.65}$$

Considering the equilibrium and compatibility requirements at the nodal circles, the relations (IV.62) of the elements are combined using the direct stiffness method and the incremental force-displacement relations for the whole shell is obtained.

$$\underset{N\times1}{\{R\}} = \underset{N\times N}{[K]}\ \underset{N\times1}{\{r\}} \tag{IV.66}$$

where N is the number of elements of the shell; $\{r\}$, and $\{R\}$ are the vectors of all incremental nodal displacements and generalized forces; and $[K]$ is the total incremental stiffness matrix of the shell.

IV.7. The Procedure of Incremental Analysis

The procedure for the analysis of large deflections of elastic-plastic shells of revolution using the finite element scheme developed in this chapter is outlined in this section. The incremental solution starts from a known initial configuration where the shell is assumed to be free of stress. Then load increments are added successively. For each one corresponding displacement increments are obtained, and the geometry and the material properties of the shell are renewed accordingly to be used as the initial values for the next increment. The details of the procedure for a typical increment of load for strain hardening materials is as follows. The displacement increments are found from (IV.66) and the increments of strain for each layer in the shell thickness are obtained from (IV.29), (IV.48), (III.14), and (III.15). The total strains are obtained from (B.5) which for the physical components of strains in axisymmetric shells of revolution becomes

$$\begin{aligned} {}^{2}\varepsilon_{11} &= {}^{1}\varepsilon_{11} + (1 + 2\,{}^{1}\varepsilon_{11})\,\varepsilon_{11} \quad , \\ {}^{2}\varepsilon_{22} &= {}^{1}\varepsilon_{22} + (1 + 2\,{}^{1}\varepsilon_{22})\,\varepsilon_{22} \quad . \end{aligned} \tag{IV.67}$$

From (III.29) the Piola stress increments are calculated and are used in (I.15) to find the total Piola stresses which are then transformed to Cauchy stresses by

$$\begin{aligned} {}^{2}\tau_{11} &= \sqrt{\frac{1+2\varepsilon_{11}}{1+2\varepsilon_{22}}}\;\; {}^{2}s_{11} \quad , \\ {}^{2}\tau_{22} &= \sqrt{\frac{1+2\varepsilon_{22}}{1+2\varepsilon_{11}}}\;\; {}^{2}s_{22} \quad . \end{aligned} \tag{IV.68}$$

The loading criterion (II.23) is checked and for loading the plastic increments of strain are used to find the increment in equivalent plastic strain (II.41) which is used to find the total equivalent plastic strain by

$$^{2}(\ \bar{\varepsilon}^{p}) = {}^{1}(\ \bar{\varepsilon}^{p}) + (\Delta\ \bar{\varepsilon}^{p}) \quad . \tag{IV.69}$$

This strain is utilized in the uniaxial stress-strain curve to find the tangent modulus and the equivalent stress $\bar{\sigma}$ (see Figure II.3). The value of $\bar{\sigma}$ is used to modify the new state of stress. The tangent modulus together with the new state of stress and strain are used in (III.30) and (III.31) to find the new material properties. The new geometry of the shell is obtained from (IV.12) and (III.7). Now the next increment of load can be added for which the above procedure is repeated.

The procedure explained here is essentially a forward integration method where the magnitude of the variables at the beginning of each increment is used for the integration during the increment. This method can be improved by various integration techniques, see, e.g., [143]. It was found in [141] that a modified Euler method gives improved results for the case of infinitesimal deflections of elastic-plastic circular plates. This modification can also be used in the present problem.

CHAPTER V: NUMERICAL EXAMPLES

In this chapter the linear incremental procedure developed in Chapter IV is applied to the large deflection elastic-plastic analysis of some axisymmetrically deformed shells of revolution. The purpose is to study the accuracy and convergence of the direct linear incremental method and, therefore, no auxiliary numerical procedures have been introduced to improve the accuracy of the results. A complete study of the nonlinear incremental procedure of Chapter IV requires either an iteration scheme or some improved integration techniques like modified Euler or Runge-Kutta method [143].

A brief description of the computer program is given and then several examples in the elastic and elastic-plastic range are solved.

V.1. Outline of Computer Program

A computer program was developed and used for the nonlinear elastic-plastic analysis of axisymmetrically loaded and supported shells of revolution. The linear incremental method of Chapter IV is used.

The program is in Fortran IV language and was used on CDC 6400 computer. The capacity of the program is limited to maintain an in-core analysis. Examples with up to 80 elements each with 20 layers can be treated. The capacity can be increased by means of out-of-core storage facilities if required.

A concise outline of the computer program is given in Fig. V.1. This chart, together with the explanations in Section IV.7, is enough to acquaint the reader with the basic steps and some details of the program. The listing and the instructions for using the program will be published in another report.

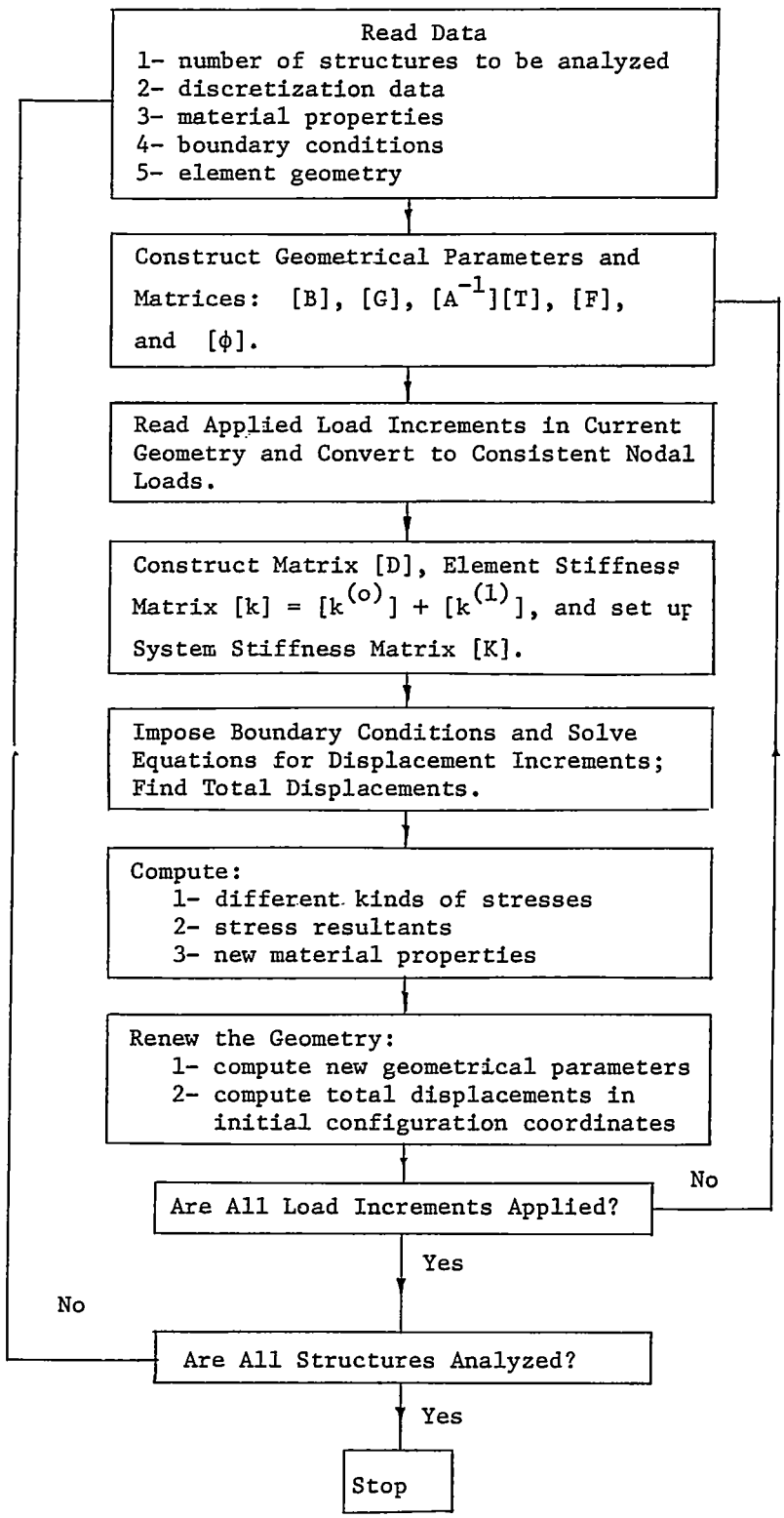

Fig. V.1 Concise Outline of Computer Program

V.2. Elastic Solutions

In this section the results of the linear incremental finite element method are compared with some other existing theoretical solutions for elastic circular plates and shallow spherical shells. The purpose is to check the accuracy and convergence of the present method in the elastic range.

V.2.1. Circular Plates

The incremental method is applied to a clamped circular elastic plate and the results of normal central deflection, and membrane and bending stresses are compared with Way's power series expansion solution [121] (see Figures V.2, and V.3). Since the plots are dimensionless, the results are applicable to any clamped circular plate with Poisson's ratio of 0.3.

As the plots in Figures V.2, and V.3 indicate, the agreement between the present results and Way's solution is good for both displacements and stresses. There is practically no difference between the results obtained for the load increments $(a/h)^4(\Delta p/E) = 0.54$ and half this value. In this example the cord length of an element was chosen as $0.055a$. The computer time used per increment of load per element is 0.65 seconds.

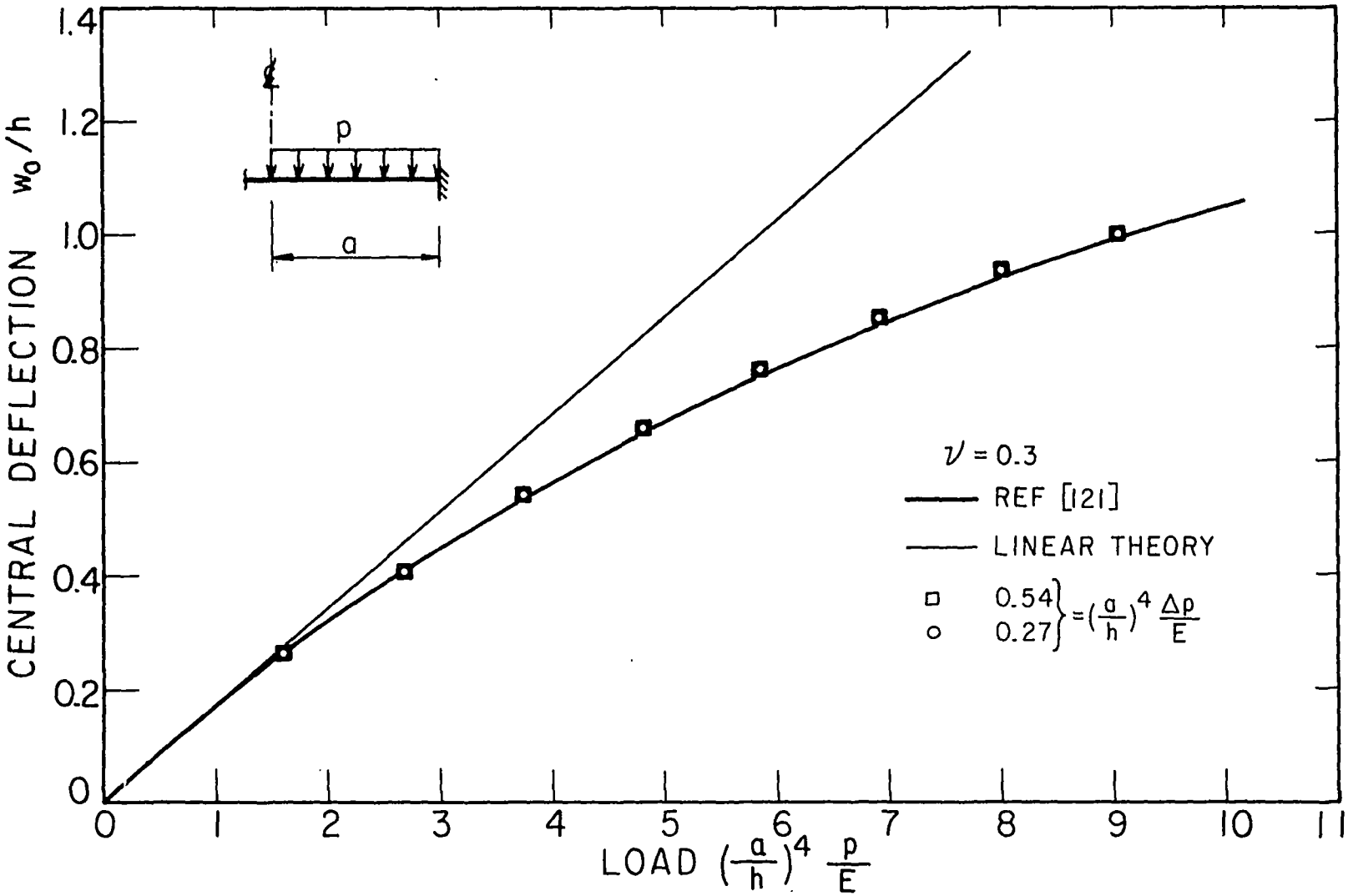

FIG. V-2 LOAD-DEFLECTION CURVE FOR CLAMPED CIRCULAR PLATE

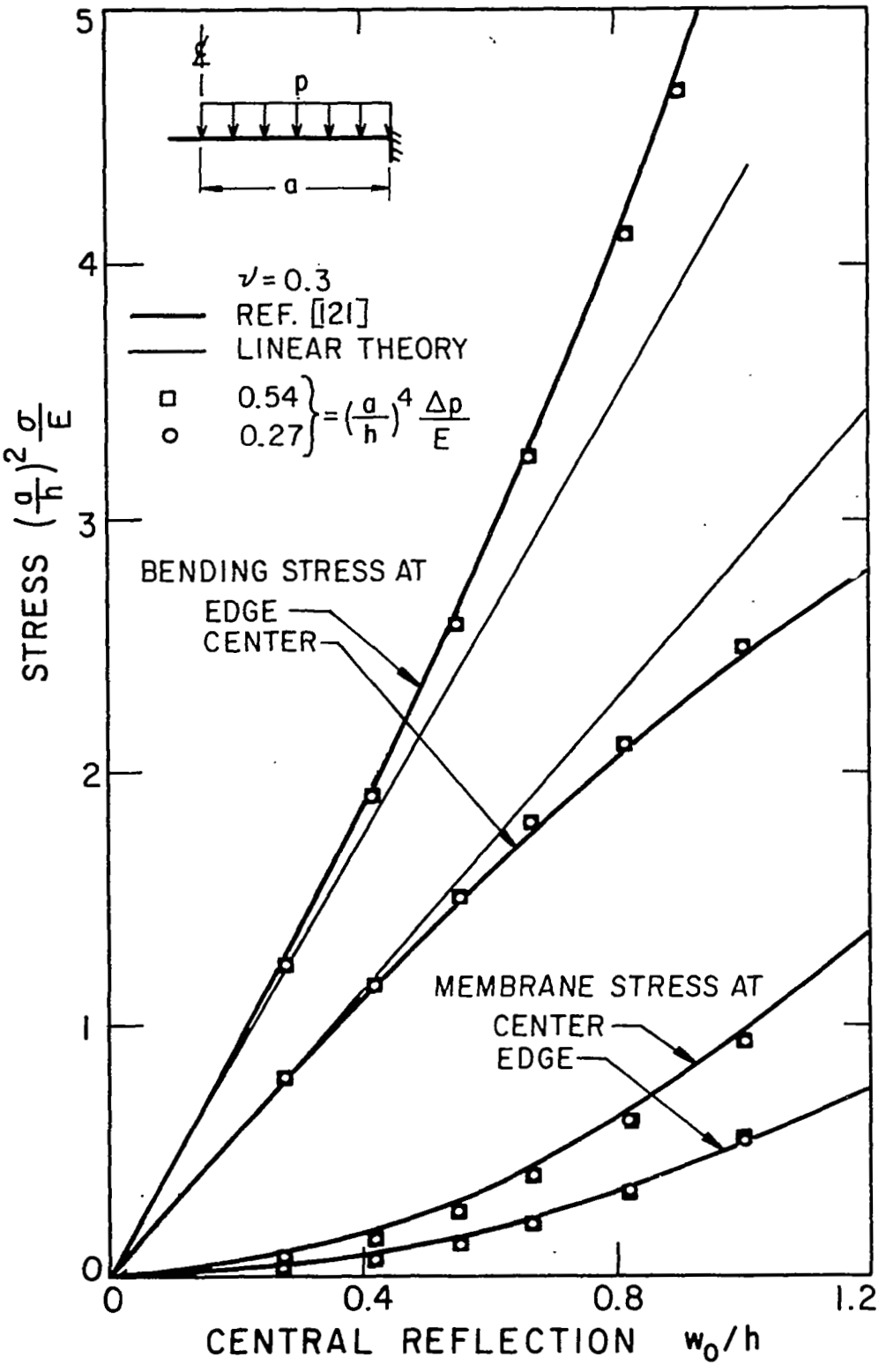

FIG. V-3 STRESSES FOR CLAMPED CIRCULAR PLATE

V.2.2. Shallow Shells

Nonlinear elastic solutions are given for two clamped shallow spherical shells with different parameters λ. The geometric parameter λ for shallow shells is defined by $\lambda = [\sqrt{12(1-\nu^2)}(a^2/hR)]^{1/2}$ where h is the thickness of the shell, and R and z are shown in Figure V.4. The values of λ for the present examples are low enough to assure axisymmetric deflections.

A. Comparison with Kornishin's Solution

In this example the results of the linear incremental method are compared with Kornishin's power series solution [144] for a shallow spherical cap with $\lambda = 2.22$ (see Figure V.4). The dimensionless results in Figure V.4 apply to any shallow spherical cap as long as $\lambda = 2.22$, Poisson's ratio $\nu = 0.3$, and the shell is thin. Values of 0.75 and 0.375 are used for the dimensionless load increments. The load-deflection curve in Figure V.4 indicates that the results by the smaller load increments are closer to Kornishin's curve for $(w_o/h) < 2$. Beyond that the results of the larger load increments are closer. This can be attributed to the fact that since in a linear incremental procedure the increments are taken along the slope to the load-deflection curve and the true slope is more closely approximated by smaller load increments, then in the present example near $(w_o/h) = 1.5$ where the tangent is almost horizontal the smaller load increments overestimate the deflection. This problem can be overcome if instead of the present linear incremental procedure the nonlinear incremental formulation of Section IV.1 is used. It can also be treated by replacing the present linear

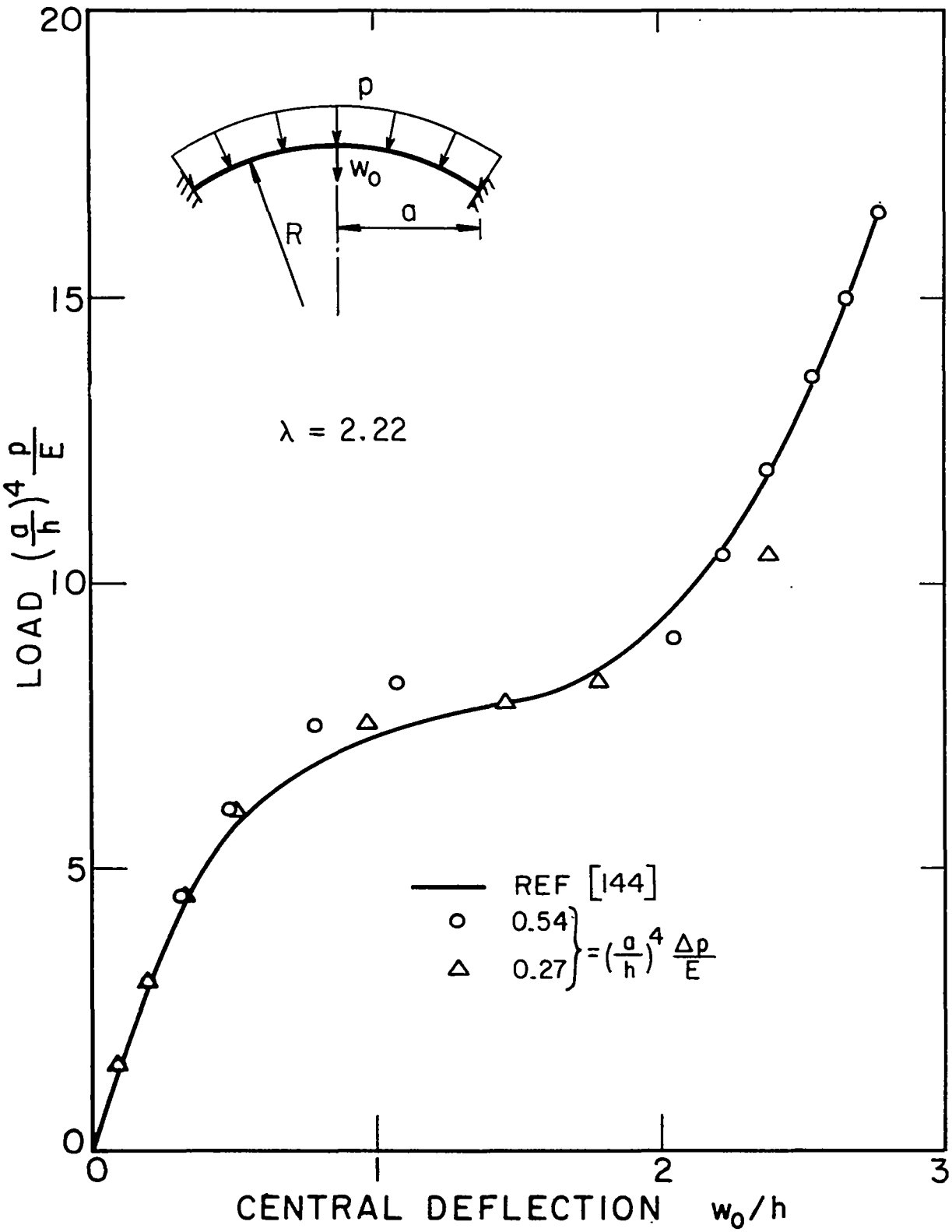

FIG. V-4 LOAD DEFLECTION CURVE FOR SHALLOW SPERICAL SHELL

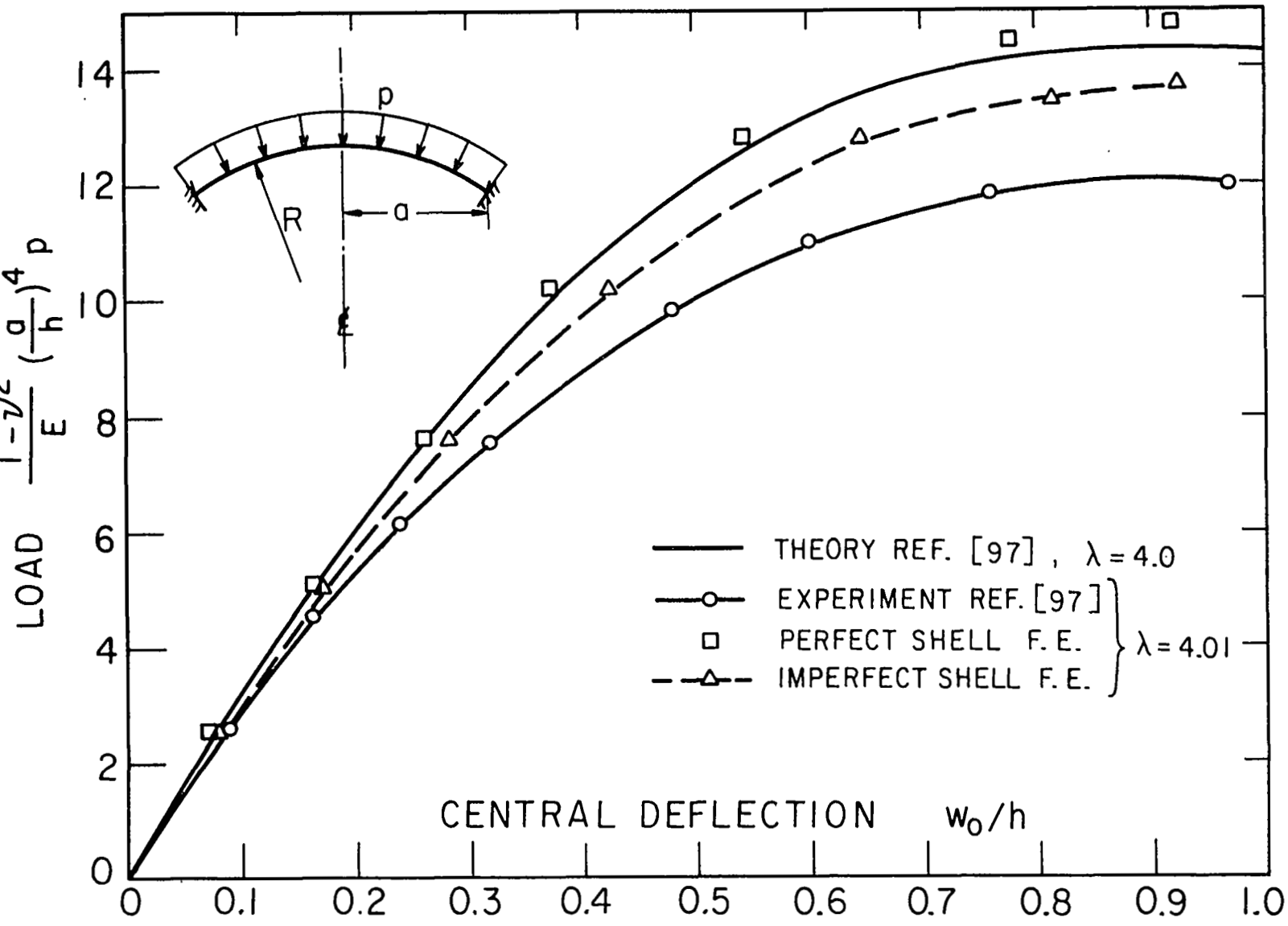

FIG. V-5 LOAD-DEFLECTION CURVE FOR SHALLOW SPHERICAL SHELL

incremental procedure which is actually Euler's forward integration method by the modified Euler or Runge-Kutta method [143].

Eighteen elements were used in the present example with finer elements near the edge of the shell. The computer time per load increment per element was 0.68 seconds.

B. Comparison with Kaplan and Fung's Results

The finite element solution is compared with Kaplan and Fung's experimental results and their theoretical perturbation solution for a shallow spherical cap with $\lambda = 4.01$ [97] (see Figure V.5). The finite element method is applied to both the initially perfect and imperfect shallow spherical cap. The geometrical imperfections measured in [97] were used. The result of the perfect shell agrees well with the theoretical solution in [97] and that of the imperfect shell is closer to the experimental observation but does not close the gap between the theoretical and experimental results.

Eighteen elements were used with finer elements at the boundary of the shell. The computer time per load increment per element was 0.68 seconds.

V.3. Elastic-Plastic Solution

The elastic-plastic behavior of a torispherical shell under internal pressure is studied. The results of nonlinear elastic-plastic analysis are reported and compared with those of nonlinear elastic and linear elastic-plastic analysis.

The geometrical dimensions of the shell are (see Figure V.6):

D = 100 in.		diameter of head skirt
R = D		radius of sphere
r = 0.2 D		meridional radius of torus
h = 0.008 D		shell thickness, uniform

The material of the shell is assumed to be elastic-perfectly plastic with yield stress $\sigma_y = 30 \times 10^3$ psi; and Young's modulus and Poisson's ratio $E = 30 \times 10^6$ psi, $\nu = 0.30$, respectively.

The shell is divided into 36 elements and the thickness of each element is divided into 16 equal layers. The convergence of the nonlinear analysis in the inelastic range is studied by using three different magnitudes for the load increments beyond the pressure of 390 psi (see Figure V.6). Below this pressure the load-deflection curve is almost linear and convergence study was considered to be unnecessary. The three load increments are 7.5, 15, and 30 psi. The results in Figure V.6 indicate that the convergence increases as the magnitude of load increments decreases and that the rate of convergence is quite rapid. The results in Figures V.7 to V.10 are for $\Delta p = 15$ psi. The average computer time used per load increment for each element is 0.765 seconds.

The comparison of the linear and nonlinear elastic-plastic load deflection curves in Figure V.6 indicates that for the same value of the apex normal deflection, w_o, the nonlinear analysis predicts higher load carrying capacity for the shell. The difference varies from zero to about 11% for displacements up to 0.4 inches. If deflection is used as the controlling factor in defining the ultimate load carrying capacity of the shell the above difference can be significant.

The variation of the normal displacement w, meridional bending moment M_s, and the circumferential in-plane force N_θ along the meridional curve of the shell are shown in Figures V.7, V.8, and V.9. It can be seen in Figure V.7 that the normal displacement of the non-linear analysis is appreciably less than that of the linear analysis all along the shell. The redistribution of stresses as a result of plastic deformation can be seen in Figures V.8 and V.9. The comparisons of linear and nonlinear elastic-plastic results in Figures V.8 indicates that for the same value of internal pressure the bending moments due to the nonlinear solution are appreciably less than the linear solution. The difference in the in-plane circumferential force for the two solutions can be seen in Figure V.9.

The elastic-plastic boundaries in the thickness of the shell for both linear and nonlinear analyses are shown in Figure V.10. In both solutions the first location in the shell which reaches the state of plasticity is the inner face of the toroidal part near the sphere edge. The plasticity for the linear solution sets in at $p = 250$ psi and for nonlinear solution at a pressure higher than this and less than $p = 280$ psi. Always the plastic regions for the linear solution propagate faster. The pattern of propagation of plastic regions is almost the same for both solutions. The plastic regions for the linear solution in the spherical part lean more towards the sphere-torus junction, whereas for the nonlinear solution they propagate faster towards the apex of the shell.

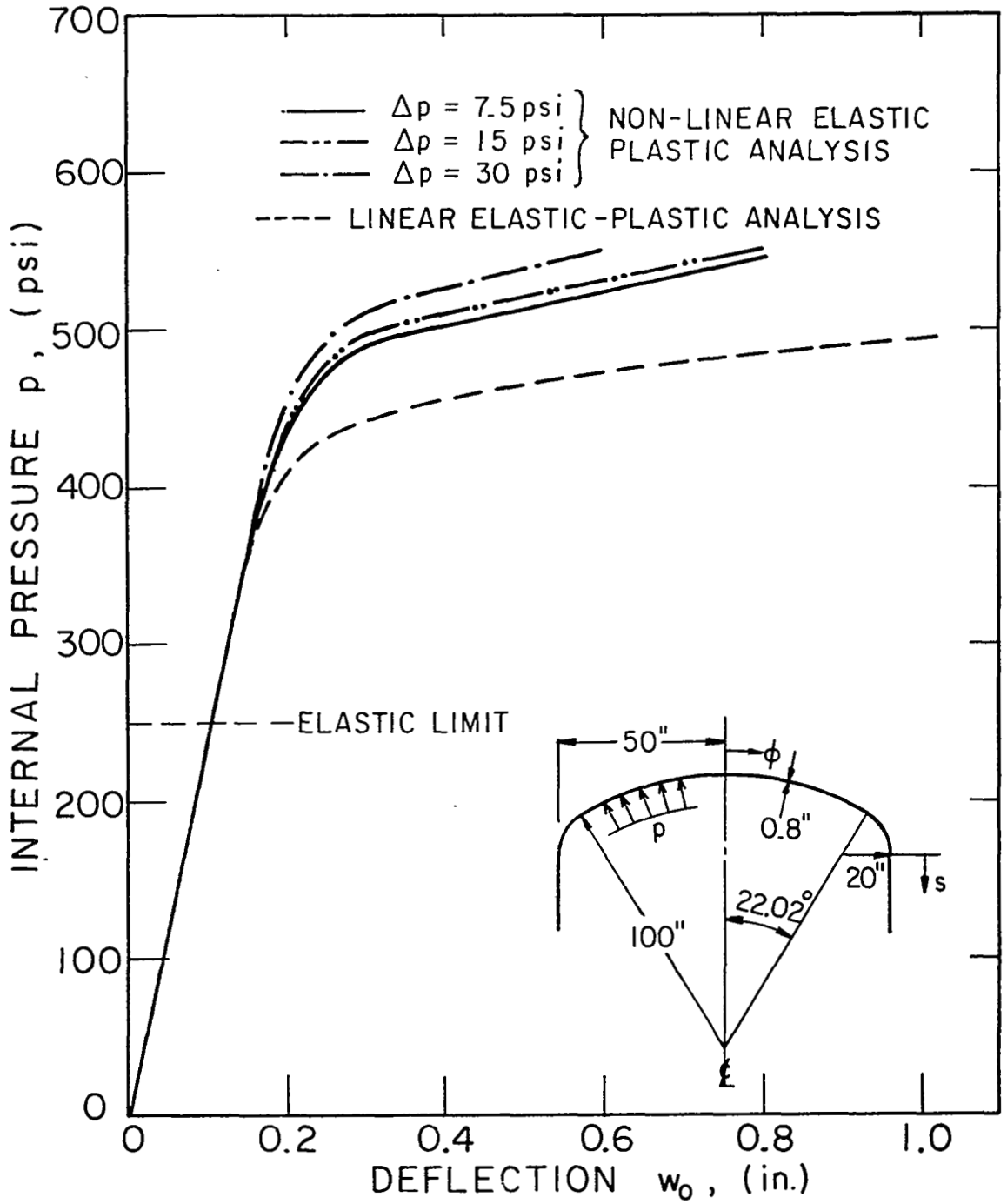

FIG. V-6 THE NORMAL DEFLECTION AT THE APEX , w_o

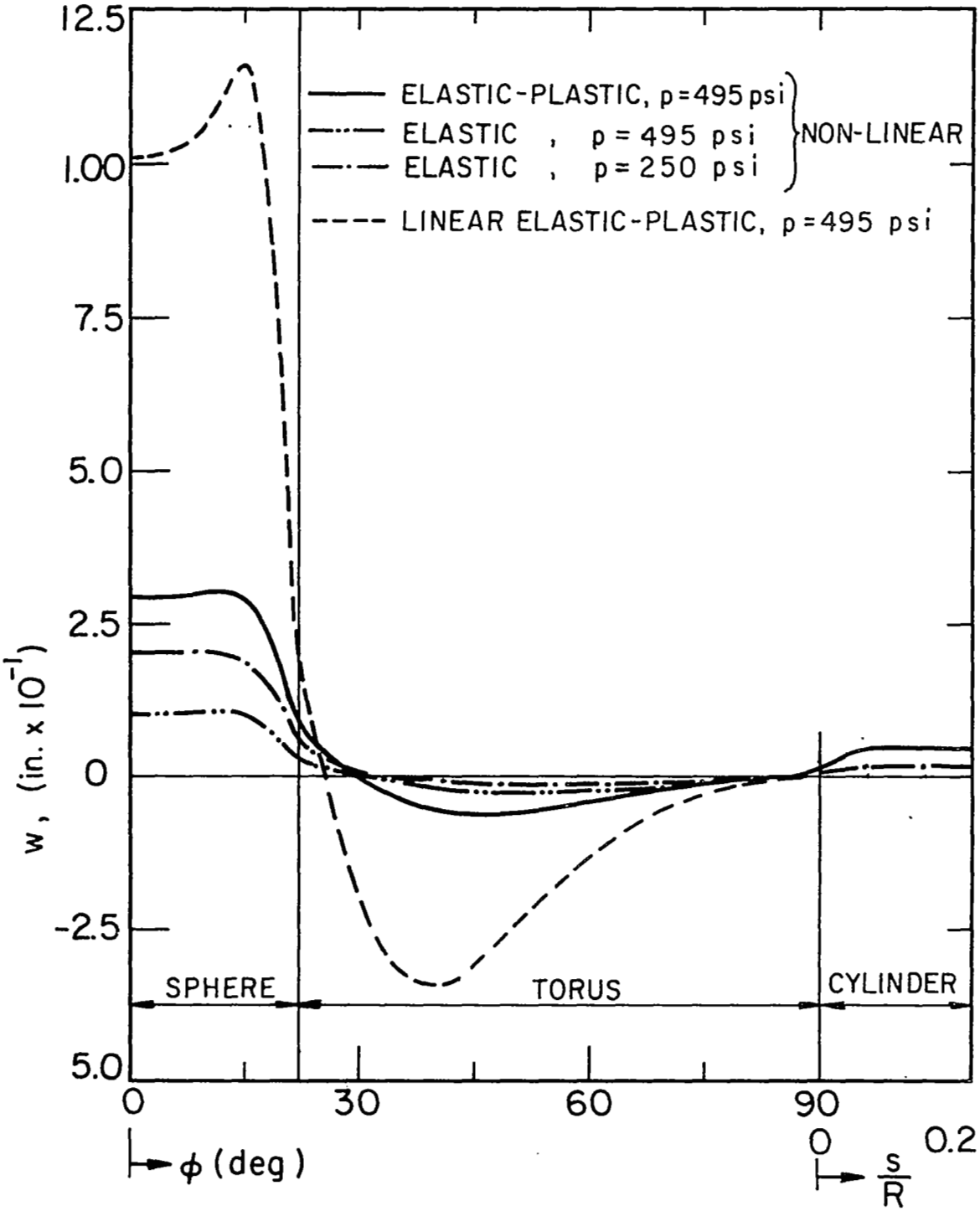

FIG. V-7 NORMAL DEFLECTIONS OF TORISPHERICAL SHELL

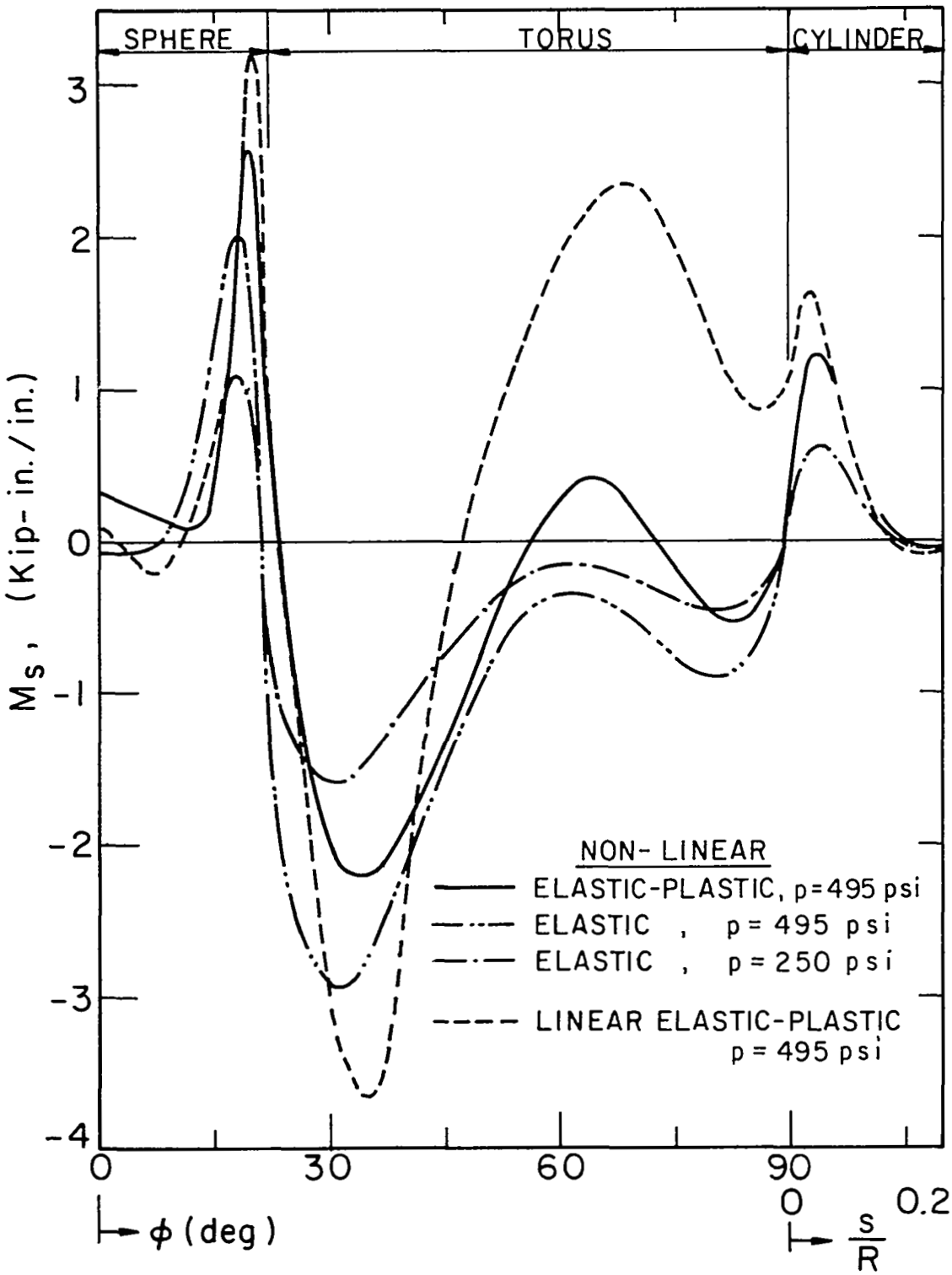

FIG. V-8 MERIDIONAL BENDING MOMENT M_s IN TORISPHERICAL SHELL

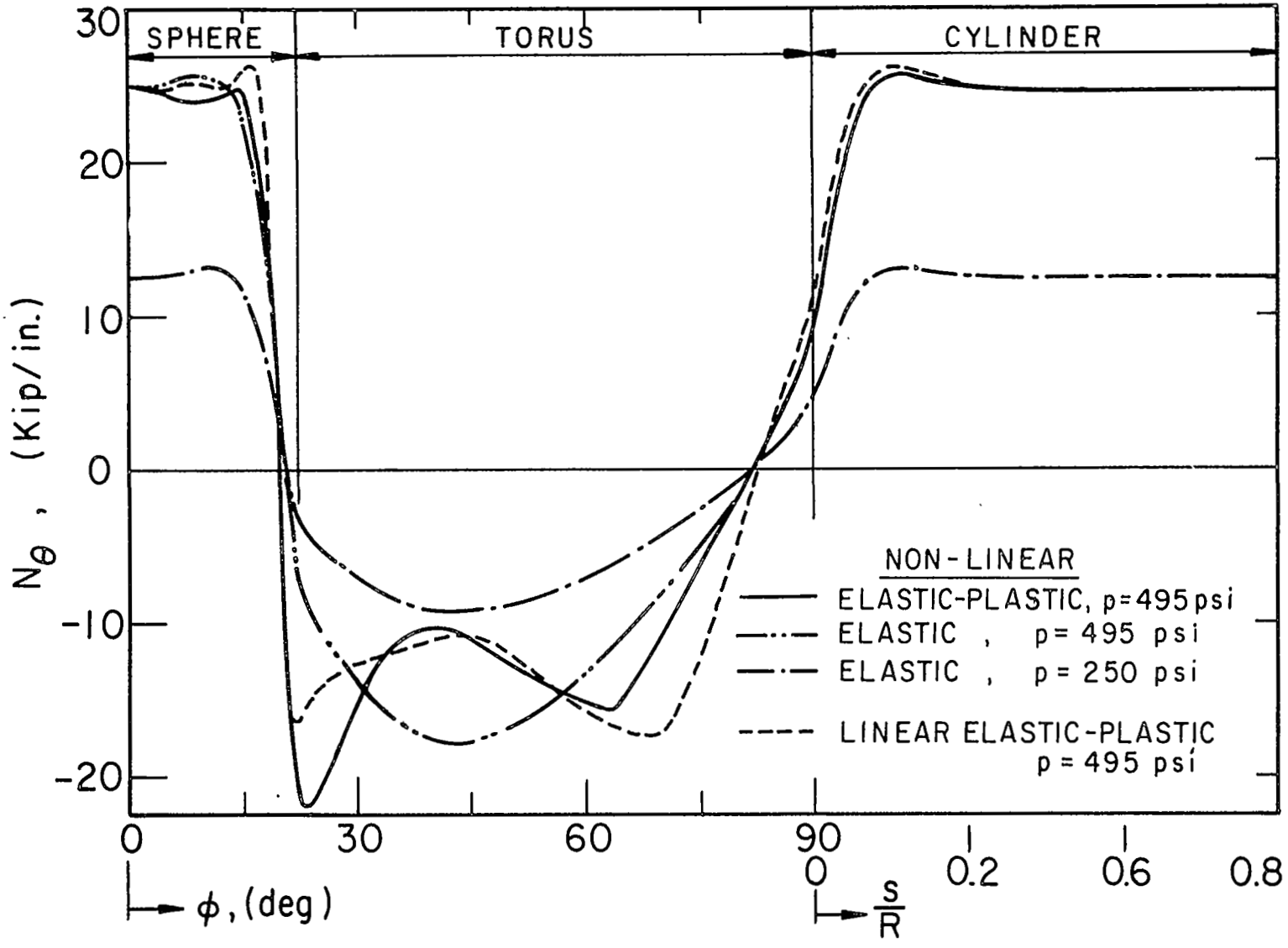

FIG. V-9 CIRCUMFERENTIAL MEMBRANE FORCE IN TORISPHERICAL SHELL

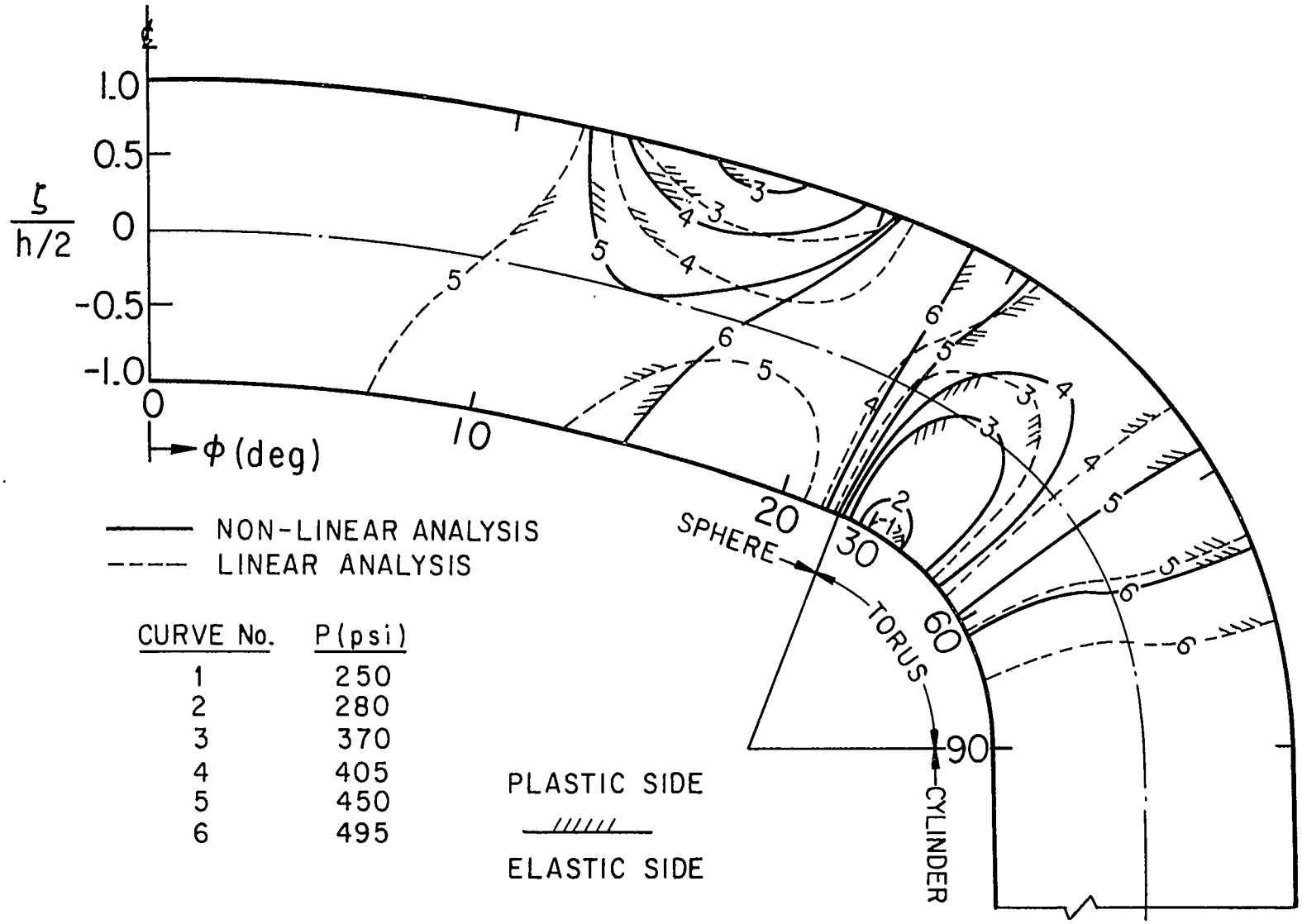

FIG. V-10 ELASTIC PLASTIC BOUNDARIES IN TORISPHERICAL SHELL

CHAPTER VI: SUMMARY AND CONCLUSIONS

An incremental variational method has been developed for the analysis of large deformations and/or displacements in continuum mechanics. Several forms of the incremental expressions of virtual work have been derived and one of them which utilizes a moving reference configuration has been used in the developments. It is shown that the incremental variational formulation leads to correct equations of equilibrium and boundary conditions.

General incremental nonlinear constitutive equations have been derived for elastic materials taking into consideration the invariance requirements in continuum mechanics and the laws of thermodynamics. Correspondingly, an incremental theory of plasticity suitable for initially isotropic materials and for the case of small deformations but large rotations has been developed by specializing and adding some features to the general theory in [50]. Using the principle of objectivity and the property of isotropy it is shown that the elastic-plastic constitutive equations remain invariant in Cartesian and initially orthogonal convected curvilinear coordinate if the Cartesian tensors are replaced by the physical components of their corresponding curvilinear tensors. This form invariance is very useful from the point of view of practical considerations since it makes it possible to bypass the complicated curvilinear tensorial form of the constitutive equations in solving problems.

The incremental method has been formulaced in the finite element form and the various stiffness matrices in the resulting incremental force-displacement relations are demonstrated. It is shown that the force-displacement relation for each increment consists of a linear and

a nonlinear part. The linear part which includes an initial stress stiffness matrix provides a first order approximation of the incremental relations.

The developed method is quite general and can be used for the analysis of large deformations of many structural problems. In this dissertation it has been specialized for the solution of large deflections of elastic-plastic thin shells of revolution with axisymmetric loading and support conditions. The displacement procedure of the finite element and the first order part of the nonlinear incremental equations have been used for the solution. A convenient matrix decomposition method has been shown for the formulation of the tangent stiffness matrix. This method can be easily applied when more nonlinear terms of the strain-displacement relations are considered.

A computer program has been written for the large deflection analysis of elastic-plastic shells of revolution. The accuracy and convergence of the linear incremental procedure has been demonstrated on some examples of circular plates, shallow shells, and shells of revolution with arbitrary meridian. It has been found that the convergence is satisfactory when the stiffness matrix of the structure is not very close to zero. For problems where the stiffness matrix becomes almost singular it is advisable to augment the procedure with an iterative scheme or an improved integration procedure. When such provisions are made the method can be easily applied for the buckling and post buckling analysis of elastic-plastic shells of revolution.

REFERENCES

1. Ames, W. F., "Nonlinear Partial Differential Equations in Engineering," Academic Press (1965).
2. Saaty, T. L., and Bram, J., "Non-Linear Mathematics," McGraw Hill (1964).
3. Mikhlin, S., "Approximate Methods for Solution of Differential and Integral Equations," translated from Russian by Scripta Technica, Inc., American Elsevier Publishing Co., Inc. (1967).
4. Lee, E. S., "Quasilinearization and Invariant Imbedding," Academic Press (1968).
5. Oliveira, E. R., "Mathematical Foundations of the Finite Element Method," Int. J. Solids Struct. 4, 10 (1968) 929-952.
6. Felippa, C. A., and Clough, R. W., "The Finite Element Method in Solid Mechanics," Symposium on Numerical Solutions of Field Problems in Continuum Mechanics, Durham, North Carolina (1968).
7. Truesdell, C., "The Mechanical Foundations of Elasticity and Fluid Dynamics," International Science Review Series Vol. 8, Part 1, Gordon and Breach (1966) 99-103.
8. Cauchy, A. L., "Sur L'Équilibre et le Mouvement Intérior des Corps Considérés Comme des Masses Continues," Ex. de Math. 4 = Oeuvres (2) 9, (1829) 342-369.
9. Murnaghan, F. D., "A Revision of the Theory of Elasticity," Anais Acad. Brasil Ci, 21 (1949) 329-336.
10. Green, A. E., Rivlin, R. S., and Shield, R. T., "General Theory of Small Elastic Deformations Superposed on Finite Elastic Deformations," Proc. R. Soc. London (A)211 (1952) 128-154.

11. Southwell, R. V., "On the General Theory of Elastic Stability," Phil. Trans. R. Soc. London (A)213 (1913-1914) 187-244.

12. Biezeno, C. B., and Hencky, H., "On the General Theory of Elastic Stability," K. Akad. Wet. Amst. Proc. 31 (1928) 569-592.

13. Biot, M. A., "Mechanics of Incremental Deformations," John Wiley and Sons (1965).

14. Prager, W., "The General Variational Principle of the Theory of Structural Stability," Quart. Appl. Math. 4, 4 (1947) 378-384.

15. Felippa, C., "Refined Finite Element Analysis of Linear and Non-linear Two-Dimensional Structures," Ph.D. Dissertation, Department of Civil Engineering, University of California, Berkeley, California (also published as SESM Report 66-22)(1966).

16. Turner, M. J., Dill, E. H., Martin, H. C., and Melosh, R. J., "Large Deflection of Structures Subjected to Heating and External Loads," J. Aerospace Sciences 27, 2 (1960) 97-106,127.

17. Gallagher, R. H., and Padlog, J., "Discrete Element Approach to Structural Instability Analysis," AIAA J. 1, 6 (1963) 1437-1439.

18. Argyris, J. H., Kelsey, S., and Kamel, H , "Matrix Methods in Structural Analysis," AGARD-ograph 72, Pergamon Press (1964).

19. Argyris, J. H., "Recent Advances in Matrix Methods of Structural Analysis," Progress in Aeronautical Sciences, Pergamon Press (1964).

20. Argyris, J. H., "Continua and Discontinua," Proc. of Conference on Matrix Methods in Structural Mechanics at Wright-Patterson Air Force Base, Dayton, Ohio, AFFDL-TR-66-80 (1965) 151-170. AD-646300

21. Argyris, J. H., "Matrix Analysis of Three Dimensional Elastic Media, Small and Large Displacements," AIAA J. 3.1 (1965) 45-52.

22. Martin, H. C., "On the Derivation of Stiffness Matrices for the Analysis of Large Deflection and Stability Problems," Proc. of Conference on Matrix Methods in Structural Mechanics at Wright-Patterson Air Force Base, Dayton, Ohio, AFFDL-TR-66-80 (1965) 697-716. AD-646300

23. Martin, H. C., "Large Deflection and Stability Analysis by the Direct Stiffness Method," NASA Tech. Report 32-931, Jet Propulsion Laboratory, Pasadena, California (1966).

24. Oden, J. T., "Calculation of Geometric Stiffness Matrices for Complex Structures," AIAA J. 4, 8 (1966) 1480-1482.

25. Turner, M. J., Martin, H. C., and Weikel, R. C., "Further Development and Applications of the Stiffness Method," AGARD-ograph 72, Pergamon Press (1964) 202-266.

26. Hartz, B. J., "Matric Formulation of Structural Stability Problems," J. of the Structural Mechanics Division, ASCE 91, ST5 (1965) 141-157.

27. Kapur, K. K., and Hartz, B. J., "Stability of Plates Using the Finite Element Method," J. of the Engineering Mechanics Division, ASCE, 92, EM2 (1966) 177-196.

28. Gallagher, R. H., Gellatly, R. A., Padlog, J., and Mallet, R. H., "A Discrete Element Procedure for Thin Shell Instability Analysis," AIAA J. 5, 1 (1967) 138-145.

29. Gallagher, R. H., and Yang, H. T. Y., "Elastic Instability Predictions for Doubly Curved Shells," Private Communication.

30. Navaratna, D. R., "Analysis of Elastic Stability of Shells of Revolution by the Finite Element Method," Proc. of the AIAA/ASME 8th Structures, Structural Dynamics, and Materials Conference, Palm Springs, California (1967) 175-183.

31. Murray, D. W., "Large Deflection Analysis of Plates," Ph.D. Dissertation, Department of Civil Engineering, University of California, Berkeley, California (also published as SESM Report 67-44) (1967).

32. Schmit, L. A., Bogner, F. K., and Fox, R. L., "Finite Deflection Structural Analysis Using Plate and Shell Discrete Elements," AIAA J. 6, 5 (1968) 781-791.

33. Purdy, D. M., and Przemieniecki, J. S., "Influence of Higher Order Terms in the Large Deflection Analysis of Frameworks," Private communication.

34. Mallett, R. H., and Marcal, P. V., "Finite Element Analysis of Nonlinear Structures," J. of the Structural Division, ASCE, 94, ST9 (1968) 2081-2105.

35. Truesdell, C., and Toupin, R. A., "The Classical Field Theories," in Handbuckh der Physik (Edited by S. Flügge), Vol. III/1 (1960) 226-793.

36. Truesdell, C., and Noll, W., "The Nonlinear Field Theories of Mechanics," in Handbuckh der Physik (Edited by S. Flügge), Vol. III/3 (1965).

37. Green, A. E., and Adkins, J. E., "Large Elastic Deformations and Nonlinear Continuum Mechanics," Oxford Press (1960).

38. Green, A. E., and Rivlin, R. S., "On Cauchy's Equations of Motion," ZAMP 15 (1964) 290-292.

39. Noll, W., "A Mathematical Theory of the Mechanical Behavior of Continuous Media," Arch. Rat. Mech. Anal. 2 (1958) 197-226.

40. Coleman, B. D., and Noll, W., "The Thermodynamics of Elastic Materials with Heat Conduction and Viscosity," Arch. Rat. Mech. Anal. 13 (1963) 167-178.

41. Carroll, M. M., "Finite Deformations of Incompressible Simple Solids. I. Isotropic Solids," Quart. J. Mech. Appl. Math. 21, 2 (1968) 147-170.

42. Carroll, M. M., "Finite Deformations of Incompressible Simple Solids. II. Transversely Isotropic Solids," Quart. J. Mech. Appl. Math. 21, 3 (1968) 270-278.

43. Naghdi, P. M., "Stress-Strain Relations in Plasticity and Thermoplasticity," in Plasticity, Proc. 2nd Symp. on Naval Struct. Mech., Pergamon Press (1960) 121-167.

44. Koiter, W. T., "General Theorems of Elastic-Plastic Solics," in Progress in Solid Mech., Vol. 1, (Edited by I. N. Sneddon and R. Hill), North Holland (1960).

45. Drucker, D. C., "A More Fundamental Approach to Plastic Stress-Strain Relations," Proc. 1st. U.S. Nat'l Congr. Appl. Mech. (1951) 487-491.

46. Il'iushin, A. A., "On the Postulate of Plasticity," Appl. Math. Mech. 25, 3 (1961) 746-752.

47. Sedov, L. I., "Foundations of the Nonlinear Mechanics of Continua," Pergamon Press (1966) Chapter III, Sect. 16-2C (translated from Russian edition 1962).

48. Backman, M. E., "Form for the Relation Between Stress and Finite Elastic and Plastic Strains Under Impulsive Loading," J. Appl. Phys. 35, 8 (1964) 2524-2533.

49. Lee, E. H., and Liu, D. T., "Finite Strain Elastic Plastic Theory with Application to Plane Wave Analysis," J. Appl. Phys. 38, 1 (1967) 19-27.

50. Green, A. E., and Naghdi, P. M., "A General Theory of an Elastic Plastic Continuum," Arch. Rat. Mech. Anal. 18, 4 (1965) 250-281.

51. Green, A. E., and Naghdi, P. M., "A Thermodynamic Development of Elastic-Plastic Continua," Proc. IUTAM Symp. on "Irreversible Aspects of Continuum Mechanics," (Vienna, 1966), Springer Verlag (1968).

52. Green, A. E., and Naghdi, P. M., "A Comment on Drucker's Postulate in the Theory of Plasticity," Acta Mech. 1, 4 (1965) 334-338.

53. Green, A. E., and Naghdi, P. M., "Plasticity Theory and Multipolar Continuum Mechanics," Mathematika 12 (1965) 21-26.

54. Green, A. E., Naghdi, P. M., and Osborn, R. B., "Theory of an Elastic-Plastic Cosserat Surface," Int. J. Solid Struct. 4, 9 (1968) 907-927.

55. Dillon, O. W., "A Thermodynamic Basis of Plasticity," Acta Mech. 4, 2 (1967) 182-195.

56. Pipkin, A. C., and Rivlin, R. S., "Mechanics of Rate Independent Materials," ZAMP, 16, 3 (1965) 313-327.

57. Bridgman, P. W., "The Compressibility of Thirty Metals as a Function of Pressure and Temperature," Proc. Am. Acad. Sci., 58 (1923) 163-242.

58. Mises, R. V., "Mechanik der Fester Koerper in Plastisch Deformation Zustard," Goettingen, Nachr. Math.-Phys., Kh. (1913) 582-592.

59. Hill, R., "The Mathematical Theory of Plasticity," Oxford, Clarendon Press (1950).

60. Naghdi, P. M., "Foundations of Elastic Shell Theory," in "Progress in Solid Mechanics." Vol. IV, editors Sneddon, I. N., and Hill, R., John Wiley, New York (1963) 1-90.

61. Synge, J. L., and Chien, W. Z., "The Intrinsic Theory of Elastic Shells and Plates," Th. v. Karman Anniv. Volume (1941) 103-120.

62. Green, A. E., and Zerna, W., "Theoretical Elasticity," Oxford, Clarendon Press (1954) Chapt. 10.

63. Wainwright, W. L., "On a Nonlinear Theory of Elastic Shells," Tech. Report No. 18, Series 131, Applied Mechanics Div., Institute of Engineering Research, University of California, Berkeley, California.

64. Naghdi, P. M., and Nordgren, R. P., "On the Nonlinear Theory of Elastic Shells Under the Kirchhoff Hypothesis," Quart. Appl. Math., 21, 1 (1963) 49-59.

65. Green, A. E., Laws, N., and Naghdi, P. M., "Rods, Plates and Shells," Report No. AM-67-8, Division of Applied Mechanics, University of California, Berkeley, California (1967).

66. Erickson, J. L., and Truesdell, C., "Exact Theory of Stress and Strain in Rods and Shells," Arch. Rat'l Mech. Anal. 1 (1958) 295-323.

67. Sanders, J. L., "Nonlinear Theories for Thin Shells," Quart. Appl. Math. 21, 1 (1963) 21-36.

68. Leonard, R. W., "Nonlinear First Approximation Thin Shell and Membrane Theory," Thesis, Virginia Polytechnic Inst. (1961).

69. Koiter, W. T., "A Consistent First Approximation in the General Theory of Thin Elastic Shells," Proc. of IUTAM Symp. on the Theory of Thin Elastic Shells, North-Holland Pub. Co. (1959) 12-33.

70. Green, A. E., Naghdi, P. M., and Wainwright, W. L., "A General Theory of a Cosserat Surface," Arch. Rat'l Mech. Anal. 20, 4 (1965) 287-308.

71. Reissner, E., "On the Theory of Thin Elastic Shells," H. Reissner Anniversary Volume, Ann Arbor, Mich. (1949) 231-247.

72. Wilson, P. E., and Spier, E. E., "Numerical Analysis of Large Axisymmetric Deformations of Thin Spherical Shells," AIAA J. 3, 9 (1965) 1716-1725.

73. Ball, R. E., and Bodeen, C. A., "A Digital Computer Program for the Geometrically Nonlinear Analysis of Axisymmetrically Loaded Thin Shells of Revolution," Dynamic Science Corp. Report No. SN-38-5 (1965).

74. Mescall, J. F., "Numerical Solutions of Nonlinear Equations of Shells of Revolution," AIAA J. 4, 11 (1966) 2041-2043.

75. Bushnell, D., "Nonlinear Axisymmetric Behavior of Shells of Revolution," AIAA J. 5, 3 (1967) 432-439.

76. Hamada, M., Seguchi, Y., Ito, S., Kaku, E., Yamakawa, K., and Oshima, I., "Numerical Method for Nonlinear Axisymmetric Bending of Arbitrary Shells of Revolution and Large Deflection Analyses of Corrugated Diaphragm and Bellows," Bulletin of JSME 11, 43 (1968) 24-33.

77. Witmer, E. A., Balmer, H. A., Leech, J. W., and Pian, H. H., "Large Dynamic Deformations of Beams, Rings, Plates, and Shells," AIAA J. 1, 8 (1963) 1848-1857.

78. Stricklin, J. A., Hsu, P. T., and Pian, H. H., "Large Elastic, Plastic and Creep Deflections of Curved Beams and Axisymmetric Shells," AIAA J. 2, 9 (1964) 1613-1620.

79. Kalnins, A., and Lestingi, J. F., "On Nonlinear Analysis of Elastic Shells of Revolution," J. Appl. Mech. 34, 1 (1967) 59-67.

80. Fox, L., "Numerical Solution of Two Point Boundary Value Problems," Oxford (1957).

81. Kalnins, A., "Analysis of Shells of Revolution Subjected to Symmetrical and Nonsymmetrical Loads," J. Appl. Mech. 31, 3 (1964) 467-476.

82. Stricklin, J. A., Haisler, W. E., MacDougall, H. R., and Stebbins, F. J., "Nonlinear Analysis of Shells of Revolution by the Matrix Displacement Method," AIAA 6th Aerospace Science Conference, Paper No. 68-177 (1968).

83. Stricklin, J. A., Deandrade, J. C., Stebbins, F., and Cwierthy, A. J., Jr., "Linear and Nonlinear Analysis of Shells of Revolution With Asymmetrical Stiffness Properties," Private Communication.

84. Navaratna, D. R., Pian, T. H. H., and Witmer, E. A., "Stability Analysis of Shells of Revolution by the Finite Element Method," AIAA J. 6, 2 (1968) 355-361.

85. Bromberg, E., and Stoker, J. J., "Nonlinear Theory of Curved Elastic Sheets," Quart. Appl. Math. 3 (1945) 246-265.

86. Jordan, P. F., "Stresses and Deformations of Thin Walled Pressurized Torus," J. Aerospace Sci. 29, 2 (1962) 213-225.

87. Sanders, J. L., Jr., and Liepins, A. A., "Toroidal Membrane Under Internal Pressure," AIAA J. 1, 9 (1963) 2105-2110.

88. Goldberg, M. A., "An Iterative Solution for Rotationally Symmetric Non-Linear Membrane Problems," Int. J. Non-Linear Mech. 1, 3 (1966) 169-178.

89. Wu, C. H., "A Nonlinear Boundary Layer for Shells of Revolution," Int. J. Engng. Sci. 6, 5 (1968) 265-281.

90. Flügge, W., and Chou, S. C., "Large Deformation Theory of Shells of Revolution," J. Appl. Mech. 34, 1 (1967) 56-58.

91. Colbroune, J. R., and Flügge, W., "The Membrane Theory of Toroidal Shell--A Singular Perturbation Problem," Int. J. Non-Linear Mech. 2, 1 (1967) 39-53.

92. Rajan, M. K. S., "Shell Theory Approach for Optimization of Arch Dam Shapes," Ph.D. Dissertation, Department of Civil Engineering, University of California, Berkeley, California (1968).

93. Weil, N. A., "An Approximate Solution for the Bursting of Thin-Walled Cylinders," Int. J. Mech. Sciences 5, 6 (1963) 487-506.

94. Salmon, M. A., "Large Plastic Deformation of Pressurized Cylinder," J. Engineering Mechanics Division, ASCE 92, EM3 (1966) 33-52.

95. Marguerre, K., "Zur Theorie der Gekrümmten Platte Grosser Formänderung," Proc. 5th Int. Cong. Appl. Mech. (1938) 93-101.

96. Reissner, E., "On Axisymmetrical Deformations of Thin Shells of Revolution," Proc. Symp. Appl. Math. Vol. III (1950) 27-52.

97. Kaplan, A., and Fung, Y. C., "A Nonlinear Theory of Bending and Buckling of Thin Elastic Shallow Spherical Shells," NACA TN 3212 (1954).

98. Reiss, E. L., Greenberg, H. J., and Keller, H. B., "Non-Linear Deflection of Shallow Spherical Shells," IX^{e} Congrés International de Mécanique Appliquée, Université de Bruxelles (1957) 362. Also J. Aero. Sciences 24, 7 (1957) 533-543.

99. Archer, R. R., "Stability Limits for a Clamped Spherical Shell Segment under Uniform Pressure," Quart. Appl. Math. 15, 4 (1958) 355-366.

100. Reiss, E. L., "Axially Symmetric Buckling of Shallow Spherical Shells under External Pressure," J. Appl. Mech. 25, 4 (1958).

101. Budiansky, B., "Buckling of Clamped Shallow Spherical Shells," Proc. of IUTAM Symp. Theory of Thin Elastic Shells, Delft (1959).

102. Weinitschke, H, J., "On the Stability Problem for Shallow Spherical Shells," J. Math. and Phys. 38, 4 (1960) 209-231.

103. Thurston, G. A., "A Numerical Solution of the Nonlinear Equations for Axisymmetric Bending of Shallow Spherical Shells," J. Appl. Mech. 28, 4 (1961) 557-562.

104. Archer, R. R., "On the Numerical Solution for the Non-Linear Equations for Shells of Revolution," J. Math. Phys. 41 (1962) 165-178.

105. Krenzke, M. A., and Kiernan, T. J., "Elastic Stability of Near Perfect Shallow Spherical Shells," AIAA J. 1, 2 (1963) 2855-2857.

106. Weinitschke, H. J., "Asymmetric Buckling of Clamped Shallow Spherical Shells," NASA TN D-1510 (1962) 481-491.

107. Huang, N. C., "Unsymmetrical Buckling of Thin Shallow Spherical Shells," J. Appl. Mech. 31, 3 (1964) 447-457.

108. Ashwell, D. G., "On the Large Deflection of a Spherical Shell with an Inward Point Load," Proc. of IUTAM Symp. Theory of Thin Elastic Shells, Delft (1959).

109. Mescall, J. F., "Large Deflection of Spherical Shells under Concentrated Loads," J. Appl. Mech. 32, 4 (1965) 936-938.

110. Penning, F. A., and Thurston, G. A., "The Stability of Shallow Spherical Shells Under Concentrated Load," NASA CR-265 (1965).

111. Evan-Ivanovski, R. M., Cheng, H. S., and Loo, T. C., "Experimental Investigations on Deformations and Stability of Spherical Shells

Subjected to Concentrated Loads at the Apex," Proc. 4th U. S. Nat'l Congr. Appl. Mech. 1 (1962) 563-571.

112. Penning, F. A., "Nonaxisymmetric Behavior of Shallow Shells Loaded at the Apex," J. Appl. Mech. 33, 3 (1966) 699-700.

113. Budiansky, B., and Hutchinson, J. W., "A Survey of Some Buckling Problems," AIAA J. 4, 9 (1966) 1505-1510.

114. Fitch, J. R., "The Buckling and Post Buckling Behavior of Spherical Caps Under Concentrated Load," Int. J. Solids Structures 4, 4 (1968) 421-446.

115. Lin, M. S., "Buckling of Spherical Sandwich Shells," Ph.D. Dissertation, Department of Civil Engineering, University of California, Berkeley, California (1968).

116. von Karman, T , "Festigkeitsprobleme im Maschinenbau," Encyklopädie der Mathematischen Wissenschaften, Vol. 4, 4 Teubner, Leipzig (1910) 348-352.

117. Berger, H. M., "A New Approach to the Analysis of Large Deflection Theory of Plates," J. Appl. Mech. 22, 4 (1955) 465-472.

118. Goldberg, M. A., "A Modified Large Deflection Theory of Plates," Proc. 4th Nat'l Congr. Appl. Mech. (1962) 611-618.

119. Wah, T., "Vibrations of Circular Plates at Large Amplitudes," J. of Engineering Mechanics Division of ASCE, 89, EM5 (1963) 1-15.

120. Sinha, S. N., "Large Deflection of Plates on Elastic Foundations," J. of Engineering Mechanics Division of ASCE, 89, EM1 (1963) 1-24.

121. Way, S., "Bending of Circular Plates with Large Deflection," ASME Transactions 56 (1934) 627-636.

122. Bromberg, E., "Non-Linear Bending of a Circular Plate under Normal Pressure," Comm. Pure Appl. Math. 9, 4 (1956) 633-659.

123. Friedrichs, K. O., and Stoker, J. J., "The Nonlinear Boundary Value Problem of the Buckled Plate," Amer. J. Math. 113, 4 (1941) 839-888.

124. Hart, V. G., and Evans, D. J., "Nonlinear Buckling of an Annular Plate by Transverse Edge Forces," J. Math. Phys. 43, 4 (1964) 275-303.

125. Keller, H. B., and Reiss, E. L., "Iterative Solutions for the Nonlinear Bending of Circular Plates," Comm. Pure Appl. Math. 11, 3 (1958) 273-292.

126. Hamada, M., and Seguchi, Y., "Large Deflection Analysis of Circular Ring Plates Under Uniform Transverse Force Along the Inner Edge," Bulletin of JSME 8, 31 (1965) 344-352.

127. Sawczuk, A., "Large Deflections of a Rigid Plastic Plate," Proc. 11th Int. Congr. Appl. Mech., Munich (Germany) 1964, Springer Verlag (1966) 224-228.

128. Jones, N., "Finite Deflections of a Rigid-Plastic Annular Plate Loaded Dynamically," Int. J. Solids Struct. 4 (1968) 593-603.

129. Jones, N., "Impulsive Loading of a Simply Supported Circular Rigid Plastic Plate," J. Appl. Mech. (1968) 59-65.

130. Ohashi, Y., and Murakami, S., "The Elasto-Plastic Bending of a Clamped Thin Circular Plate," Proc. 11th Int. Congr. Appl. Mech., Munich (Germany) 1964, Springer Verlag (1966) 212-223.

131. Ohashi, Y., and Murakami, S., "Large Deflection of Elastoplastic Bending of a Simply Supported Circular Plate Under a Uniform Load," J. Appl. Mech. 33, 4 (1966) 866-870.

132. Budiansky, B., "A Reassessment of Deformation Theories of Plasticity," J. Appl. Mech. 26 (1959) 259-264.

133. Naghdi, P. M., "Bending of Elasto-Plastic Circular Plates with Large Deflections," J. Appl. Mech. 19, 3 (1952) 393-300.

134. Ohashi, Y., and Kamiya, N., "Large Deflection of a Supported Circular Plate Having a Non-Linear Stress-Strain Relation," ZAMM 48, 3 (1968) 159-171.

135. Crose, J. G., and Ang, A. H.-S., "A Large Deflection Analysis Method for Elastic-Perfectly Plastic Circular Plates," Civil Engin. Studies, Struct. Research Series No. 323, University of Illinois, Urbana, Illinois (1967).

136. Clough, R. W., "The Finite Element Method in Structural Mechanics," in "Stress Analysis," edited by Zienkiewicz, O. C., and Holister, G. S., John Wiley (1965).

137. Fraeijs de Veubeke, B., "Displacement and Equilibrium Models in the Finite Element Method," in "Stress Analysis," edited by Zienkiewicz, O. C., and Holister, G. S., John Wiley (1965).

138. Zienkiewicz, O. C., and Cheung, Y. K., "The Finite Element Method in Structural and Continuum Mechanics," McGraw-Hill (1967).

139. Melosh, R. J., "Basis for Derivation of Matrices for the Direct Stiffness Method," AIAA J. 1, 7 (1963) 1631-1637.

140. Khojasteh-Bakht, M., "Analysis of Elastic-Plastic Shells of Revolution Under Axisymmetric Loading by the Finite Element Method," Ph.D. Dissertation, Department of Civil Engineering, University of California, Berkeley, California (also published as SESM Report 67-8)(1967).

141. Popov, E. P., Khojasteh-Bakht, M., and Yaghmai, S., "Analysis of Elastic-Plastic Circular Plates," J. of the Engineering Mechanics Division, ASCE 93, EM6 (1967).

142. Abramowitz, M., and Stegun, I. A., "Handbook of Mathematical Functions," National Bureau of Standards (1964) 887.

143. Isaacson, E., and Keller, H. B., "Analysis of Numerical Methods," John Wiley (1966).

144. Kornishin, H. S , and Isanbaeva, F. S., "Flexible Plates and Panels," Nauka, Moscow (in Russian) (1968).

145. Forsythe, G. E., and Wasow, W. R., "Finite Difference Methods for Partial Differential Equations," John Wiley and Sons (1960).

146. Bellman, R., Kalaba, R., and Wing, G. M., "Invariant Imbedding and the Reduction of Two-Point Boundary-Value Problems to Initial Value Problems," Proc. Nat'l Acad. Sci., U.S. 46 (1960) 1646.

APPENDIX A

A.1 The Principle of Virtual Work in Curvilinear Coordinates

Cauchy's relation between the traction and the Piola symmetric stress tensor in configuration 2 can be written as [35] (see Figure A.1)

$$ {}_2t^r = {}_2s^{ik}(\delta_k^r + u^r|_k)\, n_i \tag{A.1} $$

where ${}_2t^r$ are the contravariant components of traction vector which acts in configuration 2 but which is measured per unit of area of configuration 1, ${}_2s^{ik}$ are the contravariant components of the Piola Symmetric stress tensor measured per unit of area in configuration 1, u^r are the contravariant components of the displacement increment vector from configuration 1 to 2, and the vertical bar ($|$) denotes covariant differentiation.

The expression for the virtual work in configuration 2 can be written as

$$ W_v = \int_a {}_2t^r \delta u_r \, da + \int_v \rho_o {}_2f^r \delta u_r \, dv \tag{A.2} $$

Substitution of equation (A.1) into (A.2) and the application of Gauss' transformation for surface integrals into volume integrals gives

$$ W_v = \int_v \{[{}_2s^{ik}(\delta_k^r + u^r{}_{|k})]_{|i} + \rho_o {}_2f^r\}\, \delta u_r \, dv + \int_v {}_2s^{ik}(\delta_k^r + u^r{}_{|k})(\delta u_r)|_i \, dv \tag{A.3} $$

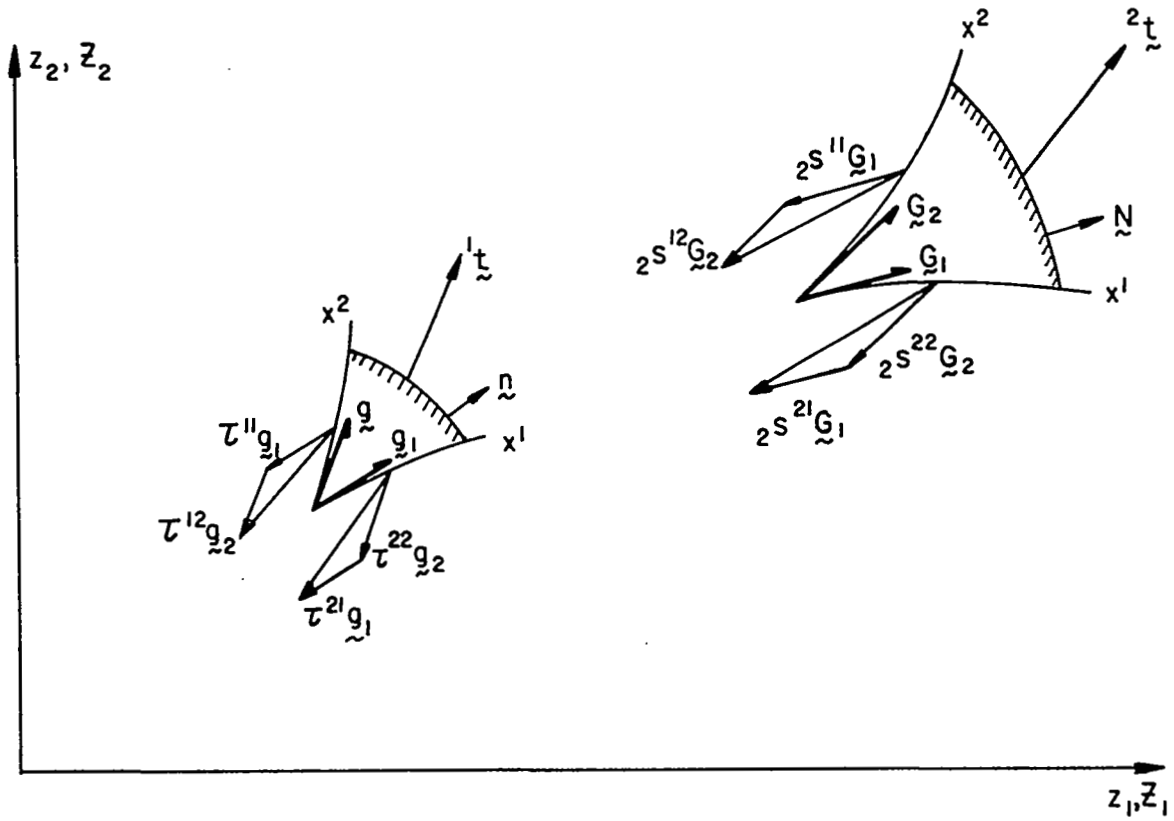
z_2, Z_2
x^2
${}^1\underset{\sim}{t}$
$\underset{\sim}{n}$
$\underset{\sim}{g}$
$\underset{\sim}{g}_1$
x^1
$\tau^{11}\underset{\sim}{g}_1$
$\tau^{12}\underset{\sim}{g}_2$
$\tau^{22}\underset{\sim}{g}_2$
$\tau^{21}\underset{\sim}{g}_1$
x^2
${}^2\underset{\sim}{t}$
${}_2S^{11}\underset{\sim}{G}_1$
$\underset{\sim}{G}_2$
$\underset{\sim}{N}$
${}_2S^{12}\underset{\sim}{G}_2$
$\underset{\sim}{G}_1$
x^1
${}_2S^{22}\underset{\sim}{G}_2$
${}_2S^{21}\underset{\sim}{G}_1$
z_1, Z_1

FIG. A-1

The integrand of the First integral of equation (A.3) consists of the equilibrium equations and is identically equal to zero; therefore,

$$W_v = \int_v {}_2s^{ik}(\delta^r_k + u^r{}_{|k})(\delta u_r)|_i \, dv \ . \qquad (A.4)$$

It can be written that

$$(\delta u_r)_{|i} = \frac{\partial(\delta u_r)}{\partial x^i} - {}_g\Gamma^s{}_{ri} \ (\delta u_s)$$

or,

$$(\delta u_r)|_i = \delta(u_{r|i})$$

This is due to the fact that the variation is applied in configuration 2 and therefore the variation of the Christoffel symbol ${}_g\Gamma^s{}_{ri}$ in configuration 1 is equal to zero. The expression for virtual work becomes

$$W_v = \int_v {}_2s^{ik} \ (\delta^r_k + u^r|_k) \ \delta(u_{r|i})dv \qquad (A.5)$$

Due to symmetry of ${}_2s^{ik}$ and the fact that $g_{ij|r} = g^{ij}{}_{|r} = 0$, then

$$\begin{aligned} {}_2s^{ik} \ u^r|_k \ \delta \ u_{r|i} &= {}_2s^{ik} \ u^r|_i \ \delta u_r|_k \\ &= {}_2s^{ik} \ (g^{rm}u_m)|_i \ \delta(g_{rn} \ u^n)|_k \\ &= {}_2s^{ik} \ \delta^m_n \ u_m|_i \ \delta \ u^r|_k \\ &= {}_2s^{ik} \ u_{r|i} \ \delta \ u^r|_k \end{aligned}$$

Therefore,

$$ {}_2s^{ik}(\delta^r_k + v^r|_k)\,\delta u_r|_i = \frac{1}{2}\,{}_2s^{ik}(\delta u_k|_i + \delta u_i|_k + u^r|_k\,\delta u_r|_i + u_r|_i\,\delta u^r|_k) \qquad (A.6) $$

$$ = {}_2s^{ik}\,\delta\varepsilon_{ik} \,. $$

in which ε_{ik} is the covariant component of the Lagrangian strain between configurations 1 and 2.

$$ \varepsilon_{ik} = \frac{1}{2}\,(u_k|_i + u_i|_k + u^m|_i\,u_m|_k) \qquad (A.7) $$

Substitution of (A.6) into (A.5) gives

$$ W_v = \int_v {}_2s^{ik}\,\delta\varepsilon_{ik} \,. \qquad (A.8) $$

The stress ${}_2s^{ik}$ can be divided into two parts

$$ {}_2s^{ik} = \tau^{ik} + s^{ik} \qquad (A.9) $$

in which τ^{ik} are in magnitude equal to the corresponding contravariants components of Cauchy stresses in configuration 1 but which are associated with base vectors $\underset{\sim}{G}$, and s^{ik} are symmetric increments of contravariant stress components of the type of symmetric Piola stresses.

Substitution of (A.9) and (A.8) into (A.2) yields

$$ \int_a {}_2t^r\,\delta u_r\,da + \int_v \rho_o\,{}_2f^r\,\delta u_r\,dv = \int_v (\tau^{ik} + s^{ik})\delta\varepsilon_{ik}\,dv \,. \qquad (A.10) $$

The expression for virtual work at configuration 1 can be written as

$$\int_a {}^{1}t^r \, \delta u_r \, da + \int_v \rho_o \, {}^{1}f^r \, \delta u_r \, dv = \int_v \tau^{ik} \delta e_{ik} \, dv \qquad \text{(A.11)}$$

in which

$$e_{ik} = \frac{1}{2}(u_i|_k + u_k|_i)$$

is the linear part of the strain increment from configuration 1 to configuration 2.

Let the increments of traction and body force be defined by

$$\begin{aligned} t^r &= {}^{2}t^r - {}^{1}t^r \text{ , and} \\ f^r &= {}^{2}f^r - {}^{1}f^r \text{ .} \end{aligned} \qquad \text{(A.12)}$$

Substitution of (A.12) into (A.10) and subtraction of (A.11) from (A.10) results in the following incremental expression for the virtual work in curvilinear coordinates

$$\int_a t^r \, \delta u_r \, da + \int_v \rho_o f^r \, \delta u_r \, dv = \int_v (\tau^{ik} \delta \eta_{ik} + s^{ik} \delta \varepsilon_{ik}) dv \qquad \text{(A.13)}$$

in which

$$\eta_{ik} = \frac{1}{2}(u_m|_k \, u^m|_i) \qquad \text{(A.14)}$$

A.2 Proof of the Validity of the Expression of Virtual Work

In this section it is shown that the expression of virtual work (A.13) results in correct equilibrium equations and boundary conditions. This proof is also applicable to the Cartesian expression of virtual work (I.27).

The equilibrium equations in configuration 1 are

$$\tau^{ir}|_i + \rho_o \, {}^1f^r = 0 \tag{A.15}$$

and the boundary conditions are

$${}^1t^r = \tau^{ir} n_i \tag{A.16}$$

The application of the principle of the balance of linear momentum to the deformable body in configuration 2 results in the equilibrium equations there.

$$\int_v \rho_o \, {}^2\underset{\sim}{f} \, dv + \int_a {}^2\underset{\sim}{t} \, da = 0 \tag{A.17}$$

Substitution of $(A.12)_2$ in the volume integral, and (A.1) and (A.9) in the surface integral of (A.17) and the application of Gauss' transformation results in

$$\int_v \{[(\tau^{ik} + s^{ik})(\delta^r_k + u^r|_k)]_{|i} + \rho_o({}^1f^r + f^r)\} dv = 0$$

This integral holds for any arbitrary volume, therefore,

$$[(\tau^{ik} + s^{ik})(\delta^r_k + u^r|_k)]_{|i} + \rho_o({}^1f^r + f^r) = 0 \tag{A.18}$$

The boundary conditions in configuration 2 are given by equation (A.1). Substitution of (A.12), (A.9) into (A.1) gives

$$ {}_1t^r + t^r = (\tau^{ik} + s^{ik})(\delta^r_k + u^r|_k)n_i \qquad (A.19) $$

Subtraction of (A.15) from (A.18) and (A.16) from (A.19) yields the incremental equations of equilibrium

$$ [s^{ik}(\delta^r_k + u^r|_k) + \tau^{ik}u^r|_k]|_i + \rho_o f^r = 0 \qquad (A.20) $$

and boundary conditions

$$ t^r = [s^{ik}(\delta^r_k + u^r|_k) + \tau^{ik}\, u^r|_k]\, n_i \ . \qquad (A.21) $$

It can be shown that by carrying out the appropriate variations for the expression of virtual work (A.13), the equilibrium equations (A.20) and the boundary conditions (A.21) are obtained. The variation of the integral on the right hand side of equation (A.13) is done as follows

$$ \int_V (\tau^{ik}\delta\eta_{ik} + s^{ik}\delta\varepsilon_{ik})dv = \int_V \frac{1}{2}\,\tau^{ik}\,\delta(u^m|_i u_m|_k)dv + $$

$$ \int_V \frac{1}{2}\, s^{ik}\,\delta(u_i|_k + u_k|_i + u_m|_i\, u^m|_k)dv $$

Because of the symmetry τ^{ik} and s^{ik}, and the fact that $\delta u_{r|i}$ is the same as $(\delta u_r)|_i$, this equation can be written as

$$ \int_V (\tau^{ik}\delta\eta_{ik} + s^{ik}\delta\varepsilon_{ik})dv = \int_V (\tau^{ik}\, u^m|_i\ \delta u_m|_k)dv + $$

$$ \int_V s^{ik}(\delta^r_k + u^m|_k)(\delta\, u_r)|_i\ dv $$

The volume integrals can be changed into surface integrals by means of Gauss transformation

$$\begin{aligned}\int_v (\tau^{ik}\,\delta\eta_{ik} + s^{ik}\delta\varepsilon_{ik})dv = &\int_a \tau^{ik}\,u^m|_i\,\delta u_m\,n_k\,da - \\ &\int_v (\tau^{ik}\,u^m|_i)|_k\,\delta u_m\,dv + \\ &\int_a s^{ik}(\delta^r_k + u^r|_k)\,\delta u_r\,n_i\,da - \\ &\int_v [s^{ik}(\delta^r_k + u^r|_k)]|_i\,\delta u_r\,dv\end{aligned} \tag{A.22}$$

Substitution of (A.22) in (A.13) yields

$$\begin{aligned}&\int_a \{t^r - [s^{ik}(\delta^r_k + u^r|_k) + \tau^{ik}\,u^r|_k]n_i\}\delta u_r\,da + \\ &\int_v \{[s^{ik}(\delta^r_k + u^r|_k) + \tau^{ik}\,u^r|_k]|_i + \rho_o\,f^r\}\delta u_r\,dv = 0\end{aligned} \tag{A.23}$$

The integrands in (A.23) must vanish identically. Therefore, the equilibrium equations

$$[s^{ik}(\delta^r_k + u^r|_k) + \tau^{ik}\,u^r|_k]|_i + \rho_o f^r = 0 \tag{A.24}$$

and boundary conditions

$$t^r = [s^{ik}(\delta^r_k + u^r|_k) + \tau^{ik}\,u^r|_k]n_i \tag{A.25}$$

are obtained which are identical to equations (A.20) and (A.21) respectively.

APPENDIX B

B.1 Superposition of Strains

Consider three configurations of a deformable body in the process of deformation (see Figure B.1). The components of the Lagrangian strain tensor between the initial and the second configuration are defined by

$$2\varepsilon_{ij} = \frac{1}{2}\left(G_{CD}\frac{\partial X^C}{\partial \bar{x}^i}\frac{\partial X^D}{\partial \bar{x}^j} - \bar{g}_{ij}\right) \tag{B.1}$$

This can be written as

$$2^2\varepsilon_{ij} = \left(g_{mn}\frac{\partial x^m}{\partial \bar{x}^i}\frac{\partial x^n}{\partial \bar{x}^j} - \bar{g}_{ij}\right) + \left(G_{CD}\frac{\partial X^C}{\partial x^m}\frac{\partial X^D}{\partial x^n} - g_{mn}\right)\frac{\partial x^m}{\partial \bar{x}^i}\frac{\partial x^n}{\partial \bar{x}^j} \quad \text{or}$$

$$2\varepsilon_{ij} = {}^1\varepsilon_{ij} + \frac{\partial x^m}{\partial \bar{x}^i}\frac{\partial x^n}{\partial \bar{x}^j}\varepsilon_{mn} \tag{B.2}$$

in which ${}^1\varepsilon_{ij}$ and ε_{mn} are the Lagrangian strains between the initial and first; and the second and first configurations respectively,

Defining ξ_{ij} by

$$\xi_{ij} = \frac{\partial x^m}{\partial \bar{x}^i}\frac{\partial x^n}{\partial \bar{x}^j}\varepsilon_{mn} \tag{B.3}$$

and substituting in (B.2) then

$$2\varepsilon_{ij} = {}^1\varepsilon_{ij} + \xi_{ij} \tag{B.4}$$

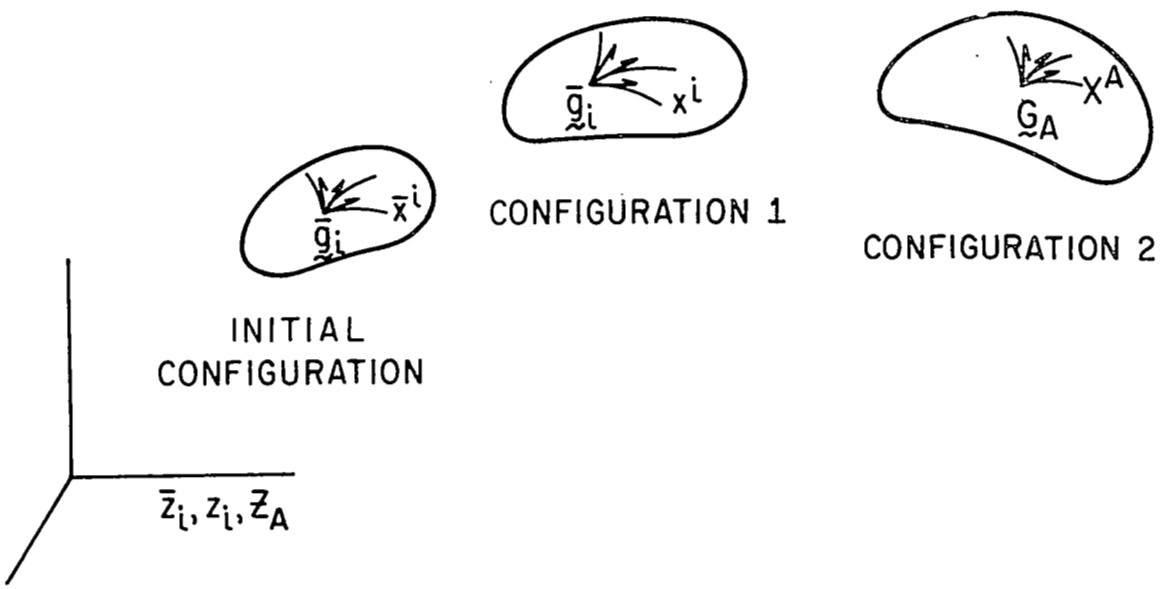
$\bar{g}_i$
$\bar{x}^i$
INITIAL
CONFIGURATION
$\bar{g}_i$
x^i
CONFIGURATION 1
G_A
X^A
CONFIGURATION 2
$\bar{z}_i, z_i, Z_A$

FIG. B - 1

If convected curvilinear coordinates are used then equation (B.2) becomes

$$^{2}\varepsilon_{ij} = {}^{1}\varepsilon_{ij} + \varepsilon_{ij} \tag{B.5}$$

The equivalent form of (B.2) in Cartesian coordinates is

$$^{2}\varepsilon_{ij} = {}^{1}\varepsilon_{ij} + \frac{\partial z_m}{\partial \bar{z}_i} \frac{\partial z_n}{\partial \bar{z}_j} \varepsilon_{mn} \tag{B.6}$$

APPENDIX C

C.1 The Principle of Virtual Work, Second Alternative

The expression of virtual work in configuration 1 can be written as

$$\int_{\bar{v}} \bar{\rho}_o \, {}^1\bar{f}_i \, \delta {}^1\bar{u}_i \, d\bar{v} + \int_{\bar{a}} {}^1\bar{t}_i \, \delta({}^1\bar{u}_i) d\bar{a} = \int_{\bar{v}} {}^1s_{ik} \, \delta {}^1\varepsilon_{ki} \, d\bar{v} \qquad (C.1)$$

in which the bar over the variables indicates that the initial configuration is the reference. In particular ${}^1\bar{u}_i$ represent the components of the displacement vector between the initial and first configurations expressed in the coordinate system of the initial configuration. The expression of virtual work in configuration 2 can be written as

$$\int_{\bar{v}} \bar{\rho}_o \, {}^2\bar{f}_i \, \delta {}^2\bar{u}_i \, d\bar{v} + \int_{\bar{a}} {}^2\bar{t}_i \, \delta({}^2\bar{u}_i) d\bar{a} = \int_{\bar{v}} {}^2\bar{s}_{ik} \, \delta {}^2\varepsilon_{ki} \, d\bar{v} \qquad (C.2)$$

It is shown in Appendix B that

$$ {}^2\varepsilon_{ki} = {}^1\varepsilon_{ki} + \xi_{ki} \, . \qquad (B.4)$$

Also define

$$\bar{f}_i = {}^2\bar{f}_i - {}^1\bar{f}_i \, ,$$

and

$$\bar{t}_i = {}^2\bar{t}_i - {}^1\bar{t}_i \qquad (C.3)$$

in which $\bar{t}_i$ denotes the increment of surface traction in the direction of the coordinates of the initial configuration and measured per unit area of $\bar{a}$, and $\bar{f}_i$ is the increment of body force per unit mass in the coordinate system of the initial configuration. Since the virtual displacements $\delta\,{}^1\underset{\sim}{u}$ and $\delta\,{}^2\underset{\sim}{u}$ (See Figure I.1) are the same as $\delta\,\underset{\sim}{u}$, then

$$\begin{aligned} \delta\,\bar{u}_i &= \delta({}^2\bar{u}_i) \text{ and} \\ \delta\,\bar{u}_i &= \delta({}^1\bar{u}_i) \end{aligned} \tag{C.4}$$

in which $\bar{u}_i$ denote the components of the increment of displacement between configurations 1, and 2 expressed in the coordinate system of the initial configuration.

Subtraction of (C.1) from (C.2) and the substitution of (B.4), (C.3), (C.4) and $(I.36)_3$ in the resulting equation yields

$$\int_{\bar{v}} \bar{\rho}_o\,\bar{f}_i\,\delta\,\bar{u}_i\,d\bar{v} + \int_{\bar{a}} \bar{t}_i\,\delta\,\bar{u}_i d\bar{a} = \int_{\bar{v}} ({}^2\bar{s}_{ik}\,\delta\,\bar{\xi}_{ki} + \bar{s}_{ik}\,\delta\,{}^1\varepsilon_{ki})d\bar{v} \tag{C.5}$$

It was shown in chapter 1 that for hyperelastic materials

$$\bar{s}_{ik} = \bar{\rho}_o \frac{\partial A}{\partial\,{}^1\varepsilon_{ki}}\,, \tag{I.40}$$

and

$${}^2\bar{s}_{ik} = \bar{\rho}_o \frac{\partial A}{\partial \bar{\xi}_{ki}} \tag{I.41}$$

Substitution of these constitutive equations in (C.5) gives

$$\int_{\bar{v}} \bar{\rho}_o\,\bar{f}_i\,\delta\,\bar{u}_i\,d\bar{v} + \int_{\bar{a}} \bar{t}_i\,\delta\,\bar{u}_i d\bar{a} = \int_{\bar{v}} \bar{\rho}_o\,\delta\,A\,d\bar{v} \tag{C.6}$$

which is an incremental expression of virtual work for elastic materials.

C.2 The Principle of Virtual Work, Third Alternative

The virtual displacements in section C.1 were taken to be $\delta(\overset{2}{\underset{\sim}{u}})$ and $\delta(\overset{1}{\underset{\sim}{u}})$. If instead of these $\delta(\underset{\sim}{u})$ is used throughout, then another form of the expression of virtual work can be obtained. As in section C.1 the components of $\underset{\sim}{u}$ are taken in the coordinate system of the initial configuration. The expression of virtual work in configuration 1 is

$$W_v = \int_{\bar{v}} \bar{\rho}_o \, {}^1\bar{f}_k \, \delta \, \bar{u}_k \, d\bar{v} + \int_{\bar{a}} {}^1\bar{t}_k \, \delta \, \bar{u}_k \, d\bar{a} \quad . \tag{C.7}$$

Substitution of

$${}^1\bar{t}_k = {}^1s_{ij} \frac{\partial z_k}{\partial \bar{z}_j} \bar{n}_i \tag{C.8}$$

into the second integral on the right hand side of (C.7), and the application of Gauss transformation results in

$$W_v = \int_{\bar{v}} [({}^1s_{ij} \, z_{k,j})_{,i} + \bar{\rho}_o \, {}^1\bar{f}_k] \, \delta \, \bar{u}_k \, d\bar{v} + \int_{\bar{v}} {}^1s_{ij} \, z_{k,j} \, \delta \, \bar{u}_{k,i} \, d\bar{v} \quad . \tag{C.9}$$

The statement of equilibrium requires that

$$({}^1s_{ij} \, z_{k,j})_{,i} + \bar{\rho}_o \, {}^1\bar{f}_k = 0 \ . \tag{C.10}$$

Therefore,

$$W_v = \int_{\bar{v}} {}^1s_{ij} \, z_{k,j} \, \delta \, \bar{u}_{k,i} \, d\bar{v} \ , \text{ or} \tag{C.11}$$

$$\int_{\bar{v}} \bar{\rho}_o \, {}^1\bar{f}_k \, \delta \, \bar{u}_k \, d\bar{v} + \int_{\bar{a}} {}^1\bar{t}_k \, \delta \, \bar{u}_k \, d\bar{a} = \int_{\bar{v}} {}^1s_{ij} \, z_{k,j} \, \delta \, \bar{u}_{k,i} \, d\bar{v} \tag{C.12}$$

The expression of virtual work in configuration 2 can be written in the same way

$$\int_{\bar{v}} \bar{\rho}_o \, {}^2\bar{f}_k \, \delta \, \bar{u}_k \, d\bar{v} + \int_{\bar{a}} {}^2\bar{t}_k \, \delta \, \bar{u}_k \, d\bar{a} = \int_{\bar{v}} {}^2\bar{s}_{ij} \, Z_{k,j} \, \delta \, \bar{u}_{k,i} \, d\bar{v} \qquad (C.13)$$

The integrand on the right hand side of (C.13) can be written as

$${}^2\bar{s}_{ij} \, Z_{k,j} \, \delta \, \bar{u}_{k,i} = ({}^1s_{ij} + \bar{s}_{ij})(z_{k,j} + \bar{u}_{k,j}) \, \delta \, \bar{u}_{k,i} \qquad (C.14)$$

Substitution of (C.14) into (C.13) and then subtraction of (C.12) from (C.13) results in

$$\int_{\bar{v}} \bar{\rho}_o \, \bar{f}_k \, \delta \, \bar{u}_k \, d\bar{v} + \int_{\bar{a}} \bar{t}_k \, \delta \, \bar{u}_k \, d\bar{a} =$$

$$\int_{\bar{v}} [{}^1s_{ij} \, \bar{u}_{k,j} \, \delta \, \bar{u}_{k,i} + \bar{s}_{ij}(z_{k,j} + \bar{u}_{k,j}) \, \delta \, \bar{u}_{k,i}] d\bar{v} \qquad (C.15)$$

Due to symmetry of ${}^1s_{ij}$ and $\bar{s}_{ij}$, then

$$\begin{aligned} {}^1s_{ij} \, \bar{u}_{k,j} \, \delta \, \bar{u}_{k,i} &= \tfrac{1}{2} \, s_{ij} \delta(\bar{u}_{k,j} \, \bar{u}_{k,i}) \, , \\ \bar{s}_{ij} \, \bar{u}_{k,j} \, \delta \, \bar{u}_{k,i} &= \tfrac{1}{2} \, s_{ij} \delta(\bar{u}_{k,j} \, \bar{u}_{k,i}) \, , \end{aligned} \qquad (C.16)$$

and

$$\begin{aligned} \bar{s}_{ij} \, z_{k,j} \, \delta \, \bar{u}_{k,i} &= \bar{s}_{ij}(\delta_{kj} + {}^1\bar{u}_{k,j}) \delta \bar{u}_{k,i} \\ &= \tfrac{1}{2} \, \bar{s}_{ij}(u_{i,j} + u_{j,i}) + \tfrac{1}{2} \, \bar{s}_{ij}({}^1\bar{u}_{k,j} \, \bar{u}_{k,i} + {}^1\bar{u}_{k,i} \, \bar{u}_{k,\,j}) \end{aligned} \qquad (C.17)$$

Define

$$\bar{\varepsilon}_{ij} = \frac{1}{2}\left(\bar{u}_{i,j} + \bar{u}_{j,i} + \bar{u}_{k,i}\,\bar{u}_{k,j}\right)$$

$$\bar{\eta}_{ij} = \frac{1}{2}\left(\bar{u}_{k,i}\,\bar{u}_{k,j}\right) \tag{C.18}$$

$$\bar{\xi}_{ij} = \bar{\varepsilon}_{ij} + \frac{1}{2}\left({}^{1}\bar{u}_{k,j}\,\bar{u}_{k,i} + {}^{1}\bar{u}_{k,i}\,\bar{u}_{k,j}\right)$$

in which $\bar{\varepsilon}_{ij}$ nas the same form as the increment of Lagrangian strain between configurations 1 and 2 but involves displacement components which are in the coordinate system of the initial configuration. Substitution of (C.18), (C.17), and (C.16) into (C.15) gives

$$\int_{\bar{v}} \bar{\rho}_o\,\bar{f}_k\,\delta\,\bar{u}_k\,d\bar{v} + \int_{\bar{a}} \bar{t}_k\,\delta\,\bar{u}_k\,d\bar{a} = \int_{\bar{v}} \left({}^{1}\bar{s}_{ij}\,\delta\,\bar{\eta}_{ij} + \bar{s}_{ij}\,\delta\,\bar{\xi}_{ij}\right)d\bar{v} \tag{C.19}$$

APPENDIX D

D.1 The Physical Components of Stress Tensors

The deformation of a continuum may be expressed in Cartesian, and curvilinear coordinates by

$$Z_A = Z_A(z_i) \ . \tag{D.1}$$

and

$$X^A = X^A(x^i) \tag{D.2}$$

respectively (see Figures D.1, and D.2 for a two dimensional picture). In Cartesian coordinates the stress tensor π can be expressed in terms of Cauchy (τ_{AB}), Piola symmetric (s_{ij}) and unsymmetric (T_{Ai}) components as follows.

$$\pi = \underset{\sim}{i}_A \, \tau_{AB} \, \underset{\sim}{i}_B = J^{-1} \, \underset{\sim}{G}_i \, s_{ij} \, \underset{\sim}{G}_j = J^{-1} \, \underset{\sim}{i}_A \, T_{Ak} \, \underset{\sim}{G}_k \tag{D.3}$$

in which $\underset{\sim}{i}$ is the unit base vector, G is the convected base vector, and J is the Jacobian of transformation (D.1). The convected base vectors can be written as

$$\underset{\sim}{G}_i = \frac{\partial \underset{\sim}{R}}{\partial z_i} = \frac{\partial \underset{\sim}{R}}{\partial Z_A} \frac{\partial Z_A}{\partial z_i} = \underset{\sim}{i}_A \, Z_{A,i} \tag{D.4}$$

Substitution of (D.4) into (D.3) results in

$$\tau_{AB} = J^{-1} \, Z_{A,i} \, s_{ij} \, Z_{B,j} = J^{-1} \, T_{Ak} \, Z_{B,k} \tag{D.5}$$

The same relationships in curvilinear coordinates are

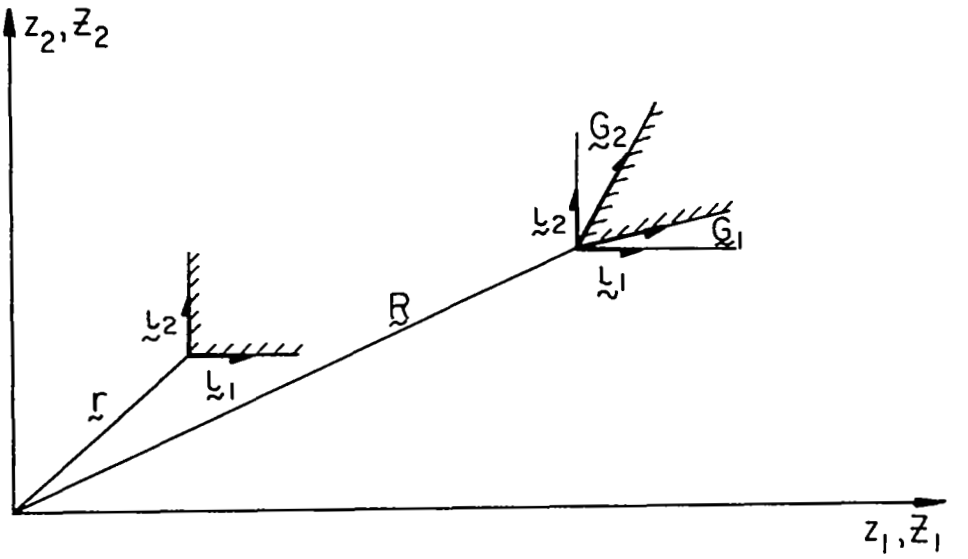
z_2, Z_2
G_2
L_2
G_1
L_1
R
L_2
r
L_1
z_1, Z_1

FIG. D-1

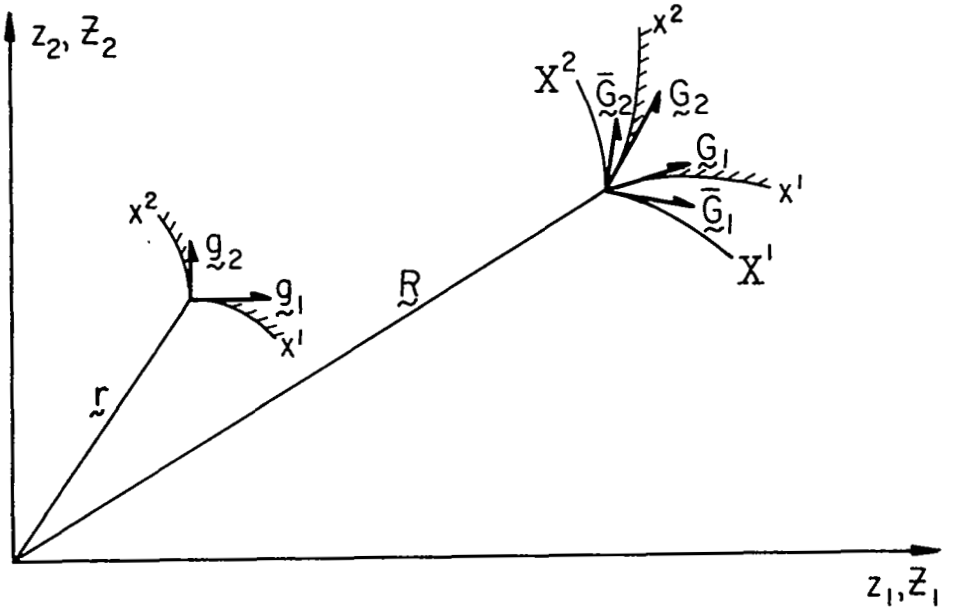
z_2, Z_2
x^2
X^2
$\bar{G}_2$
G_2
G_1
x'
$\bar{G}_1$
X'
x^2
g_2
g_1
x'
R
r
z_1, Z_1

FIG. D-2

$$\pi = \bar{\underset{\sim}{G}}_A \, \tau^{AB} \, \bar{\underset{\sim}{G}}_B = J^{-1} \, \underset{\sim}{G}_i \, s^{ij} \, \underset{\sim}{G}_j = J^{-1} \, \bar{\underset{\sim}{G}}_A \, T^{Ak} \, \underset{\sim}{G}_k \, , \tag{D.6}$$

$$\underset{\sim}{G}_i = \frac{\partial \underset{\sim}{R}}{\partial x^i} = \bar{\underset{\sim}{G}}_A \, X^A_{,i} \, , \quad \text{and} \tag{D.7}$$

$$\tau^{AB} = J^{-1} \, X^A_{,i} \, s^{ij} \, X^B_{,j} = J^{-1} \, T^{Ak} \, X^B_{,k} \tag{D.8}$$

The physical components of s^{ij}, and T^{Ak} are defined such that they transform to the physical components of τ^{AB} by equation (D.5). In fact the stresses in (D.5) are the physical components. In orthogonal curvilinear coordinates the physical components of τ^{AB} and $X^A_{,i}$ are

$$\tau^*_{AB} = \tau^{AB} (\bar{G}_{(AA)} \bar{G}_{(BB)})^{\frac{1}{2}} \quad \text{(no sum)} \, , \tag{D.9}$$

and

$$X^*_{A,i} = X^A_{,i} \, (\bar{G}_{(AA)} \, g^{(ii)})^{\frac{1}{2}} \quad \text{(no sum)} \, . \tag{D.10}$$

Substitution of (D.9) and (D.10) into (D.8) gives

$$\begin{aligned} \tau^*_{AB} &= J^{-1} \, X^*_{A,i} \, (\sqrt{g_{(ii)} g_{(jj)}} \, s^{ij}) \, X^*_{B,j} = \\ &= J^{-1} \, X^*_{B,k} \, [\sqrt{\bar{G}_{(BB)} g_{(kk)}} \, T^{Ak}] \end{aligned} \tag{D.11}$$

By comparison of (D.11) and (D.5) the physical components of s^{ij} and T^{Ak} are

$$s^*_{ij} = \sqrt{g_{(ii)} g_{(jj)}} \, s^{ij} \quad \text{(no sum)} \, , \tag{D.12}$$

and

$$T^*_{Ak} = \sqrt{\bar{G}_{(BB)} \, g_{(kk)}} \, T^{Ak} \quad \text{(no sum)} \, . \tag{D.13}$$

APPENDIX E

The Strain Displacement Equations for Axisymmetric Shells of Revolution

The Lagrange strain tensor will be subjected to Kirchoff's hypothesis and and will be specialized for axisymmetric shells of revolution. Since convected coordinates are convenient to use in axisymmetrically deformed shells of revolution (see III.4.). This type of coordinate system will be adopted throughout the derivations. The Lagrange strain tensor ε_{ij} between two configurations of the shell, say configuration 1 and 2 in Figure B.1, is defined as

$$\varepsilon_{ij} = \frac{1}{2}(u'_i|_j + u'_j|_i + u'^k|_i \; u'_k|_j \tag{E.1}$$

where $\underset{\sim}{u}'$ is the displacement vector between the material points in the shell space in configurations 1 and 2. The vector $\underset{\sim}{u}'$ can be expressed in terms of its shifted components on the middle surface of the shell space in configuration 1 as

$$u'_\alpha = \mu^\gamma_\alpha \, u_\gamma \; ; \; u'^\alpha = (\mu^{-1})^\alpha_\gamma \, u^\gamma \tag{E.2}$$

where the space shifters are [60]

$$\mu^\gamma_\alpha = \delta^\gamma_\alpha - x^3 b^\gamma_\alpha \; , \tag{E.3}$$

$$(\mu^{-1})^\gamma_\alpha = \frac{1}{\mu} \; \delta^{\gamma\nu}_{\alpha\lambda} \, \mu^\lambda_\nu \tag{E.4}$$

and

$$\mu = \det[\mu^\gamma_\alpha] \tag{E.5}$$

in which b^γ_α are the curvatures of the middle surface at configuration 1.

Also

$$u_3' = u'^3 = u_3 = u^3 \tag{E.6}$$

Substitution of (E.2) through (E.6) into (E.1) results in [60].

$$\begin{aligned} 2\varepsilon_{\alpha\beta} = {} & \mu_\alpha^\lambda(u_{\lambda||\beta} - b_{\lambda\beta}u_3) + \mu_\beta^\lambda(u_{\lambda||\alpha} - b_{\lambda\alpha}u_3) \\ & + (u_{\delta||\beta} - b_{\delta\beta}\,u_3)(u^\delta{}_{||\alpha} - b_\alpha^\delta\,u_3) \\ & + (u_{3,\alpha} + b_\alpha^\nu\,u_\nu)(u_{3,\beta} + b_\beta^\lambda\,u_\lambda)\ , \end{aligned} \tag{E.7}$$

$$\begin{aligned} 2\varepsilon_{3\alpha} = {} & \mu_\alpha^\gamma\,u_{\gamma,3} + (u_{3,\alpha} + b_\alpha^\lambda u_\lambda) + \\ & u^\lambda{}_{,3}(u_{\lambda||\alpha} - b_{\lambda\alpha}u_3) + u_{3,3}(u_{3,\alpha} + b_\alpha^\lambda\,u_\lambda)\ , \end{aligned} \tag{E.8}$$

and

$$2\varepsilon_{33} = 2u_{3,3} + (u_{3,3})^2 + u_{\lambda,3}u^\lambda{}_{,3}\ , \tag{E.9}$$

where

$$\begin{aligned} u_{\alpha||\beta} &= u_{\alpha,\beta} - \Gamma_{\alpha\beta}^\lambda\,u_\lambda\ , \\ u^\alpha{}_{||\beta} &= u^\alpha{}_{,\beta} + \Gamma_{\delta\beta}^\alpha\,u^\delta \end{aligned} \tag{E.10}$$

In axisymmetric shells of revolution where the deformations are restricted to Kirchoff's hypothesis the only non-zero components of the metric tensor of the middle surface will be

$$a_{11} = \alpha^2\ ,\ a_{22} = r^2 \tag{E.11}$$

where

$$\alpha^2 = (r_{,1})^2 + (z_{,1})^2 \quad . \tag{E.12}$$

The corresponding metrics associated with the contravariant base vectors will be

$$a^{11} = \alpha^{-2} \ , \ a^{22} = r^{-2} \ . \tag{E.13}$$

The components of the second fundamental form are

$$b_{11} = - \alpha \, \phi_{,1} \ , \ b_{22} = -r \sin \phi \ . \tag{E.14}$$

and the corresponding principle curvatures are

$$\begin{aligned} b^1_1 &= \frac{b_{11}}{a_{11}} = - \frac{1}{R_s} \ , \text{ and} \\ b^2_2 &= \frac{b_{22}}{a_{22}} = - \frac{1}{R_\theta} \ . \end{aligned} \tag{E.15}$$

The Christoffel symbols which are defined as

$$\Gamma^\alpha_{\beta\gamma} = \frac{1}{2} a^{\alpha\lambda} (a_{\lambda\beta,\gamma} + a_{\lambda\gamma,\beta} - a_{\beta\gamma,\lambda}) \tag{E.16}$$

will become

$$\begin{aligned} &\Gamma^1_{11} = \frac{\alpha_{,1}}{\alpha} \ , \ \Gamma^1_{12} = 0 \ , \ \Gamma^1_{22} = - \frac{r r_{,1}}{\alpha^2} \ , \\ &\Gamma^2_{11} = 0 \ , \ \Gamma^2_{12} = \frac{r_{,1}}{r} \ , \ \Gamma^2_{22} = 0 \ . \end{aligned} \tag{E.17}$$

The space shifters which are different from zero are

$$\mu^1_1 = 1 + x^3 \frac{\phi_{,11}}{\alpha} \ , \ \mu^2_2 = 1 + x^3 \frac{\sin \phi}{r} \ . \tag{E.18}$$

In axisymmetrically deformed shells of revolution ε_{12} and ε_{23} will be equal to zero. Also if Kirchhoff's hypothesis is accepted then ε_{13} and ε_{33} will vanish. Therefore, the only non zero components of strain are ε_{11} and ε_{22}. The expressions for these two components of strain are obtained from (E.7) after substitution of (E.10) to (E.18) into this equation. These strains are

$$2\varepsilon_{11} = 2(1 + \frac{x^3}{R_s})[(u_{1,1} - \frac{\alpha_{,1}}{\alpha} u_1) + \frac{\alpha^2}{R_s} u_3] + \frac{1}{\alpha^2}[(u_{1,1} - \frac{\alpha_{,1}}{\alpha} u_1) + \frac{\alpha^2}{R_s} u_3]^2 + (u_{3,1} - \frac{u_1}{R_s})^2 \tag{E.19}$$

$$2\varepsilon_{22} = 2(1 + \frac{x^3}{R_\theta})(rr_{,1} u^1 + r \sin \phi \, u_3) + (r_{,1}u^1 + \sin \phi \, u_3)^2 \tag{E.20}$$

Consider the displacement vector $\underset{\sim}{u}'$. Subject to Kirchhoff's hypothesis it can be written as (see Figure E.1)

$$\underset{\sim}{u}' = \underset{\sim}{v} + x^3 (\underset{\sim}{A}_3 - \underset{\sim}{a}_3) \tag{E.21}$$

where $\underset{\sim}{v}$ is the displacement vector of the middle surface. Let $\underset{\sim}{\omega}$ be defined as the difference between the normal unit vectors

$$\underset{\sim}{\omega} = \underset{\sim}{A}_3 - \underset{\sim}{a}_3 , \tag{E.22}$$

hence

$$\underset{\sim}{u}' = \underset{\sim}{v} + x^3 \underset{\sim}{\omega} \tag{E.23}$$

$$= (v^1 + x^3\omega^1)\underset{\sim}{a}_1 + (v^3 + x^3\omega^3)\underset{\sim}{a}_3$$

Also $\underset{\sim}{u}'$ can be expressed in terms of its shifted components as

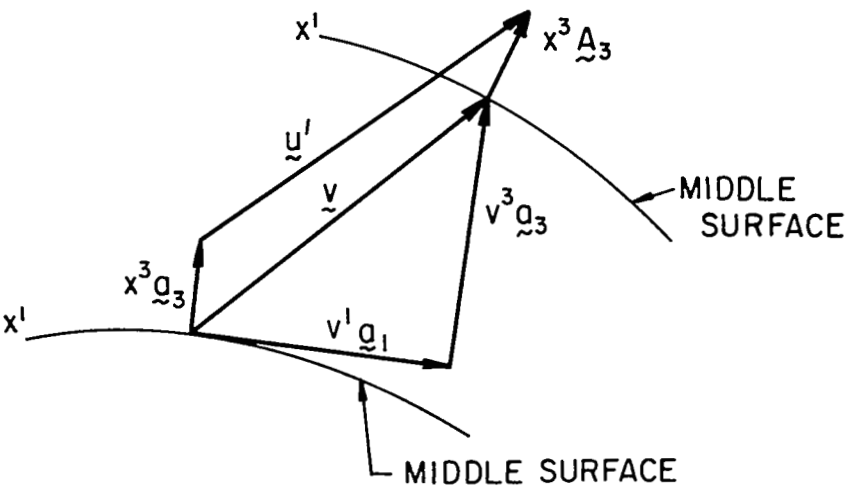
x¹
x³ A₃
u'
v
v³ a₃
MIDDLE SURFACE
x³ a₃
x¹
v¹ a₁
MIDDLE SURFACE

FIG. E-1

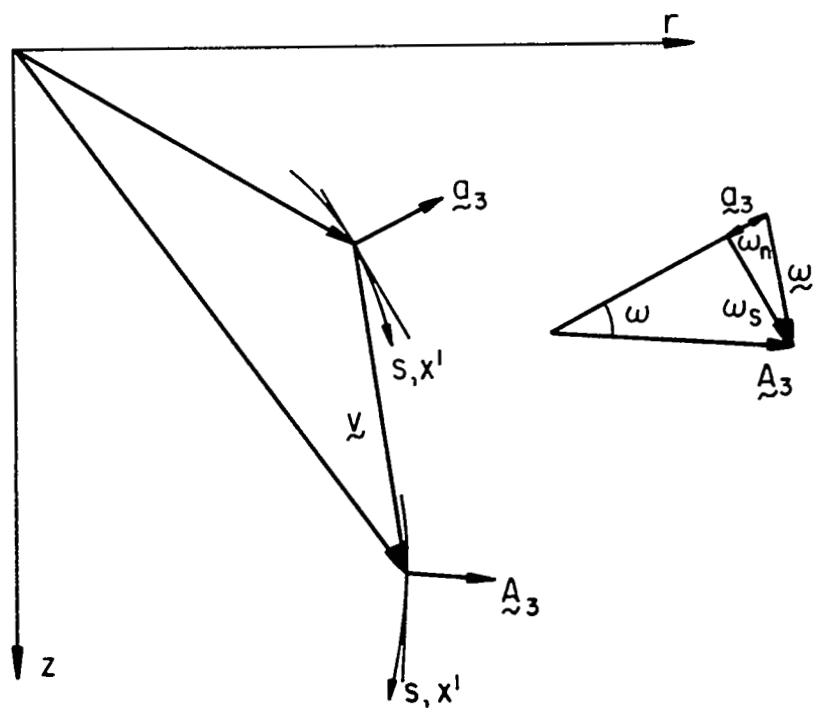
r
a₃
S, x¹
v
A₃
z
S, x¹
a₃
ωn
ω
ωs
ω
A₃

FIG. E-2

$$\underset{\sim}{u}' = u^1 \underset{\sim}{a}_1 + u^3 \underset{\sim}{a}_3 \ . \tag{E.25}$$

Therefore,

$$u' = v^1 + x^3 \omega^1 \ , \text{ and } \ u^3 = v^3 + x^3 \omega^3 \ . \tag{E.25}$$

Similarly,

$$u_1 = v_1 + x^3 \omega_1 \ , \text{ and } \ u_3 = u^3 = v_3 + x^3 \omega_3 \ . \tag{E.26}$$

Substitution of (E.25) and (E.26) into (E.19) and (E.20) gives

$$\begin{aligned} 2\varepsilon_{11} = 2(1 + \frac{x^3}{R_s})\{&(v_{1,1} - \frac{\alpha_{,1}}{\alpha} v_1) + \frac{\alpha^2}{R_s} v_3 + x^3 [(\omega_{1,1} - \frac{\alpha_{,1}}{\alpha} \omega_1) \\ &+ \frac{\alpha^2}{R_s} \omega_3] \} + \frac{1}{\alpha^2} \{(v_{1,1} - \frac{\alpha_{,1}}{\alpha} v_1) + \frac{\alpha^2}{R_s} v_3 \\ &+ x^3 [(\omega_{1,1} - \frac{\alpha_{,1}}{\alpha} \omega_1) + \frac{\alpha^2}{R_s} \omega_3]\}^2 \\ &+ [(v_{3,1} - \frac{v_1}{R_s}) + x^3(\omega_{3,1} - \frac{\omega_1}{R_s})]^2 \end{aligned} \tag{E.27}$$

$$\begin{aligned} 2\varepsilon_{22} = 2(1 + \frac{x^3}{R_\theta})&[(rr_{,1}v^1 + r \sin\phi \ v^3) + x^3(rr_{,1} \omega^1 + r \sin\phi \ \omega^3)] \\ &+ [(r_{,1}v^1 + \sin\phi \ v^3) + x^3(r_{,1} \omega^1 + \sin\phi \ \omega^3)]^2 \end{aligned} \tag{E.28}$$

Let u , w , ω_s , ω_n $\varepsilon_{\theta\theta}$, ε_{ss} denote the physical components of $\underset{\sim}{v}$, $\underset{\sim}{\omega}$, and $\varepsilon_{\alpha\beta}$ respectively. Then

$$u = v^1\alpha = \frac{v_1}{\alpha} \ , \ w = v^3 = v_3 \tag{E.29}$$

$$\omega_s = \omega^1\alpha = \frac{\omega_1}{\alpha} \ , \ \omega_n = \omega^3 = \omega_3 \tag{E.30}$$

$$\varepsilon_{\theta\theta} = \frac{\varepsilon_{22}}{r^2} \quad , \ \varepsilon_{ss} = \frac{\varepsilon_{11}}{\alpha^2} \tag{E.31}$$

Substitution of (E.29), (E.30), and (E.31) into (E.27), and (E.28) gives the strain-displacement relationships in terms of the physical components.

$$\varepsilon_{ss} = e_s + \frac{1}{2} e_s^2 + \frac{\chi^2}{2} + \zeta[(\omega_{s,s} + \frac{\omega_n}{R_s}) + \frac{e_s}{R_s} + e_s(\omega_{s,s} + \frac{\omega_n}{R_s}) - \chi(\omega_{n,s} - \frac{\omega_s}{R_s})] \quad \text{(E.32)}$$

$$+ \zeta^2 [\frac{1}{R_s} (\omega_{s,s} + \frac{\omega_n}{R_s}) + \frac{1}{2} (\omega_{s,s} + \frac{\omega_n}{R_s})^2 + \frac{1}{2} (\omega_{n,s} - \frac{\omega_s}{R_s})^2]$$

$$\varepsilon_{\theta\theta} = e_\theta + \frac{1}{2} e_\theta^2 + \zeta[\omega_r(1 + e_\theta) + \frac{e_\theta}{R_\theta}] + \zeta^2[\frac{\omega_r}{R_\theta} + \frac{1}{2} \omega_r^2] \quad \text{(E.33)}$$

where

$$e_\theta = \frac{1}{r} (u \cos \phi + w \sin \phi) \quad \text{(E.34)}$$

$$e_s = u_{,s} + \frac{w}{R_s} \quad \text{(E.35)}$$

$$\chi = \frac{u}{R_s} - w_{,s} \quad \text{(E.36)}$$

$$\omega_r = \frac{\omega_s \cos \phi + \omega_n \sin \phi}{r} \quad \text{(E.37)}$$

It can be seen in Figure (E.2) that the components of the rotation vector $\underset{\sim}{\omega}$ can be written as

$$\omega_s = \sin \omega \quad \text{(E.38)}$$

$$\omega_n = \cos \omega - 1 \quad \text{(E.39)}$$

When Kirchhoff's hypothesis prevails, it is possible to find ω_s and ω_n in terms of the middle surface displacements u and w. Kirchhoff's hypothesis requires that

$$\varepsilon_{33} = 0 \ , \ \varepsilon_{31} = 0 \ . \tag{E.40}$$

Substitution of the physical components of the variables in (E.8) and (E.9) in view of (E.40) results in three independent equations

$$\omega_s(1 + e_s) - \chi(1 + \omega_n) = 0 \ , \tag{E.41}$$

$$\omega_s[\frac{1}{R_s} + \omega_{s,s} + \frac{\omega_n}{R_s}] + (1 + \omega_n)(\omega_{n,s} - \frac{\omega_s}{R_s}) = 0 \ , \tag{E.42}$$

$$\omega_n^2 + 2\,\omega_n + \omega_s^2 = 0 \ , \tag{E.43}$$

from which ω_n , and ω_s can be found. The expression for ω_s , and ω_n are

$$\omega_s = \frac{\chi}{(1 + 2e_s + e_s^2 + \chi)^{\frac{1}{2}}} \tag{E.44}$$

$$\omega_n = \frac{1 + e_s}{(1 + 2e_s + e_s^2 + \chi)^{\frac{1}{2}}} - 1 \tag{E.45}$$

APPENDIX F

THE EXPRESSION OF VIRTUAL WORK FOR AXISYMMETRIC SHELLS OF REVOLUTION

Let the surface of the shell in configuration 1 be denoted by a' and the displacement vector between the material points in the shell space in configurations 1 and 2 be called $\underset{\sim}{u}'$ (see Figure E.1). Then, in the absence of body forces, the expression of virtual work (A.13) can be written as

$$\int_{a'} t^{r}\delta u_{r}' \, da' = \int_{v} (\tau^{ik}\delta\eta_{ik} + s^{ik}\delta\varepsilon_{ik}) \, dv \qquad (A.13)$$

The surface a' consists of the outside, inside and edge surfaces of the shell where tractions are specified. In vectorial notation the surface integral can be written as

$$\int_{a'} \underset{\sim}{t} \cdot \delta\underset{\sim}{u}' \, da' = \int_{a_o} \underset{\sim}{t} \cdot \delta\underset{\sim}{u}' \, da' + \int_{a_i} \underset{\sim}{t} \cdot \delta\underset{\sim}{u}' \, da' + \int_{a_e} \underset{\sim}{t} \cdot \delta\underset{\sim}{u}' \, da' \; . \qquad (F.1)$$

Consider the integral over the inside surface of the shell. For axisymmetric shells of revolution

$$\underset{\sim}{t} = t^{1}\underset{\sim}{g}_{1} + t^{3}\underset{\sim}{g}_{3} \quad , \qquad (F.2)$$

and since [60]

$$\underset{\sim}{g}_{1} = \mu_{1}^{1} \, \underset{\sim}{a}_{1} \quad , \quad \underset{\sim}{g}_{3} = \underset{\sim}{a}_{3} \qquad (F.3)$$

where μ_{1}^{1} is the space shifter defined in (E.3), then

$$\underset{\sim}{t} = \mu_{1}^{1} \, t^{1}\underset{\sim}{a}_{1} + t^{3}\underset{\sim}{a}_{3} \quad . \qquad (F.4)$$

Also, similar to (E.24), the displacement vector $\underset{\sim}{u}'$ can be written as

$$\underset{\sim}{u}' = u_1 \underset{\sim}{a}^1 + u_3 \underset{\sim}{a}^3 \tag{F.5}$$

The relationship between the surface differential da' on the inside surface and the surface differential da on the middle surface of the shell can be established by noting that

$$da' = \underset{\sim}{g}_1 \times \underset{\sim}{g}_2 \, dx^1 \, dx^2 \quad , \tag{F.6}$$

and

$$da = \underset{\sim}{a}_1 \times \underset{\sim}{a}_2 \, dx^1 \, dx^2 \tag{F.7}$$

Then in view of $(F.3)_1$ and (E.5)

$$da' = \mu \, da \tag{F.8}$$

Substitution of (F.4), (F.5) amd (F.8) into the inside surface integral of (F.1) results in

$$\int_{a_i'} \underset{\sim}{t} \cdot \delta \underset{\sim}{u}' \, da' = \int_a ([\mu \mu_1^1 \, t^1]_{-h/2} \, \delta u_1 + [\mu t^3]_{-h/2} \, \delta u_3) \, da \tag{F.9}$$

where $[\quad]_{-h/2}$ indicates that the variables inside the bracket are evaluated at $x_3 = -h/2$, h being the thickness of the shell. If the tensors in (F.9) are expressed in terms of their physical components then

$$\int_{a_i'} \underset{\sim}{t} \cdot \delta \underset{\sim}{u}' \, da' = \int_a ([\mu t_s]_{-h/2} \, \delta u_1^* + [\mu t_n]_{-h/2} \, \delta u_3^*) \, da \tag{F.10}$$

where the physical components are defined as

$$\begin{aligned} t_s &= \sqrt{g_{11}} \; t^1 \quad , \quad t_n = t^3 \\ u_1^* &= \sqrt{a_{11}} \; u_1 \quad , \quad u_3^* = u_3 \quad . \end{aligned} \tag{F.11}$$

Substitution of (E.26), (E.29), and (E.30) in (F.10) and a similar equation for the outside surface integral leads to

$$\int_{a_o'+a_i'} \underset{\sim}{t} \cdot \delta\underset{\sim}{u}\, da' = \int_a ([\mu t_s]_{-h/2}^{h/2}\, \delta u + [\mu t_n]_{-h/2}^{h/2}\, \delta w + [\mu t_s \zeta]_{-h/2}^{h/2}\, \delta\omega_s + [\mu t_n \zeta]_{-h/2}^{h/2}\, \delta\omega_n)\, da \qquad (F.12)$$

where, in view of (III.12) and (III.13),

$$\delta\omega_s = (1-e_s)\,\delta\chi - \chi\delta e_s \quad , \qquad (F.13)$$

$$\delta\omega_n = -\chi\delta\chi \quad . \qquad (F.14)$$

Let us assume that

$$\delta\omega_s \doteq \delta\chi \quad , \quad \delta\omega_n \doteq 0 \qquad (F.15)$$

then equation (F.12) becomes

$$\int_{a_o'+a_i'} \underset{\sim}{t} \cdot \delta\underset{\sim}{u}'\, da' = \int_a (\tilde{p}_s\, \delta u + \tilde{p}_n\, \delta w + \tilde{m}\, \delta\chi)\, da \qquad (F.16)$$

where

$$\tilde{p}_s = [\mu t_s]_{-h/2}^{h/2} \quad , \quad \tilde{p}_n = [\mu t_n]_{-h/2}^{h/2} \quad , \quad \tilde{m} = [\mu\zeta t_s]_{-h/2}^{h/2} \qquad (F.17)$$

In the same manner the integral over the edge surface in (F.1) can be changed into an integral over the edge contour of the middle surface.

$$\int_{a_e} \underset{\sim}{t} \cdot \delta\underset{\sim}{u}'\, da' = \int_c (\tilde{N}_s\, \delta u + \tilde{Q}\, \delta w + \tilde{M}_s\, \delta\chi)\, dc \qquad (F.18)$$

where

$$\tilde{N}_s = \int_{-h/2}^{h/2} \left(1 + \frac{\zeta}{R_\theta}\right) t_s \, d\zeta$$

$$\tilde{Q}_s = \int_{-h/2}^{h/2} \left(1 + \frac{\zeta}{R_\theta}\right) t_{sn} \, d\zeta \qquad \text{(F.19)}$$

$$\tilde{M}_s = \int_{-h/2}^{h/2} \left(1 + \frac{\zeta}{R_\theta}\right) t_s \zeta \, d\zeta$$

For axisymmetrically deformed shells of revolution, under Kirchhoff's hypothesis, the volume integral in (A.13) reduces to

$$\int_v (\tau^{ik}\delta\eta_{ik} + s^{ik}\delta\varepsilon_{ik}) \, dv = \int_v (\tau^{11}\delta\eta_{11} + \tau^{22}\delta\eta_{22} + s^{11}\delta\varepsilon_{11} + s^{22}\delta\varepsilon_{22}) \, dv \qquad \text{(F.20)}$$

Let τ_{ss}, $\tau_{\theta\theta}$, s_{ss}, $s_{\theta\theta}$ be the physical components of τ^{11}, τ^{22}, s^{11}, s^{22}, and η_{ss}, $\eta_{\theta\theta}$, ε_{ss}, $\varepsilon_{\theta\theta}$ be the physical components of η_{11}, η_{22}, ε_{11} and ε_{22}. Then (F.20) becomes

$$\int_v \tau^{ik}\delta\eta_{ik} + s^{ik}\delta\varepsilon_{ik}) \, dv = \int_v (\tau_{ss}\delta\eta_{ss} + \tau_{\theta\theta}\delta\eta_{\theta\theta} + s_{ss}\delta\varepsilon_{ss} + s_{\theta\theta}\delta\varepsilon_{\theta\theta}) \, dv \qquad \text{(F.21)}$$

APPENDIX G: Some Matrices for the Axisymmetric Shells of Revolution

G.1. [B] Matrix for a Ring Element, see Equation (IV.29).
4×6

$$
\begin{bmatrix}
0 & \rho & 0 & \eta'\rho & 2\xi\eta'\rho & 3\xi^2\eta'\rho \\
\frac{\sin\psi}{r} & \xi\frac{\sin\psi}{r} & \frac{\cos\psi}{r} & \xi\frac{\cos\psi}{r} & \xi^2\frac{\cos\psi}{r} & \xi^3\frac{\cos\psi}{r} \\
0 & -\eta'^2\Phi & 0 & \eta'\Phi & 2\xi\eta'\Phi-\mu & 3\xi(\xi\eta'\Phi-\mu) \\
\frac{\sin\psi\sin\phi}{r^2} & \eta'\Psi+\frac{\xi\sin\psi\sin\phi}{r^2} & \frac{\cos\psi\sin\phi}{r^2} & -\Psi+\frac{\xi\cos\psi\sin\phi}{r^2} & -2\xi\Psi+\frac{\xi^2\cos\psi\sin\phi}{r^2} & -3\xi^2\Psi+\frac{\xi^3\cos\psi\sin\phi}{r^2}
\end{bmatrix}
$$

where

$$\rho = \frac{1}{\ell(1+\eta'^2)} \quad , \quad \mu = \frac{2}{\ell^2(1+\eta'^2)^{3/2}} \quad , \quad \Phi = \frac{\eta''}{\ell^2(1+\eta'^2)^{5/2}} \quad ,$$

$$\Psi = \frac{\sin\psi+\eta'\cos\psi}{\ell r(1+\eta'^2)^{3/2}} \quad .$$

G.2. [B] Matrix for a Cap Element, see Equation (IV.29)
4×6

$$\begin{bmatrix} 0 & 0 & 0 & \rho(1+\eta'\tan\beta_i) & 2\xi\eta'\rho & 3\xi^2\eta'\rho \\ 0 & 0 & 0 & \dfrac{1}{\bar{r}\cos\beta_1} & \dfrac{\xi\cos\psi}{\bar{r}} & \dfrac{\xi^2\cos\psi}{\bar{r}} \\ 0 & 0 & 0 & \Phi(\eta'\tan\beta_1-\eta'^2) & 2\xi\eta'\Phi-\mu & 3\xi(\xi\eta'\Phi-\mu) \\ 0 & 0 & 0 & \dfrac{\eta'-\tan\beta_1}{\xi}\Psi+\dfrac{\sin\phi}{\xi\bar{r}^2\cos\beta_1} & -2\Psi+\dfrac{\cos\psi\sin\phi}{\bar{r}^2} & -3\xi\Psi+\dfrac{\xi\cos\psi\sin\phi}{\bar{r}^2} \end{bmatrix}$$

where

$$\rho = \frac{1}{\ell(1+\eta'^2)} \quad , \quad \mu = \frac{2}{\ell^2(1+\eta'^2)^{3/2}} \quad , \quad \Phi = \frac{\eta''}{\ell^2(1+\eta'^2)^{5/2}} \quad ,$$

$$\Psi = \frac{\sin\psi+\eta'\cos\psi}{\ell\bar{r}(1+\eta'^2)^{3/2}} \quad , \quad \bar{r} = \frac{r}{\xi} \quad .$$

G.3. $[\phi(\xi)]$ Matrix for a Ring Element, see Equation (IV.52)
3×6

$$\begin{bmatrix} 1 & \xi & 0 & 0 & 0 & 0 \\ 0 & 0 & 1 & \xi & \xi^2 & \xi^3 \\ 0 & \dfrac{\eta'}{\ell(1+\eta'^2)} & 0 & \dfrac{-1}{\ell(1+\eta'^2)} & \dfrac{-2\xi}{\ell(1+\eta'^2)} & \dfrac{-3\xi^2}{\ell(1+\eta'^2)} \end{bmatrix}$$

G.4. $[\phi(\xi)]$ Matrix for a Cap Element, see Equation (IV.52)
3×6

$$\begin{bmatrix} 0 & 0 & -\cos\psi & \xi & 0 & 0 \\ 0 & 0 & \sin\psi & \xi\tan\beta_1 & \xi^2 & \xi^3 \\ 0 & 0 & 0 & \dfrac{\eta'-\tan\beta_1}{\ell(1+\eta'^2)} & \dfrac{-2\xi}{\ell(1+\eta'^2)} & \dfrac{-3\xi^2}{\ell(1+\eta'^2)} \end{bmatrix}$$

G.5. [G] Matrix for a Ring Element, see Equation (IV.48)
4×6

$$\begin{bmatrix} 0 & \eta'\rho & 0 & -\rho & -2\xi\rho & -3\xi^2\rho \\ 0 & 0 & 0 & 0 & 0 & 0 \\ 0 & \eta'\rho & 0 & -\rho & -2\xi\rho & -3\xi^2\rho \\ 0 & \eta'\rho & 0 & -\rho & -2\xi\rho & -3\xi^2\rho \end{bmatrix}$$

G.6. [G] Matrix for a Cap Element, see Equation (IV.48)
4×6

$$\begin{bmatrix} 0 & 0 & 0 & \rho(\eta'-\tan\beta_1) & -2\xi\rho & -3\xi^2\rho \\ 0 & 0 & 0 & 0 & 0 & 0 \\ 0 & 0 & 0 & \rho(\eta'-\tan\beta_1) & -2\xi\rho & -3\xi^2\rho \\ 0 & 0 & 0 & \rho(\eta'-\tan\beta_1) & -2\xi\rho & -3\xi^2\rho \end{bmatrix}$$

G.7. [F] Matrix, see Equation (IV.36)
4×4

For Ring Element:

$$\begin{bmatrix} 1 & 0 & 0 & 0 \\ 0 & 0 & 0 & 0 \\ 0 & 0 & -\frac{\Phi}{\rho} & 0 \\ 0 & 0 & 0 & \frac{\sin\phi}{r} \end{bmatrix}$$

For Cap Element:

$$\begin{bmatrix} 1 & 0 & 0 & 0 \\ 0 & 0 & 0 & 0 \\ 0 & 0 & -\frac{\Phi}{\rho} & 0 \\ 0 & 0 & 0 & \frac{\sin\phi}{\xi\bar{r}} \end{bmatrix}$$

where

$$\rho = \frac{1}{\ell(1+\eta'^2)} \quad , \quad \Phi = \frac{\eta''}{\ell^2(1+\eta'^2)^{5/2}}$$

G.8. [A] Matrix for a Ring Element, see Equation (IV.57)
6×6

$$\begin{bmatrix} 1 & 0 & 0 & 0 & 0 & 0 \\ 0 & 0 & 1 & 0 & 0 & 0 \\ 0 & \frac{\sin\beta_i\cos\beta_i}{\ell} & 0 & \frac{-\cos^2\beta_i}{\ell} & 0 & 0 \\ 1 & 1 & 0 & 0 & 0 & 0 \\ 0 & 0 & 1 & 1 & 1 & 1 \\ 0 & \frac{\sin\beta_j\cos\beta_j}{\ell} & 0 & \frac{-2\cos^2\beta_j}{\ell} & \frac{-\cos^2\beta_j}{\ell} & \frac{-3\cos^2\beta_j}{\ell} \end{bmatrix}$$

G.9. [A] Matrix for a Cap Element, see Equation (IV.57)
6×6

$$\begin{bmatrix} 0 & 0 & -\cos\psi & 0 & 0 & 0 \\ 0 & 0 & \sin\psi & 0 & 0 & 0 \\ 0 & 0 & 0 & 0 & 0 & 0 \\ 0 & 0 & -\cos\psi & 1 & 0 & 0 \\ 0 & 0 & \sin\psi & \tan\beta_1 & 1 & 1 \\ 0 & 0 & 0 & \frac{\cos^2\beta_2(\tan\beta_2-\tan\beta_1)}{\ell} & \frac{-2}{\ell}\cos^2\beta_2 & \frac{-3}{\ell}\cos^2\beta_2 \end{bmatrix}$$

G.10. $[A^{-1}]_{6\times6}$ Matrix for a Ring Element, see Equation (IV.59)

$$\begin{bmatrix}
1 & 0 & 0 & 0 & 0 & 0 \\
-1 & 0 & 0 & 1 & 0 & 0 \\
0 & 1 & 0 & 0 & 0 & 0 \\
-\tan\beta_i & 0 & -\ell(1+\tan^2\beta_i) & \tan\beta_i & 0 & 0 \\
2\tan\beta_i+\tan\beta_j & -3 & 2\ell(1+\tan^2\beta_i) & -(2\tan\beta_i+\tan\beta_j) & 3 & \ell(1+\tan^2\beta_j) \\
-(\tan\beta_i+\tan\beta_j) & 2 & -\ell(1+\tan^2\beta_i) & \tan\beta_i+\tan\beta_j & -2 & -(1+\tan^2\beta_j)
\end{bmatrix}$$

G.11. $[A^{-1}]_{6\times6}$ Matrix for a Cap Element, see Equation (IV.59)

$$\begin{bmatrix}
0 & 0 & 0 & 0 & 0 & 0 \\
0 & 0 & 0 & 0 & 0 & 0 \\
0 & 1 & 0 & 0 & 0 & 0 \\
0 & \cos\psi & 0 & 1 & 0 & 0 \\
0 & \dfrac{-2}{\cos\beta_1} - \dfrac{\cos\psi}{\cos\beta_2} & 0 & -2\tan\beta_1-\tan\beta_2 & 3 & \ell(1+\tan^2\beta_2) \\
0 & \dfrac{1}{\cos\beta_1} + \dfrac{\cos\psi}{\cos\beta_2} & 0 & \tan\beta_1+\tan\beta_2 & -2 & -\ell(1+\tan^2\beta_2)
\end{bmatrix}$$

G.12. [T] Matrix, see Equation (IV.60)

$$[T]_{6\times6} = \begin{bmatrix} T_i & 0 \\ 0 & T_j \end{bmatrix}$$

where

$$[T_i]_{3\times3} = \begin{bmatrix} \cos\beta_i & -\sin\beta_i & 0 \\ \sin\beta_i & \cos\beta_i & 0 \\ 0 & 0 & 1 \end{bmatrix}$$

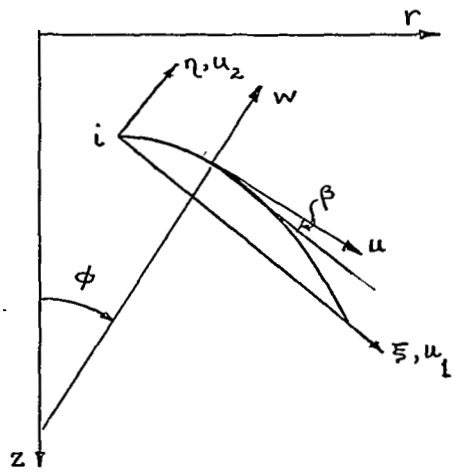

FIG. G-1